Supporting Information

Low-molecular weight organogel matrices as crystallisation media for active pharmaceutical ingredients

Alarqam Zyaad Tareq,[a,b] Matthew Hyder,[a] Ann M. Chippindale,[a] Nicholas J. Spencer,[a] Saeed D. Mohan,[c] Amanpreet Kaur,[c] James E. Hallett[a], Thomas Zinn[d], Kenneth Shankland[e] and Wayne Hayes[a]*

[a] Department of Chemistry, University of Reading, Whiteknights, Reading, RG6 6DX, UK.
[b] Department of Chemistry, Faculty of Science, University of Zakho, Duhok 42001, Iraq.
[c] Centre for Advanced Microscopy, Chemical Analysis Facility, University of Reading, Whiteknights, Reading, RG6 6ED, UK.
[d] Diamond Light Source, Diamond Light Source Ltd., Harwell Science & Innovation Campus, Didcot OX11 0DE, U.K.
[e] School of Pharmacy, University of Reading, Whiteknights, Reading RG6 6AD, UK.

*Corresponding author e-mail: w.c.hayes@reading.ac.uk

Table of Contents

General procedures

(A) Protection amine via benzyl chloroformate (CbzCl)

Synthesis of 4-(((Benzyloxy) carbonyl) amino) butanoic acid (**4**)[1]

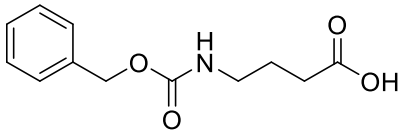

γ-Aminobutyric acid (GABA) (1.00 g, 9.70 mmol, 1.0 equiv.) was dissolved in 4 M $NaOH_{(aq)}$ (10 mL). The mixture was then cooled to –5 °C, and benzyl chloroformate (CbzCl) (1.99 g, 11.64 mmol, 1.2 equiv.) in THF was added dropwise. After one hour, the solution was allowed to warm to room temperature and stirred for 18 hours. The reaction mixture was washed with diethyl ether (3 × 50 mL), and the aqueous layer was cooled to 0 °C and then acidified with 6 M $HCl_{(aq)}$ to a pH of 3 and the resulting white precipitate was filtered and washed with ice cold 0.1 M $HCl_{(aq)}$ (3 × 50 mL) then water (3 × 50 mL), the resulting solid was dried *in vacuo* to afford the desired product 4-(((Benzyloxy) carbonyl) amino) butanoic acid (1.96 g, 85 %) as a white solid. Mp 61–62 °C; FTIR ATR (v/cm^{-1}): 3328, 2922, 1684,1545, 1496, 1449, 1429, 1412, 1363, 1256, 1103; ^{1}H NMR (400 MHz, $CDCl_3$) δ 10.75 (s, 1H), 7.39 – 7.28 (m, 5H), 5.09 (s, 2H), 5.00 (s, 1H), 3.29 – 3.18 (m, 2H), 2.39 (t, *J* = 7.3 Hz, 2H), 1.89 – 1.78 (m, 2H); ^{13}C NMR (100 MHz, $CDCl_3$) δ 178.7, 156.7, 136.5, 128.7, 128.3, 128.3, 66.9, 40.4, 31.3, 25.1; FTMS (ESI) *m/z* [M + H$^+$] calculated for $C_{12}H_{15}NO_4$ = 237.1001; found = 237.1074.

(B) General Coupling Method[2]

A general protocol for the coupling of the 4-(((Benzyloxy) carbonyl) amino) butanoic acid (**1**) with the corresponding amine is as follows. DMAP (0.10 equiv.) was added to a mixture of 4-(((Benzyloxy) carbonyl) amino) butanoic acid (**1**) (1.00 equiv.) and EDC.HCl (1.10 equiv.) in dichloromethane (250 mL), the reaction mixture was stirred at room temperature for 10 minutes and then the corresponding amine (1.05 equiv.) was added. The resulting mixture was stirred overnight at room temperature and monitored via thin layer chromatography. The solution was then poured into ice cold sat. $NaHCO_{3(aq)}$ (250 mL) and the aqueous phase was extracted with CH_2Cl_2 (3 × 250 mL). The combined organic layers were washed with brine (2 × 250 mL), then dried over $MgSO_4$, filtered, and the residual solvent was removed *in vacuo* to afford the desired product.

(C) General Deprotection Method[1, 3]

To a solution of CbzCl-protected amine (**5a, 5b, 5d,** or **5e**) (1 mmol) in absolute ethanol (EtOH) (100-150 mL), 10% palladium on activated carbon (Pd/C) (10%, wt./wt.) was added with constant stirring and the reaction mixture was hydrogenated (with the aid of a hydrogen balloons) at room temperature for 16 hours. The catalyst was removed by filtration and the solvent was removed *in vacuo*, affording the desired product with sufficient purity for use in subsequent steps.

(D) General Synthesis of LMWGs

A general synthetic protocol for the LMWGs is as follows. To a solution of hexyl or octyl isocyanate or hexamethylene diisocyanate (HDI) (1.00 equiv.) in dry THF or $CHCl_3$ (50 mL) the corresponding amine (1.00 equiv. or 2.00 equiv. for HDI) was added dropwise. The resulting mixture was stirred overnight at 60 °C under Argon. Each reaction was monitored via FTIR spectroscopy, until the isocyanate absorbance band at 2272-2248 cm^{-1} was no longer evident. The solid product was then filtered and washed with THF or $CHCl_3$ (50 × 3 mL) and dried *in vacuo* to afford the desired product.

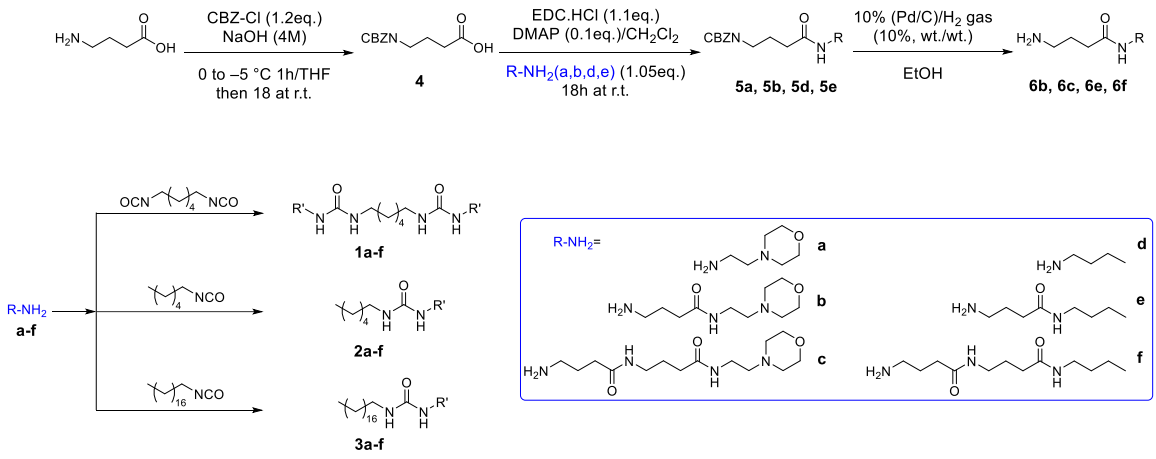

Scheme S1: The synthetic route used to synthesis the LMWGs compounds.

Synthesis of benzyl (4-((2-morpholinoethyl) amino)-4-oxobutyl) carbamate (**5a**).

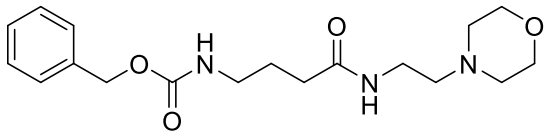

Compound **5a** was obtained as a light-pink solid (2.63 g, 7.51 mmol, 89%) following the general coupling method outlined above from **4** (2.00 g, 8.43 mmol, 1.00 equiv.), EDC.HCl (1.78 g, 9.27 mmol, 1.10 equiv.), DMAP (0.10 g, 0.84 mmol, 0.10 equiv.), and 4-(2-aminoethyl) morpholine (1.15 g, 8.85 mmol, 1.05 equiv.). Mp = 108-110 °C.

FTIR ATR (v/cm^{-1}): 3308, 2967, 2935, 2850, 2817, 1686, 1637,1586, 1544, 1498, 1450, 1381, 1320, 1257, 1114; ^{1}H NMR (400 MHz, $CDCl_3$) δ 7.37 – 7.27 (m, H_a, 5H), 6.31 (s, 1H), 5.27 (s, 1H), 5.07 (s, 2H), 3.71 – 3.65 (m, 4H), 3.37 – 3.30 (m, 2H), 3.27 – 3.19 (m, 2H), 2.47 – 2.40 (m, 6H), 2.22 (t, *J* = 7.1 Hz, 2H), 1.87 – 1.78 (m, 2H); ^{13}C NMR (100 MHz, $CDCl_3$) δ 172.7, 156.9, 136.7, 128.6, 128.2, 128.2, 66.9, 66.7, 57.2, 53.4, 40.4, 35.7, 33.7, 26.1.; FTMS (ESI) *m/z* [M + H$^+$] calculated for $C_{18}H_{27}N_3O_4$ = 349.2002; found = 349.2074.

Synthesis of 4-amino-*N*-(2-morpholinoethyl) butanamide (**6a**).

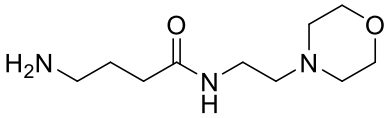

Compound **6a** was obtained as viscous (1.21 g, 5.62 mmol, 98%) by following the general deprotection method outlined above from **5a** (2.00 g, 5.72 mmol).

FTIR ATR (v/cm^{-1}): 3289, 2935, 2856, 2813, 1640, 1549, 1494, 1446, 1359, 1267, 1144, 1113; ^{1}H NMR (400 MHz, $CDCl_3$) δ 6.35 (s, 1H), 3.67 (t, 4H), 3.36 – 3.27 (m, 2H), 2.73 (t, *J* = 6.8 Hz, 2H), 2.49 – 2.38 (m, 6H), 2.24 (t, *J* = 7.4 Hz, 2H), 2.17 (s, 2H), 1.82 – 1.70 (m, 2H); ^{13}C NMR (100 MHz, $CDCl_3$) δ 172.9, 66.9, 57.2, 53.4, 41.4, 35.7, 33.9, 28.9; FTMS (ESI) *m/z* [M + H$^+$] calculated for $C_{10}H_{21}N_3O_2$ = 215.1634; found = 215.1707.

Synthesis of benzyl (4-((4-((2-morpholino ethyl) amino)-4-oxobutyl) amino)-4-oxobutyl) carbamate (**5b**).

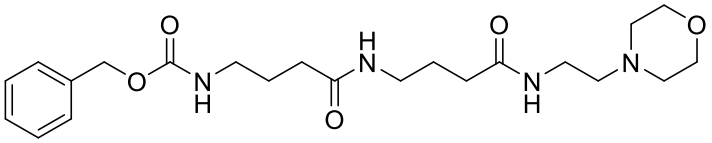

Compound **5b** was obtained as a light-pink solid (2.74 g, 6.31 mmol, 75%) by following the general coupling method outlined above from **4** (2.00 g, 8.43 mmol, 1.00 equiv.), EDC.HCl (1.78 g, 9.27 mmol, 1.1 equiv.), DMAP (103 mg, 0.84 mmol, 0.10 equiv.), and **6a** (1.91 g, 8.85 mmol, 1.05 equiv.). Mp = 121-123 °C.

FTIR ATR (v/cm^{-1}): 3365, 3298, 3263, 2967, 2917, 2887, 2812, 1707, 1696, 1655, 1641, 1531, 1497, 1470, 1305, 1269, 1141, 1114; ^{1}H NMR (400 MHz, $CDCl_3$) δ 7.38 – 7.27 (m, 5H), 6.69 (t, *J* = 5.7 Hz, 1H), 6.51 (t, *J* = 5.3 Hz, 1H), 5.34 (t, *J* = 6.0 Hz, 1H), 5.07 (s, 2H), 3.70 – 3.63 (m, 4H), 3.36 – 3.18 (m, 6H), 2.46 – 2.38 (m, 6H), 2.25 – 2.16 (m, 4H), 1.86 – 1.75 (m, 4H); ^{13}C NMR (100 MHz, $CDCl_3$) δ 173.0, 172.9, 157.0, 136.6, 128.6, 128.2, 128.1, 66.9, 66.8, 57.2, 53.5, 40.4, 39.1, 35.9, 33.9, 33.7, 26.2, 25.5; FTMS (ESI) *m/z* [M + H$^+$] calculated for $C_{22}H_{34}N_4O_5$ = 434.2529; found = 434.2602.

Synthesis of 4-amino-*N*-(4-((2-morpholino ethyl) amino)-4-oxobutyl) butanamide (**6b**).

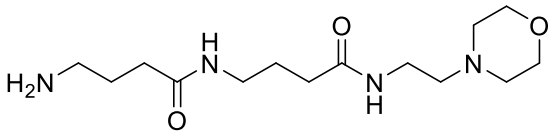

Compound **6b** was obtained as viscous (1.35 g, 4.50 mmol, 97%) by following the general deprotection method outlined above from **5b** (2.00 g, 4.60 mmol).

FTIR ATR (v/cm^{-1}): 3282, 2935, 1634, 1549, 1446, 1266, 1238, 1143; ^{1}H NMR (400 MHz, DMSO-d_6) δ 7.84 – 7.72 (m, 2H), 3.55 (t, *J* = 4.6 Hz, 4H), 3.18 – 3.09 (m, 4H), 3.04 – 2.96 (m, 2H), 2.38 – 2.28 (m, 6H), 2.10 – 2.01 (m, 4H), 1.63 – 1.49 (m, 4H); ^{13}C NMR (100 MHz, DMSO-d_6) δ 172.1, 171.7, 66.1, 57.5, 53.2, 41.1, 38.1, 35.7, 33.0, 32.9, 29.4, 25.5; FTMS (ESI) *m/z* [M + H$^+$] calculated for $C_{14}H_{28}N_4O_3$ = 300.2161; found = 300.2234.

Synthesis of benzyl (4-(butyl amino)-4-oxobutyl) carbamate (**5d**).

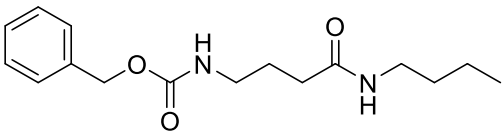

Compound **5d** was obtained as an off-white solid (2.23 g, 7.64 mmol, 90%) by following the general coupling procedure outlined above from **4** (2.00 g, 8.43 mmol, 1.00 equiv.), EDC.HCl (1.78 g, 9.27 mmol, 1.10 equiv.), DMAP (0.10 g, 0.84 mmol, 0.10 equiv.), and *n*-butylamine (0.64 g, 8.85 mmol, 1.05 equiv.). Mp = 138-141 °C.

FTIR ATR (v/cm^{-1}): 3335, 3306, 2955, 2931, 2872, 1682, 1634,1534, 1494, 1454, 1426, 1378, 1316, 1227, 1137; ^{1}H NMR (400 MHz, $CDCl_3$) δ 7.37 – 7.27 (m, 5H), 6.04 (s, 1H), 5.23 (s, 1H), 5.08 (s, 2H), 3.26 – 3.17 (m, 4H), 2.18 (t, *J* = 7.0 Hz,

2H), 1.85 – 1.76 (m, 2H), 1.51 – 1.41 (m, 2H), 1.38 – 1.27 (m, 2H), 0.90 (t, *J* = 7.3 Hz, 3H); ^{13}C NMR (100 MHz, $CDCl_3$) δ 172.6, 157.0, 136.7, 128.6, 128.2, 128.2, 66.8, 40.4, 39.4, 33.8, 31.7, 26.3, 20.2, 13.9; FTMS (ESI) *m/z* [M + H^+] calculated for $C_{16}H_{24}N_2O_3$ = 292.1787; found = 292.1860.

Synthesis of 4-amino-*N*-butylbutanamide (**6d**).

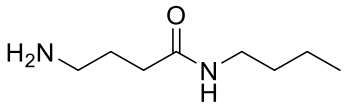

Compound **6d** was obtained as viscous (1.05 g, 6.65 mmol, 97%) by following the general deprotection method outlined above from **5d** (2.00 g, 6.84 mmol).

FTIR ATR (v/cm^{-1}): 3283, 2955, 2829, 2863, 1639, 1548, 1450, 1367, 1289, 1226, 1149, 1052; ^{1}H NMR (400 MHz, $CDCl_3$) δ 6.08 (s, 1H), 3.23 – 3.15 (m, 2H), 2.71 (t, *J* = 6.8 Hz, 2H), 2.21 (t, *J* = 7.4 Hz, 2H), 1.79 – 1.69 (m, 2H), 1.49 (s, 2H), 1.47 – 1.39 (m, 2H), 1.35 – 1.25 (m, 2H), 0.88 (t, *J* = 7.3 Hz, 3H); ^{13}C NMR (100 MHz, $CDCl_3$) δ 172.9, 41.6, 39.3, 34.2, 31.8, 29.3, 20.2, 13.8; FTMS (ESI) *m/z* [M + H^+] calculated for $C_8H_{18}N_2O$ = 158.1419; found = 158.1492.

Synthesis of benzyl (4-((4-(butyl amino)-4-oxobutyl) amino)-4-oxobutyl) carbamate (**5e**).

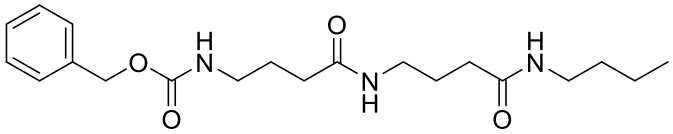

Compound **5e** was obtained as white solid (2.46 g, 6.52 mmol, 77%) by following the general coupling procedure outlined above from **4** (2.00 g, 8.43 mmol, 1.00 equiv.), EDC.HCl (1.78 g, 9.27 mmol, 1.10 equiv.), DMAP (0.10 g, 0.84 mmol, 0.10 equiv.), and **6d** (1.40 g, 8.85 mmol, 1.05 equiv.). Mp = 155-157 °C.

FTIR ATR (v/cm^{-1}): 3337, 3341, 2960, 2932, 2873, 1683, 1629, 1533, 1476, 1425, 1378, 1321, 1288, 1275, 1217, 1138; ^{1}H NMR (400 MHz, DMSO-d_6) δ 7.77 (t, *J* = 5.6 Hz, 1H), 7.72 (t, *J* = 5.6 Hz, 1H), 7.39 – 7.28 (m, 5H), 7.26 (t, *J* = 5.7 Hz, 1H), 5.00 (s, 2H), 3.04 – 2.95 (m, 6H), 2.08 – 2.00 (m, 4H), 1.65 – 1.54 (m, 4H), 1.40 – 1.30 (m, 2H), 1.30 – 1.20 (m, 2H), 0.85 (t, *J* = 7.2 Hz, 3H); ^{13}C NMR (100 MHz, DMSO-d_6) δ 171.6, 171.5, 156.1, 137.3, 128.4, 127.8, 65.2, 39.9, 38.2, 38.1, 32.9, 32.8, 31.3, 25.7, 25.5, 19.6, 13.7; FTMS (ESI) *m/z* [M + H^+] calculated for $C_{20}H_{31}N_3O_4$ = 377.2315; found = 377.2387.

Synthesis of 4-amino-*N*-(4-(butyl amino)-4-oxobutyl) butanamide (**6e**).

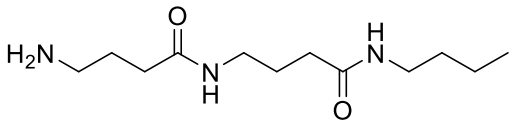

Compound **6e** was obtained as viscous (1.25 g, 5.13 mmol, 96%) by following the general deprotection method outlined above from **5e** (2.00 g, 5.30 mmol).

FTIR ATR (v/cm^{-1}): 3300, 2931, 1628, 1543, 1426, 1283, 1228, 1155; ^{1}H NMR (400 MHz, DMSO-d_6) δ 7.91 – 7.81 (m, 2H), 3.07 – 2.97 (m, 4H), 2.51 (t, J = 7.1 Hz, 2H), 2.12 – 2.02 (m, 4H), 1.65 – 1.51 (m, 4H), 1.41 – 1.32 (m, 2H), 1.31 – 1.21 (m, 2H), 0.86 (t, J = 7.3 Hz, 3H); ^{13}C NMR (100 MHz, DMSO-d_6) δ 172.1, 171.5, 41.3, 38.1, 38.1, 33.1, 32.9, 31.3, 29.6, 25.6, 19.6, 13.7; FTMS (ESI) *m/z* [M + H$^+$] calculated for $C_{12}H_{25}N_3O_2$ = 243.1947; found = 243.2020.

Synthesis of 1,1'-(hexane-1,6-diyl)bis(3-(2-morpholinoethyl)urea) (**1a**)

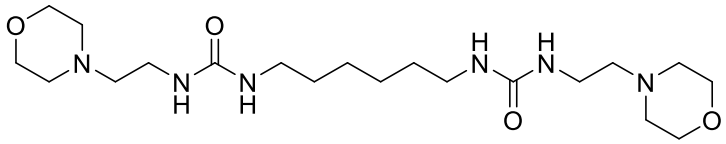

Compound **1a** was obtained as off-white powder (2.89 g, 6.73 mmol, 92%) by following the general synthesis of LMWGs outlined above from 4-(2-aminoethyl)morpholine (2.00 g, 15.63 mmol) and HDI (1.23 g, 7.32 mmol). Mp 190-192 °C

FTIR ATR (v/cm^{-1}): 3343, 3312, 2933, 1619,1573, 1517, 1250, 1115; ^{1}H NMR (400 MHz, DMSO-d_6) δ 5.95 (t, J = 5.6 Hz, 2H), 5.66 (t, J = 5.6 Hz, 2H), 3.56 (t, J = 4.6 Hz, 8H), 3.12 – 3.04 (m, 4H), 2.99 – 2.90 (m, 4H), 2.39 – 2.25 (m, 12H), 1.39 – 1.28 (m, 4H), 1.27 – 1.18 (m, 4H); ^{13}C NMR (100 MHz, DMSO-d_6) δ 158.0, 66.2, 58.3, 53.3, 39.1, 36.3, 30.0, 26.1; FTMS (ESI) *m/z* [M + H$^+$] calculated for $C_{20}H_{40}N_6O_4$ = 428.3111; found = 428.3180.

Synthesis of N^1,N^{20}-bis(2-morpholinoethyl)-6,15-dioxo-5,7,14,16-tetraazaicosanediamide (**1b**)

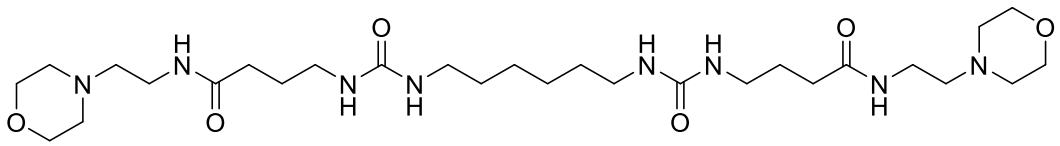

Compound **1b** was obtained as pink powder (2.38 g, 3.96 mmol, 89%) by following the general synthesis of LMWGs outlined above from **6a** (2.00 g, 9.29 mmol) and HDI (0.74 g, 4.42 mmol). Mp 200-202 °C

FTIR ATR (v/cm^{-1}): 3323, 3282, 2931, 1640, 1610,1553, 1477, 1117; ^{1}H NMR (400 MHz, DMSO-d_6) δ 7.75 (t, J = 5.7 Hz, 2H), 5.80 – 5.73 (m, 4H), 3.55 (t, J = 4.6 Hz, 8H), 3.19 – 3.11 (m, 4H), 2.98 – 2.90 (m, 8H), 2.39 – 2.27 (m, 12H), 2.03 (t, J = 7.5 Hz, 4H), 1.60 – 1.50 (m, 4H), 1.33 (t, J = 6.8 Hz, 4H), 1.25 – 1.20 (m, 4H); ^{13}C NMR (100 MHz, DMSO-d_6) δ 171.8, 158.1, 66.2, 57.5, 53.2, 39.3, 39.2, 35.7, 32.9, 30.0, 26.5, 26.1; FTMS (ESI) *m/z* [M + H$^+$] calculated for $C_{28}H_{54}N_8O_6$ = 598.4166; found = 598.4235.

Synthesis of N^{1},N^{20}-bis(4-((2-morpholinoethyl)amino)-4-oxobutyl)-6,15-dioxo-5,7,14,16-tetraazaicosanediamide (**1c**)

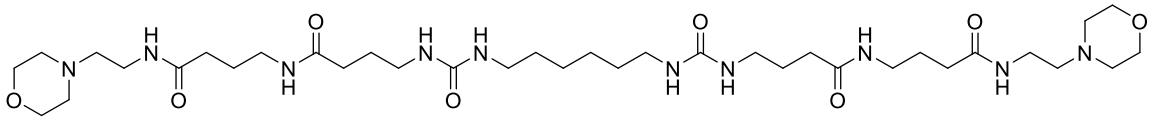

Compound **1c** was obtained as pink powder (2.23 g, 2.90 mmol, 87%) by following the general synthesis of LMWGs outlined above from **6b** (2.00 g, 6.66 mmol) and HDI (0.55 g, 3.33 mmol). Mp 199-201 °C

FTIR ATR (v/cm^{-1}): 3286, 2933, 2857, 1637, 1615,1548, 1476, 1260, 1115; ^{1}H NMR (400 MHz, DMSO-d_6) δ 7.82 – 7.73 (m, 4H), 5.82 – 5.74 (m, 4H), 3.55 (t, J = 4.7 Hz, 8H), 3.20 – 3.10 (m, 4H), 3.03 – 2.98 (m, 4H), 2.97 – 2.91 (m, 8H), 2.39 – 2.27 (m, 12H), 2.11 – 1.98 (m, 8H), 1.65 – 1.50 (m, 8H), 1.32 (t, J = 6.8 Hz, 4H), 1.25 – 1.18 (m, 4H); ^{13}C NMR (100 MHz, DMSO-d_6) δ 171.8, 158.2, 66.2, 57.5, 53.3, 38.1, 35.8, 32.9, 30.0, 26.5, 26.2, 25.5; FTMS (ESI) *m/z* [M + H$^+$] calculated for $C_{36}H_{68}N_{10}O_8$ = 768.5222; found = 768.5291.

Synthesis of 1,1'-(hexane-1,6-diyl)bis(3-butylurea) (**1d**)

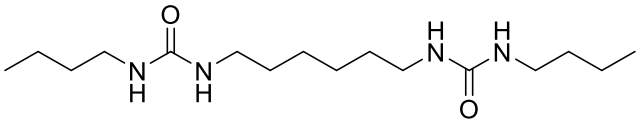

Compound **1d** was obtained as white powder (3.89 g, 12.33 mmol, 95%) by following the general synthesis of LMWGs outlined above from *n*-butylamine (2.00 g, 27.53 mmol) and **5** (2.19 g, 13.03 mmol). Mp 204-206 °C

FTIR ATR (v/cm^{-1}): 3322, 2931,1614,1568, 1478, 1243; ^{1}H NMR (400 MHz, DMSO-d_6) δ 5.74 – 5.67 (m, 4H), 3.00 – 2.89 (m, 8H), 1.38 – 1.18 (m, 16H), 0.86

(t, J = 7.1 Hz, 6H); FTMS (ESI) *m/z* [M + H^+] calculated for $C_{16}H_{34}N_4O_2$ = 314.2682; found = 314.2750.

Synthesis of N^1,N^{20}-dibutyl-6,15-dioxo-5,7,14,16-tetraazaicosanediamide (**1e**)

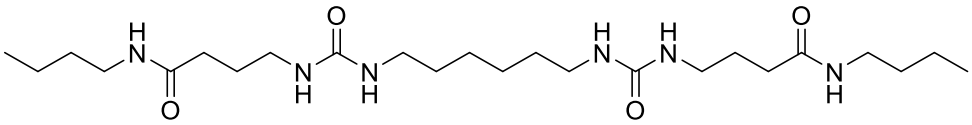

Compound **1e** was obtained as solid white (2.74 g, 5.64 mmol, 93%) by following the general synthesis of LMWGs outlined above from **6d** (2.00 g, 12.64 mmol) and HDI (1.01 g, 6.02 mmol). Mp 231-233 °C

FTIR ATR (v/cm^{-1}): 3309, 3282, 2931, 1639, 1610,1580, 1475, 1251; ^{1}H NMR (400 MHz, DMSO-d_6) δ 7.76 (s, 2H), 5.76 (s, 4H), 3.06 – 2.89 (m, 12H), 2.06 – 1.98 (m, 4H), 1.65 – 1.50 (m, 4H), 1.40 – 1.20 (m,16H), 0.87 (t, J = 7.2 Hz, 6H); FTMS (ESI) *m/z* [M + H^+] calculated for $C_{24}H_{48}N_6O_4$ = 484.3737; found = 484.3810.

Synthesis of N^1,N^{20}-bis(4-(butylamino)-4-oxobutyl)-6,15-dioxo-5,7,14,16-tetraazaicosanediamide (**1f**)

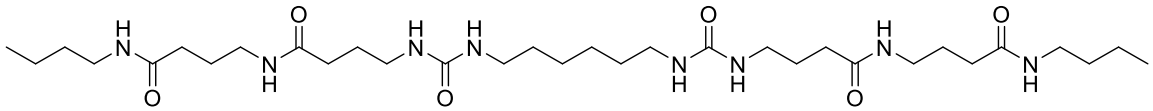

Compound **1f** was obtained as solid white (2.43 g, 3.71 mmol, 90%) by following the general synthesis of LMWGs outlined above from **6e** (2.00 g, 8.22 mmol) and HDI (0.69 g, 4.11 mmol). Mp 240-242 °C

FTIR ATR (v/cm^{-1}): 3292, 2973, 2927, 2882, 1638, 1614,1581, 1542, 1476, 1418, 1259, 1228; ^{1}H NMR (400 MHz, DMSO-d_6) δ 7.78 (d, J = 14.8 Hz, 4H), 5.77 (s, 4H), 3.07 – 2.93 (m, 16H), 2.14 – 1.97 (m, 8H), 1.40 – 1.19 (m, 24H), 0.86 (t, J = 7.2 Hz, 6H); FTMS (ESI) *m/z* [M + H^+] calculated for $C_{32}H_{62}N_8O_6$ = 654.4792; found = 654.4862.

Synthesis of 1-hexyl-3-(2-morpholinoethyl)urea (**2a**).

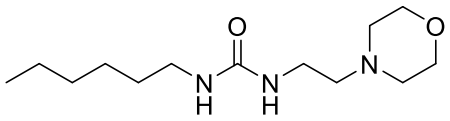

Compound **2a** was obtained as light viscous (3.62 g, 5.114.07 mmol, 91%) by following the general synthesis of LMWGs outlined above from 4-(2-aminoethyl)morpholine (2.00 g, 15.36 mmol) and hexyl isocyanate (1.95 g, 15.36 mmol). Mp 64-66 °C

FTIR ATR (v/cm^{-1}): 3345, 3311,2980, 2955, 2930, 2866,1618,1572, 1516, 1461, 1248, 1113; ^{1}H NMR (400 MHz, $CDCl_3$) δ 4.97 (t, *J* = 5.1 Hz, 1H), 4.80 (s, 1H), 3.71 (t, *J* = 4.6 Hz, 4H), 3.31 – 3.25 (m, 2H), 3.17 – 3.11 (m, 2H), 2.53 – 2.47 (m, 6H), 1.53 – 1.44 (m, 2H), 1.36 – 1.23 (m, 6H), 0.88 (d, *J* = 6.9 Hz, 3H).; ^{13}C NMR (100 MHz, $CDCl_3$) δ 158.7, 66.9, 58.3, 53.5, 40.8, 36.9, 31.7, 30.4, 26.7, 22.7, 14.2; FTMS (ESI) *m/z* [M + H$^+$] calculated for $C_{13}H_{27}N_3O_2$ = 257.2103; found = 257.2171.

Synthesis of 4-(3-hexylureido)-N-(2-morpholinoethyl)butanamide (**2b**).

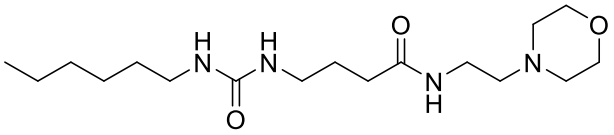

Compound **2b** was obtained as light viscous (2.95 g, 8.61 mmol, 92%) by following the general synthesis of LMWGs outlined above from **6a** (2.00 g, 9.29 mmol) and hexyl isocyanate (1.18 g, 9.29 mmol). Mp 112-114 °C

FTIR ATR (v/cm^{-1}): 3341, 3287, 2979, 2954, 2931, 2930, 2863,1644, 1610,1551, 1474, 1279, 1212, 1114; ^{1}H NMR (400 MHz, $CDCl_3$) δ 7.09 (t, *J* = 5.2 Hz, 1H), 5.76 (t, *J* = 5.9 Hz, 1H), 5.49 (t, *J* = 5.6 Hz, 1H), 3.62 (t, *J* = 4.6 Hz, 4H), 3.30 – 3.23 (m, 2H), 3.15 – 3.08 (m, 2H), 3.07 – 2.99 (m, 2H), 2.46 – 2.37 (m, 6H), 2.17 (t, *J* = 7.1 Hz, 2H), 1.74 – 1.64 (m, 2H), 1.42 – 1.32 (m, 2H), 1.27 – 1.13 (m, 6H), 0.83 – 0.76 (m, 3H); ^{13}C NMR (100 MHz, $CDCl_3$) δ 173.4, 159.4, 66.7, 57.2, 53.4, 40.3, 39.2, 35.9, 33.5, 31.5, 30.3, 26.8, 26.6, 22.5, 14.0; FTMS (ESI) *m/z* [M + H$^+$] calculated for $C_{17}H_{34}N_4O_3$ = 342.2631; found = 342.2703.

Synthesis of 4-(3-hexylureido)-N-(4-((2-morpholinoethyl)amino)-4-oxobutyl)butanamide (**2c**).

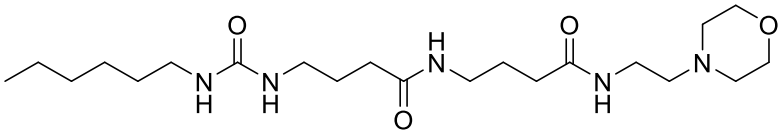

Compound **2c** was obtained as light viscous (2.43 g, 5.67 mmol, 85%) by following the general synthesis of LMWGs outlined above from **6b** (2.00 g, 6.66 mmol) and hexyl isocyanate (0.85 g, 6.66 mmol). Mp 130-132 °C

FTIR ATR (v/cm^{-1}): 3464, 3305, 3271, 3092, 2954, 2924, 2856, 2814,1675, 1645, 1626,1568, 1461, 1302, 1219, 1112; ^{1}H NMR (400 MHz, $CDCl_3$) δ 7.49 (t, *J* = 5.8 Hz, 1H), 7.13 (t, *J* = 5.5 Hz, 1H), 5.59 (t, *J* = 6.0 Hz, 1H), 5.31 (t, *J* = 5.7 Hz, 1H), 3.69 (t, *J* = 4.7 Hz, 4H), 3.39 – 3.32 (m, 2H), 3.30 – 3.23 (m, 2H), 3.21 – 3.15 (m, 2H), 3.10 (t, *J* = 3.2 Hz, 2H), 2.50 (t, *J* = 6.0 Hz, 6H), 2.29 – 2.19 (m, 4H), 1.87 – 1.70 (m, 4H), 1.49 – 1.39 (m, 2H), 1.33 – 1.20 (m, 6H), 0.89 – 0.82 (m, 3H); ^{13}C NMR (100 MHz, $CDCl_3$) δ 173.6, 173.2, 159.5, 66.8, 57.5, 53.5, 40.66, 40.6, 39.2, 38.6, 35.9, 33.7, 33.6, 31.7, 30.4, 27.1, 26.7, 25.7, 22.7, 14.1; FTMS (ESI) *m/z* [M + H$^+$] calculated for $C_{21}H_{41}N_5O_4$ = 427.3159; found = 427.3224.

Synthesis of 1-butyl-3-hexylurea (**2d**).

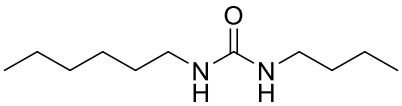

Compound **2d** was obtained as light viscous (5.30 g, 26.45 mmol, 96%) by following the general synthesis of LMWGs outlined above from *n*-butylamine (2.00 g, 27.35 mmol) and hexyl isocyanate (3.48 g, 27.35 mmol). Mp 52-54 °C

FTIR ATR (v/cm^{-1}): 3324, 2953, 2928, 2870, 1651, 1571, 1478, 1462,1378, 1244, 1224,1156, 1054; ^{1}H NMR (400 MHz, $CDCl_3$) δ 4.43 (s, 2H), 3.18 – 3.11 (m, 4H), 1.52 – 1.42 (m, 4H), 1.39 – 1.23 (m, 8H), 0.95 – 0.84 (m, 6H); ^{13}C NMR (100 MHz, $CDCl_3$) δ 158.7, 40.8, 40.5, 32.5, 31.7, 30.3, 26.7, 22.7, 20.2, 14.2, 13.9; FTMS (ESI) *m/z* [M + H$^+$] calculated for $C_{11}H_{24}N_2O$ = 200.1889; found = 200.1956.

Synthesis of N-butyl-4-(3-hexylureido)butanamide (**2e**).

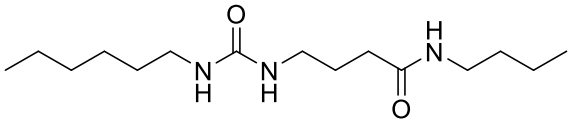

Compound **2e** was obtained as light viscous (2.92 g, 10.22 mmol, 80%) by following the general synthesis of LMWGs outlined above from **6d** (2.00 g, 12.64 mmol) and hexyl isocyanate (1.61 g, 12.64 mmol). Mp 158-160 °C

FTIR ATR (v/cm^{-1}): 3353, 3273, 2953, 2927, 2871, 1712, 1669, 1546, 1466, 1393, 1298, 1213, 1096; ^{1}H NMR (400 MHz, DMSO-d_6) δ 7.77 (t, *J* = 5.6 Hz, 1H), 5.82 – 5.73 (m, 2H), 3.05 – 2.89 (m, 6H), 2.02 (t, *J* = 7.5 Hz, 2H), 1.60 – 1.50 (m, 2H), 1.40 – 1.19 (m, 12H), 0.90 – 0.81 (m, 6H); ^{13}C NMR (100 MHz, DMSO-d_6) δ 171.7, 158.2, 38.9, 38.1, 32.9, 31.3, 31.1, 30.0, 26.5, 26.1, 22.1, 19.6, 13.9, 13.7; FTMS (ESI) *m/z* [M + H$^+$] calculated for $C_{15}H_{31}N_3O_2$ = 285.2416; found = 285.2488.

Sunthesis of N-butyl-4-(4-(3-hexylureido)butanamido)butanamide (**2f**).

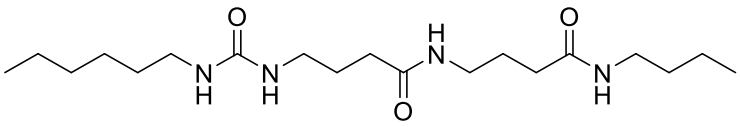

Compound **2af** was obtained as light viscous (2.65 g, 7.14 mmol, 86%) by following the general synthesis of LMWGs outlined above from **6e** (2.00 g, 8.22 mmol) and hexyl isocyanate (1.05 g, 8.22 mmol). Mp 180-182 °C.

FTIR ATR (v/cm^{-1}): 3649, 3299, 2979, 2919, 2871, 1714, 1628, 1540, 1474, 1375,1252, 1223, 1086; ^{1}H NMR (400 MHz, DMSO-d_6) δ 7.82 – 7.72 (m, 2H), 5.80 – 5.73 (m, 2H), 3.05 – 2.91 (m, 8H), 2.06 – 1.99 (m, 4H), 1.63 – 1.51 (m, 4H), 1.40 – 1.20 (m, 12H), 0.89 – 0.82 (m, 6H); ^{13}C NMR (100 MHz, DMSO-d_6) δ 172.2, 172.0, 158.6, 38.6, 38.6, 33.4, 31.7, 31.5, 30.5, 26.9, 26.6, 26.0, 22.6, 20.1, 14.4, 14.1; FTMS (ESI) *m/z* [M + H^{+}] calculated for $C_{15}H_{31}N_3O_2$ = 370.2944; found = 370.3017.

Synthesis of 1-(2-morpholinoethyl)-3-octadecylurea (**3a**).

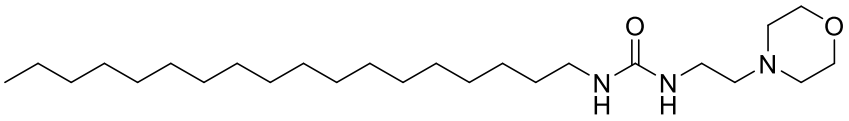

Compound **3a** was obtained as light viscous (2.87 g, 6.74 mmol, 87%) by following the general synthesis of LMWGs outlined above from 4-(2-aminoethyl)morpholine (1.00 g, 7.68 mmol) and octadecyl isocyanate (2.27 g, 7.68 mmol). Mp 108-110 °C

FTIR ATR (v/cm^{-1}): 3343, 2953, 2918, 2847,1615,1576, 1515, 1467, 1118; ^{1}H NMR (400 MHz, $CDCl_3$) δ 4.81 (t, *J* = 5.1 Hz, 1H), 4.69 (s, 1H), 3.70 (t, *J* = 4.6 Hz, 4H), 3.30 – 3.23 (m, 2H), 3.18 – 3.11 (m, 2H), 2.50 – 2.42 (m, 6H), 1.49 (t, *J* = 7.0 Hz, 2H), 1.31 – 1.21 (m, 30H), 0.87 (t, *J* = 6.8 Hz, 3H); ^{13}C NMR (100 MHz, $CDCl_3$) δ 158.6, 67.1, 58.2, 53.5, 40.8, 37.1, 32.1, 30.4, 29.8, 29.8, 29.7, 29.5, 27.1, 22.8, 14.3 ; FTMS (ESI) *m/z* [M + H^{+}] calculated for $C_{25}H_{51}N_3O_2$ = 425.4000; found = 425.4044.

Synthesis of N-(2-morpholinoethyl)-4-(3-octadecylureido)butanamide (**3b**).

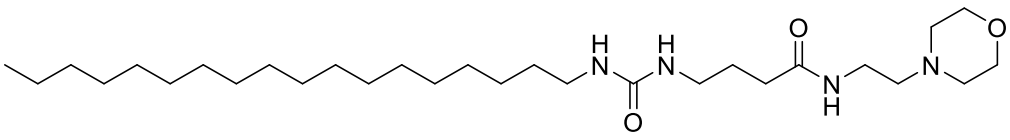

Compound **3b** was obtained as light viscous (1.96 g, 3.83 mmol, 82%) by following the general synthesis of LMWGs outlined above from **6a** (1.00 g, 4.64 mmol) and octadecyl isocyanate (1.37 g, 4.64 mmol). Mp 130-132 °C

FTIR ATR (v/cm^{-1}): 3449, 3339, 3284, 2980, 2917, 2847, 1638, 1610, 1555, 1467, 1405, 1280,1216, 1118; ^{1}H NMR (400 MHz, $CDCl_3$) δ 6.45 (s, 1H), 4.80 (t, *J* = 5.9 Hz, 1H), 4.52 (t, *J* = 5.6 Hz, 1H), 3.75 – 3.67 (m, 4H), 3.39 – 3.32 (m, 2H), 3.28 – 3.22 (m, 2H), 3.17 – 3.09 (m, 2H), 2.51 – 2.41 (m, 6H), 2.26 (t, *J* = 6.7 Hz, 2H), 1.87 – 1.77 (m, 2H), 1.53 – 1.42 (m, 2H), 1.25 (s, 30H), 0.88 (t, *J* = 6.7 Hz, 3H); ^{13}C NMR (100 MHz, $CDCl_3$) δ 173.2, 158.7, 67.1, 57.3, 53.5, 40.9, 39.9, 35.9, 33.8, 32.1, 30.4, 29.8, 29.5, 27.1, 26.5, 22.8, 14.3; FTMS (ESI) *m/z* [M + H$^+$] calculated for $C_{29}H_{58}N_4O_3$ = 510.4509; found = 510.4574.

Synthesis of N-(2-morpholinoethyl)-4-(4-(3-octadecylureido) butanamido) butanamide (**3c**).

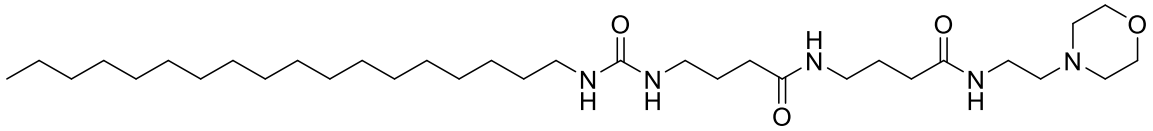

Compound **3c** was obtained as light viscous (1.44 g, 2.42 mmol, 72%) by following the general synthesis of LMWGs outlined above from **6b** (1.00 g, 3.33 mmol) and octadecyl isocyanate (0.98 g, 3.33 mmol). Mp 146-148 °C

FTIR ATR (v/cm^{-1}): 3303, 2980, 2916, 2848, 1635, 1613, 1577, 1544, 1470, 1378, 1147,1114; ^{1}H NMR (400 MHz, $CDCl_3$) δ 7.04 (s, 1H), 6.86 (s, 1H), 4.91 (s, 1H), 4.67 (s, 1H), 3.72 (t, *J* = 4.6 Hz, 4H), 3.41 – 3.35 (m, 2H), 3.34 – 3.28 (m, 2H), 3.27 – 3.20 (m, 2H), 3.17 – 3.09 (m, 2H), 2.58 – 2.45 (m, 6H), 2.31 – 2.22 (m, 3H), 1.90 – 1.74 (m, 4H), 1.53 – 1.43 (m, 2H), 1.25 (s, 30H), 0.88 (t, *J* = 6.7 Hz, 3H); ^{13}C NMR (100 MHz, $CDCl_3$) δ 173.5, 173.1, 159.0, 66.9, 57.5, 53.6, 40.9, 39.6, 38.8, 35.8, 33.8, 33.7, 32.1, 30.4, 29.8, 29.5, 27.1, 26.8, 25.6, 22.8, 14.3; FTMS (ESI) *m/z* [M + H$^+$] calculated for $C_{33}H_{65}N_5O_4$ = 595.5037; found = 595.5109.

Synthesis of 1-butyl-3-octadecylurea (**3d**).

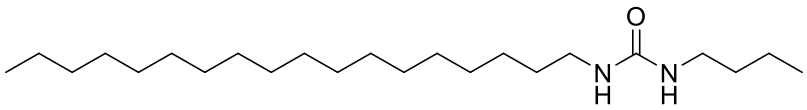

Compound **3d** was obtained as light viscous (4.32 g, 11.71 mmol, 85%) by following the general synthesis of LMWGs outlined above from *n*-butylamine (1.00 g, 13.67 mmol) and octadecyl isocyanate (4.04 g, 13.67 mmol). Mp 98-100 °C

FTIR ATR (v/cm^{-1}): 3340, 3325, 2916, 2871, 2847, 1615, 1569, 1467, 1375, 1235; ^{1}H NMR (400 MHz, $CDCl_3$) δ 4.23 (t, *J* = 5.7 Hz, 2H), 3.19 – 3.10 (m, 4H), 1.52 –

1.43 (m, 4H), 1.25 (s, 32H), 0.96 – 0.84 (m, 6H); ^{13}C NMR (100 MHz, $CDCl_3$) δ 158.4, 40.9, 40.5, 32.5, 32.1, 30.4, 30.0, 29.8, 29.8, 29.7, 29.5, 27.1, 22.8, 20.2, 14.3, 13.9; FTMS (ESI) *m/z* [M + H^+] calculated for $C_{23}H_{48}N_2O$ = 368.3767; found = 368.3839.

Synthesis of N-butyl-4-(3-octadecylureido)butanamide (**3e**).

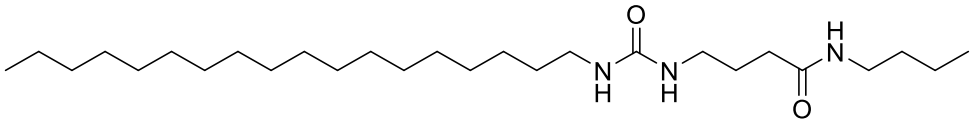

Compound **3e** was obtained as light viscous (12.41 g, 5.30 mmol, 83%) by following the general synthesis of LMWGs outlined above from **6d** (1.00 g, 6.32 mmol) and octadecyl isocyanate (10.87 g, 6.32 mmol). Mp 154-156 °C

FTIR ATR (v/cm^{-1}): 3309, 2955, 2919, 2846, 1641, 1609, 1548, 1480, 1460, 1420, 1377, 1244, 1199; ^{1}H NMR (400 MHz, $CDCl_3$) δ 6.13 (s, 1H), 4.64 (s, 1H), 4.38 (s, 1H), 3.28 – 3.09 (m, 6H), 2.23 (t, *J* = 6.6 Hz, 2H), 1.84 – 1.76 (m, 2H), 1.52 – 1.44 (m, 4H), 1.25 (s, 32H), 0.95 – 0.85 (m, 6H); FTMS (ESI) *m/z* [M + H^+] calculated for $C_{27}H_{55}N_3O_2$ = 453.4294; found = 453.4367.

Synthesis of N-butyl-4-(4-(3-octadecylureido)butanamido)butanamide (**3e**).

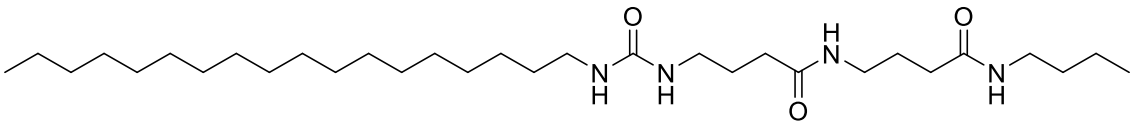

Compound **3e** was obtained as light viscous (1.76 g, 3.27 mmol, 79%) by following the general synthesis of LMWGs outlined above from **6e** (1.00 g, 4.11 mmol) and octadecyl isocyanate (1.21 g, 4.11 mmol). Mp 187-189 °C

FTIR ATR (v/cm^{-1}): 3302, 2955, 2917, 2847, 1639, 1610, 1544, 1461, 1419, 1375, 1263, 1199; ^{1}H NMR (400 MHz, $CDCl_3$) δ 5.34 (d, *J* = 6.8 Hz, 2H), 4.58 (s, 1H), 4.36 (s, 1H), 3.35 – 3.08 (m, 4H), 2.29 – 2.13 (m, 4H), 2.08 – 1.96 (m, 4H), 1.92 – 1.76 (m, 4H), 1.38 – 1.15 (m, 30H), 0.98 – 0.77 (m, 6H); FTMS (ESI) *m/z* [M + H^+] calculated for $C_{31}H_{62}N_4O_3$ = 538.4822; found = 538.4895.

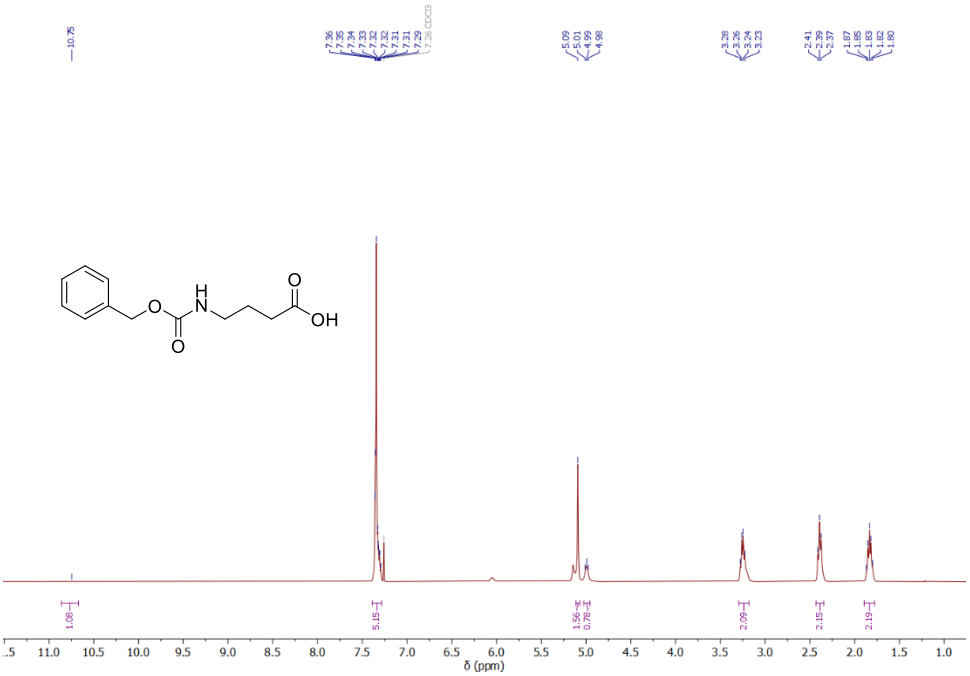

Figure S1. ^{1}H NMR spectrum of compound **4** (400 MHz, $CDCl_3$, at 25 °C).

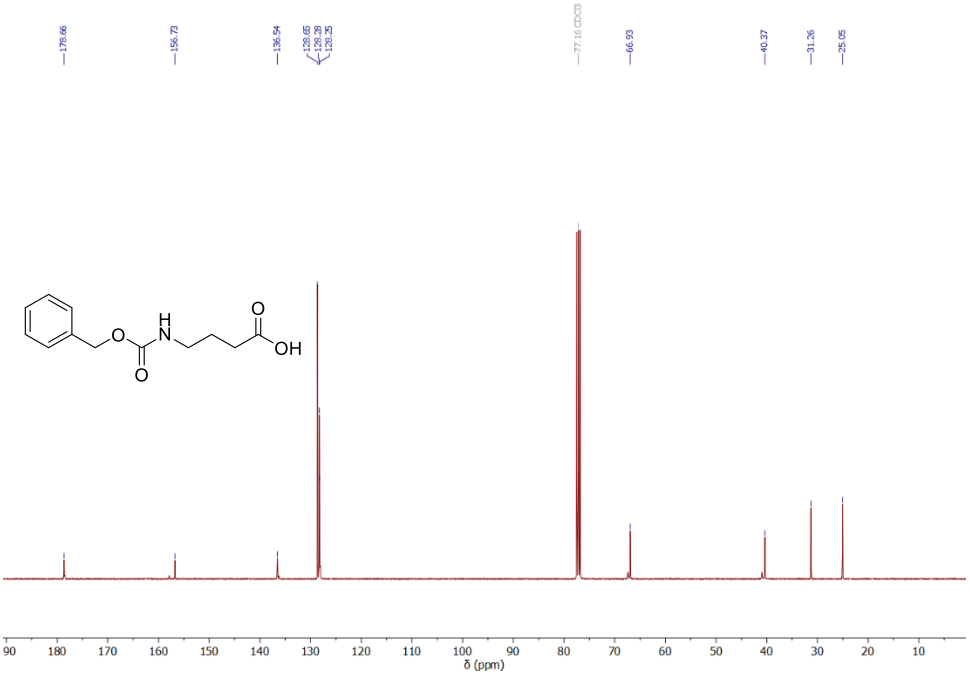

Figure S2. ^{13}C NMR spectrum of compound **4** (100 MHz, $CDCl_3$, at 25 °C).

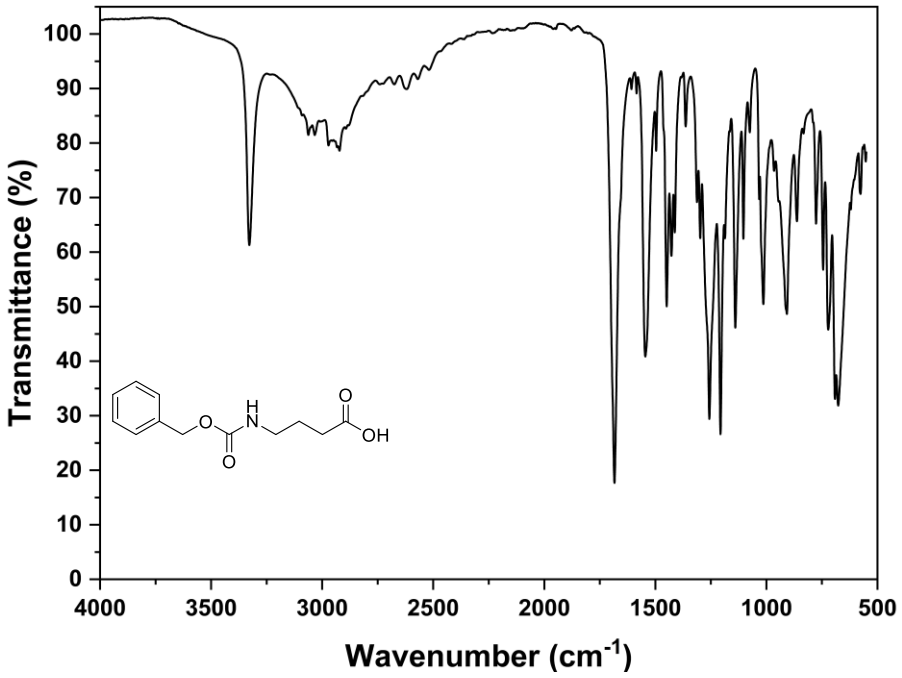

Figure S3. The FTIR spectrum of of compound **4**.

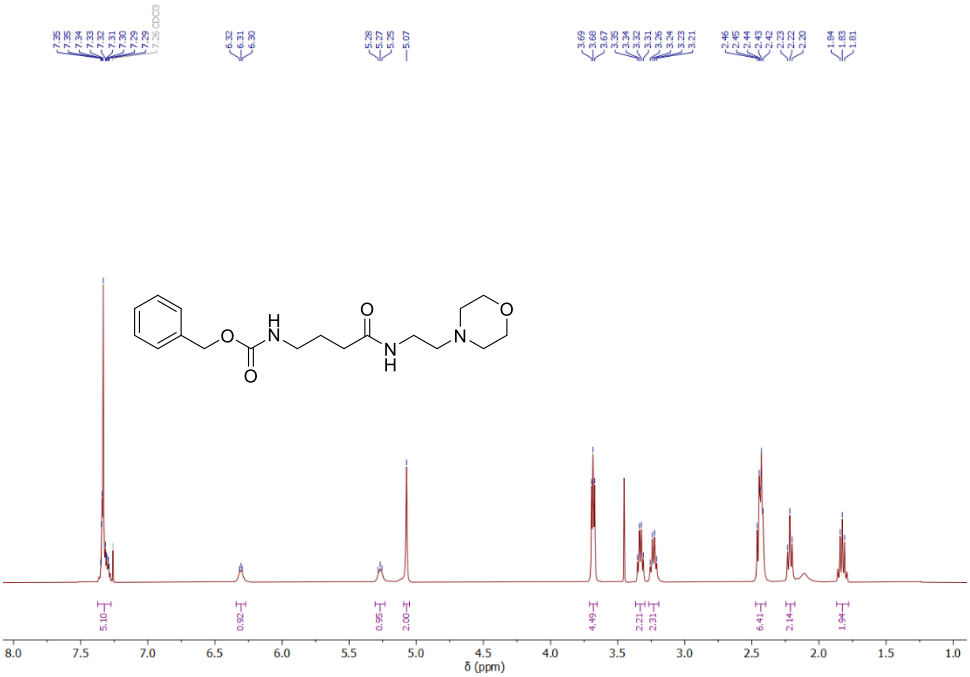

Figure S4. ^{1}H NMR spectrum of compound **5a** (400 MHz, $CDCl_3$, at 25 °C).

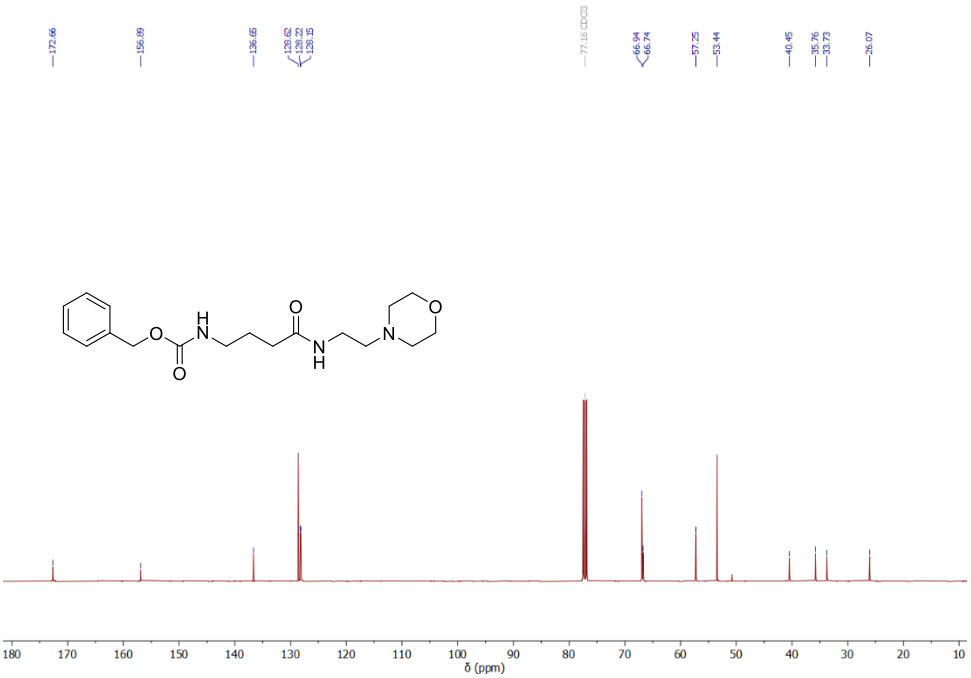

Figure S5. ^{13}C NMR spectrum of compound **5a** (100 MHz, $CDCl_3$, at 25 °C).

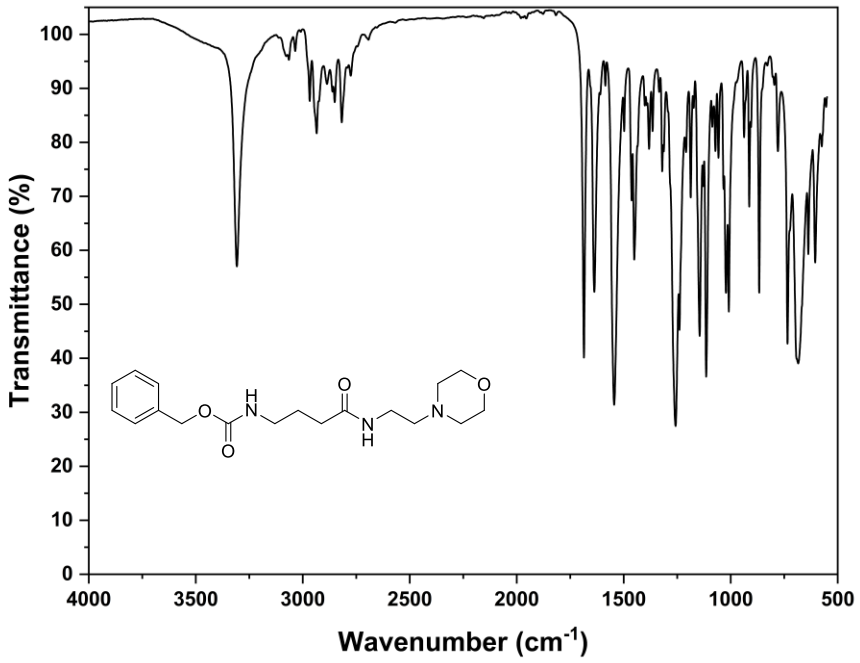

Figure S6. The FTIR spectrum of of compound **5a**.

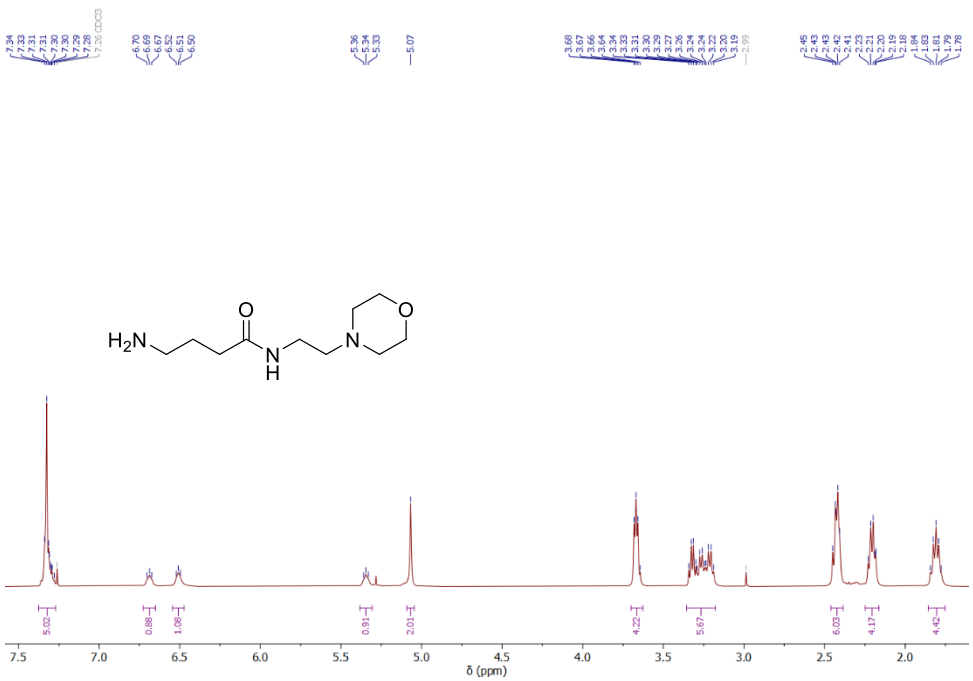

Figure S7. ^{1}H NMR spectrum of compound **6a** (400 MHz, $CDCl_3$, at 25 °C).

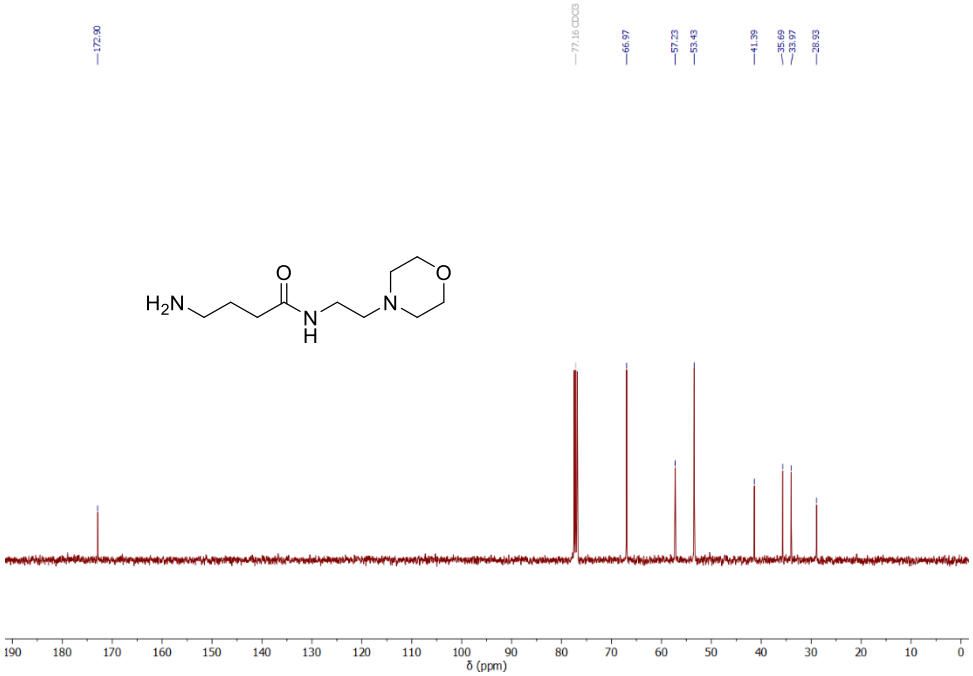

Figure S8. ^{13}C NMR spectrum of compound **6a** (100 MHz, CDCl3, at 25 °C).

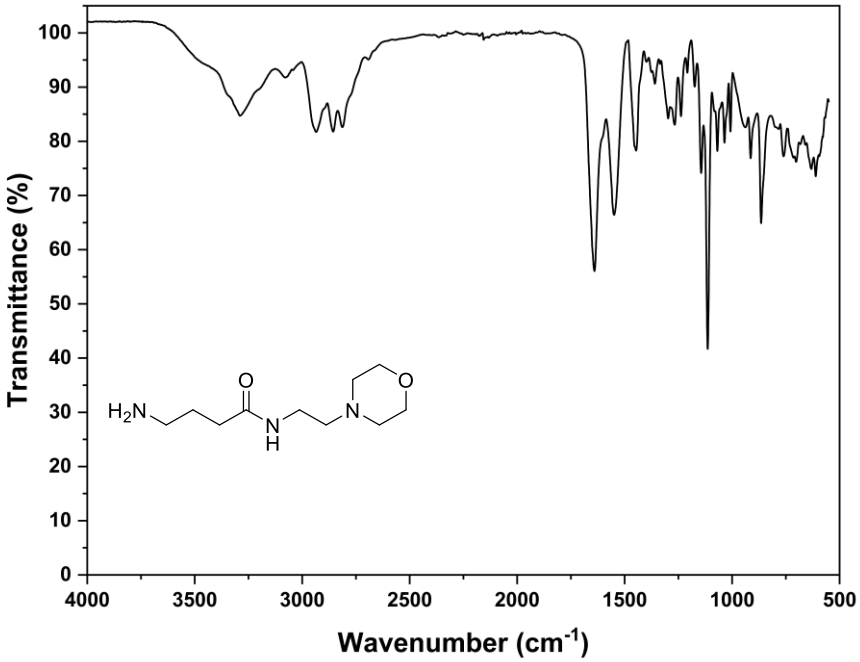

Figure S9. The FTIR spectrum of compound **6a**.

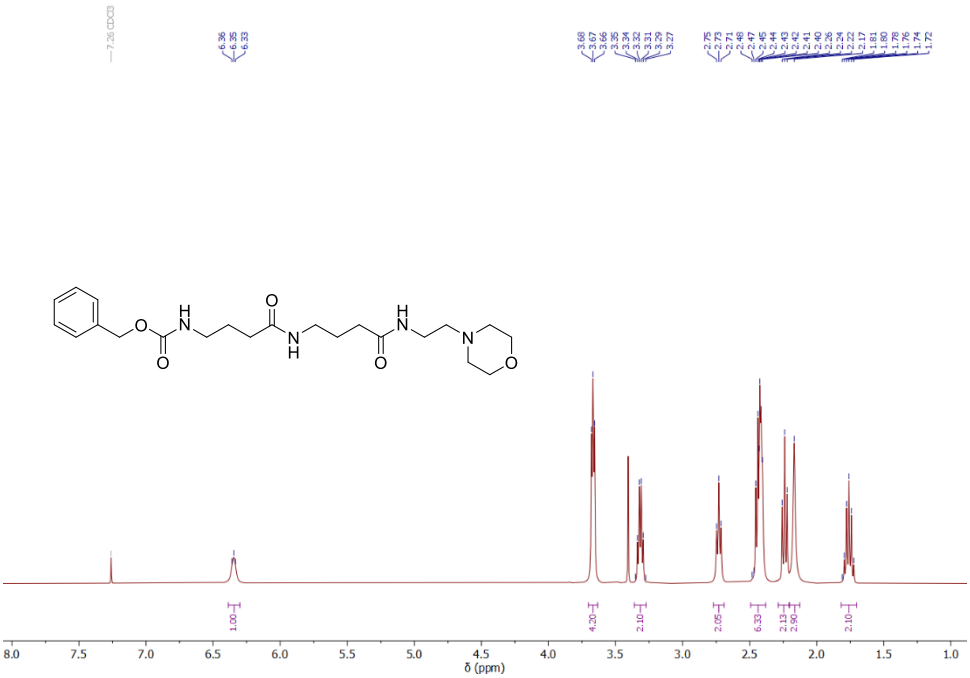

Figure S10. ^{1}H NMR spectrum of compound **5b** (400 MHz, $CDCl_3$, at 25 °C).

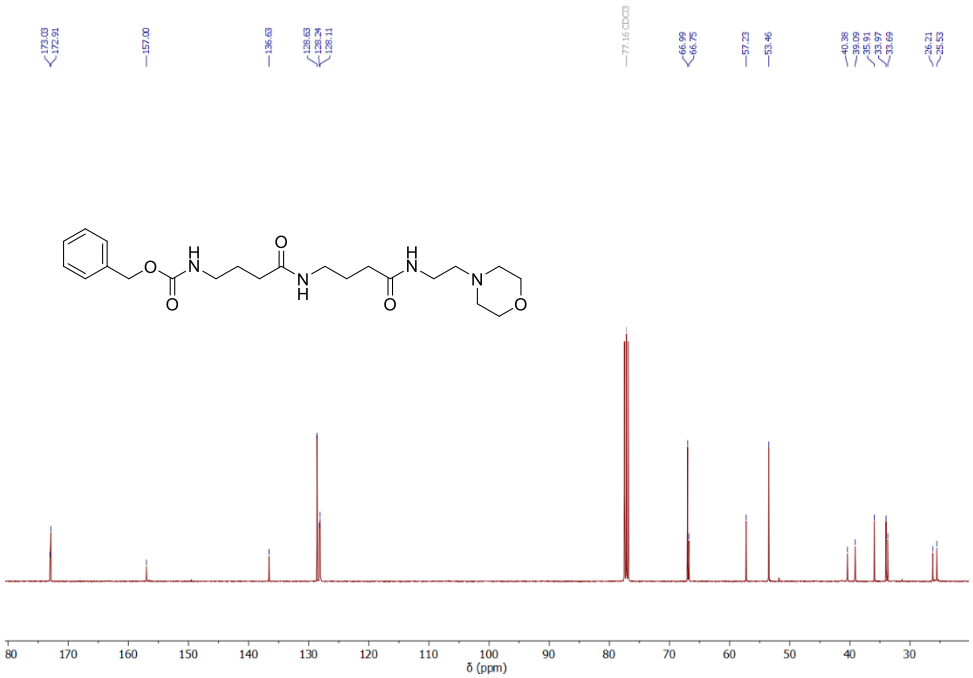

Figure S11. ^{13}C NMR spectrum of compound **5b** (100 MHz, $CDCl_3$, at 25 °C).

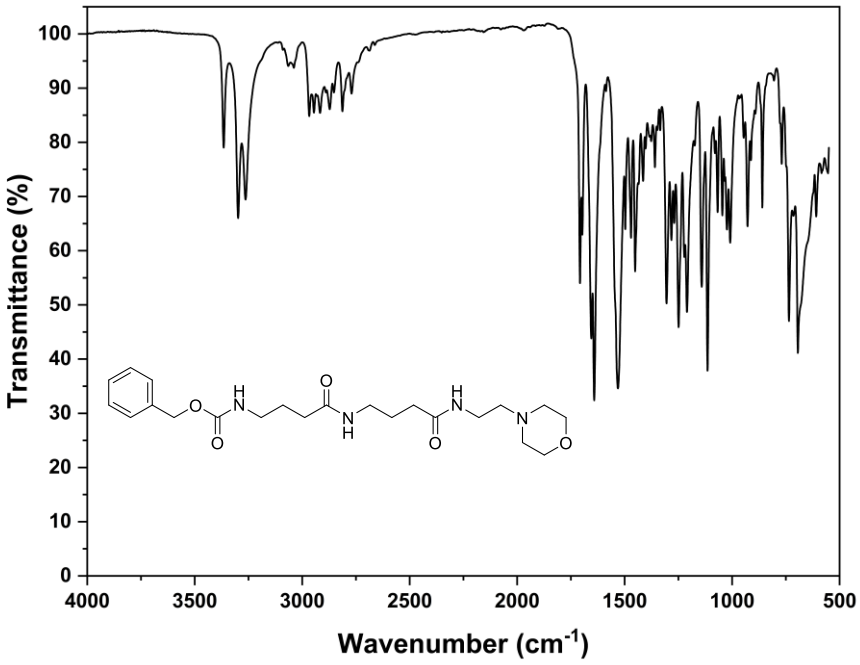

Figure S12. The FTIR spectrum of compound **5b**.

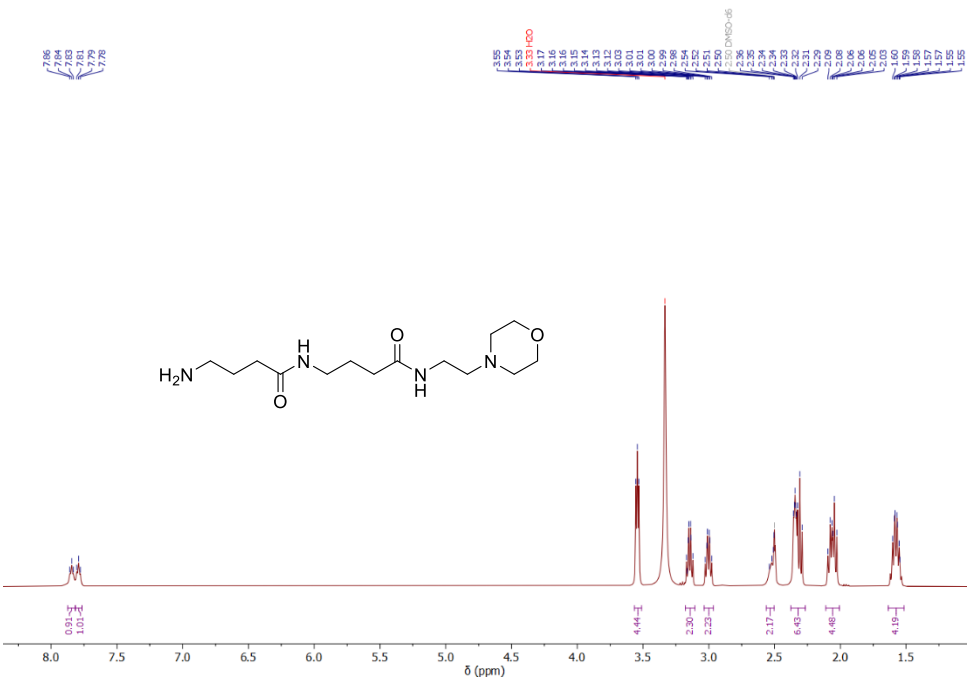

Figure S13. ^{1}H NMR spectrum of compound **6b** (400 MHz, DMSO-d_6, at 25 °C).

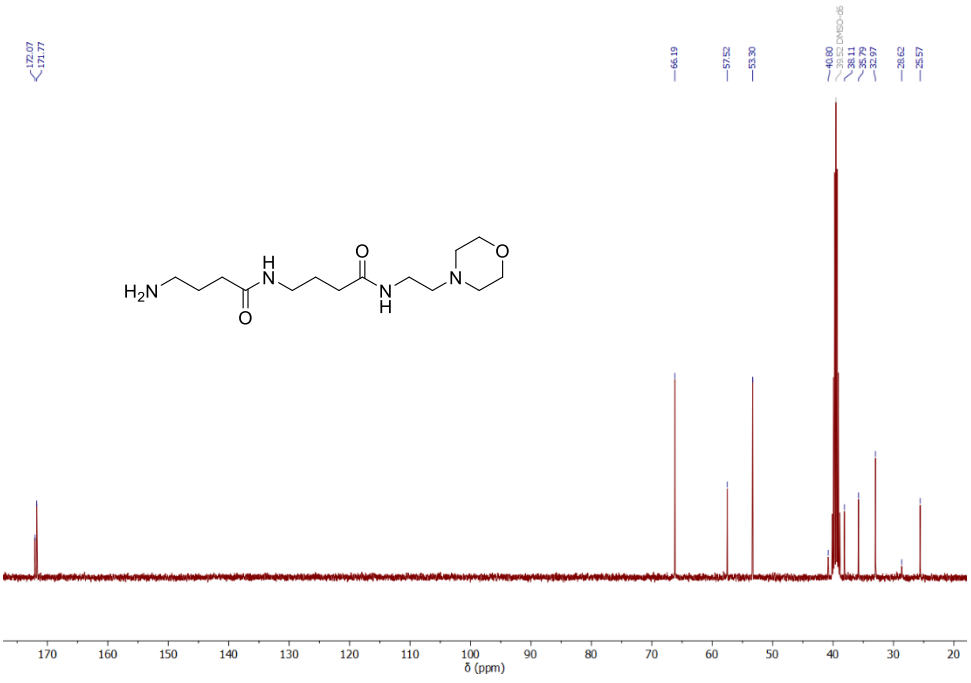

Figure S14. ^{13}C NMR spectrum of compound **6b** (100 MHz, DMSO-d_6, at 25 °C).

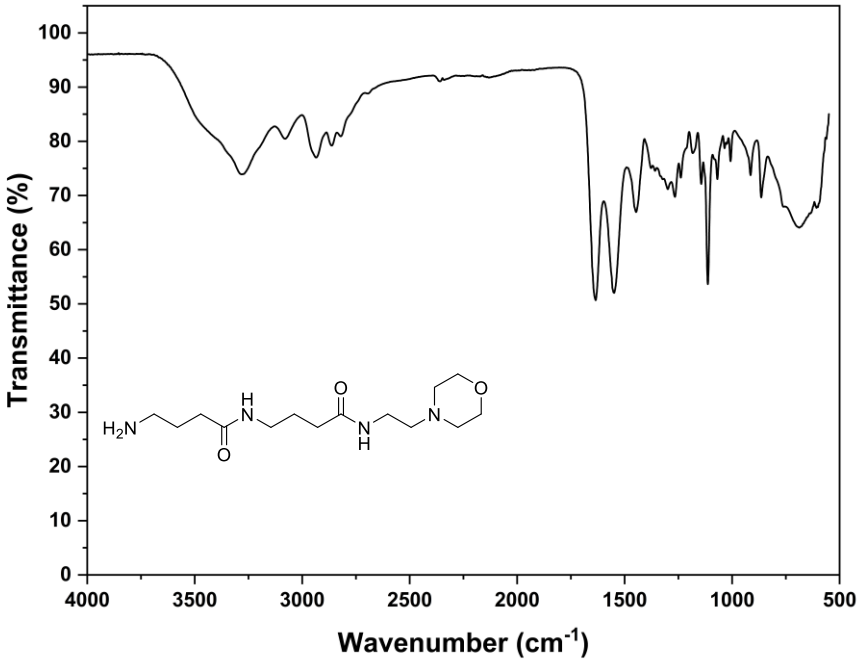

Figure S15. The FTIR spectrum of compound **6b**.

Figure S16. ^{1}H NMR spectrum of compound **5d** (400 MHz, $CDCl_3$, at 25 °C).

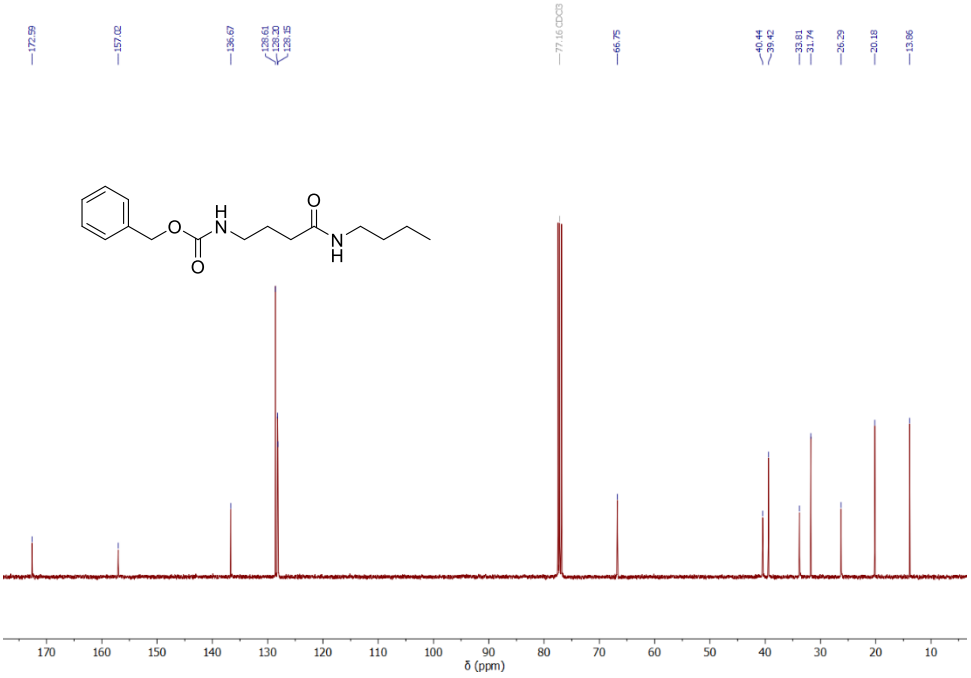

Figure S17. ^{13}C NMR spectrum of compound **5d** (100 MHz, $CDCl_3$, at 25 °C).

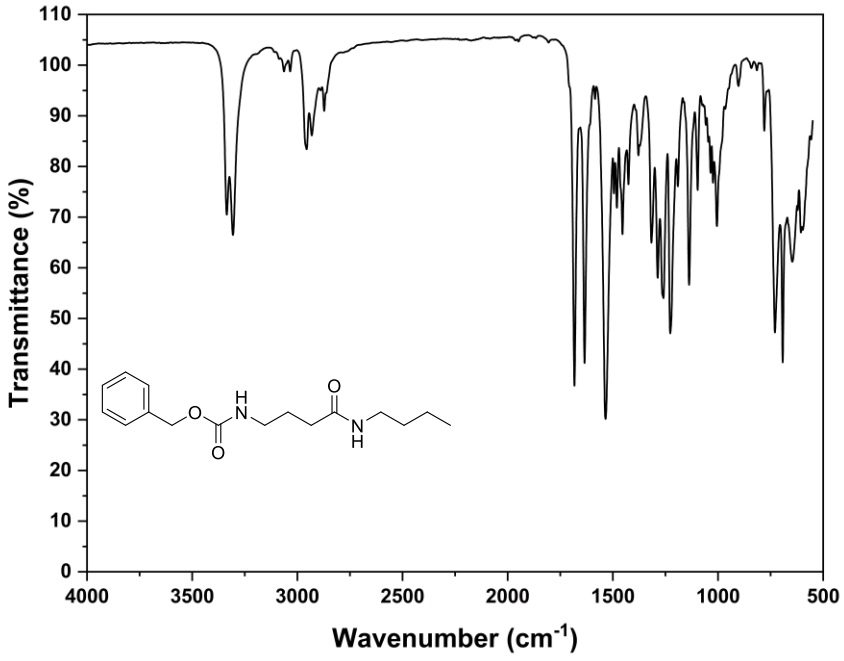

Figure S18. The FTIR spectrum of compound **5d**.

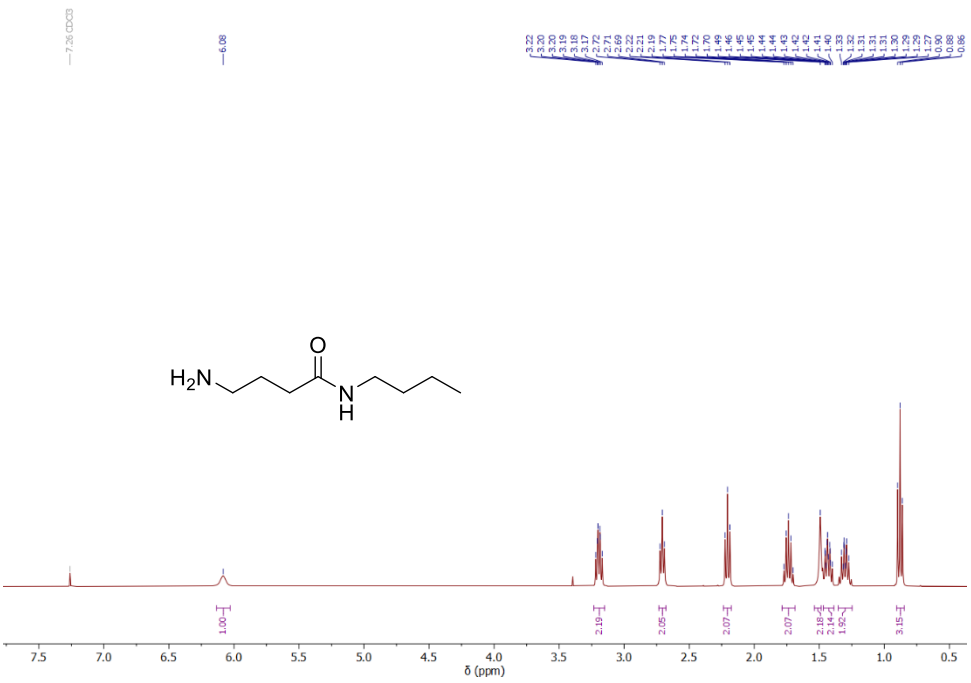

Figure S19. ^{1}H NMR spectrum of compound **6d** (400 MHz, $CDCl_3$, at 25 °C).

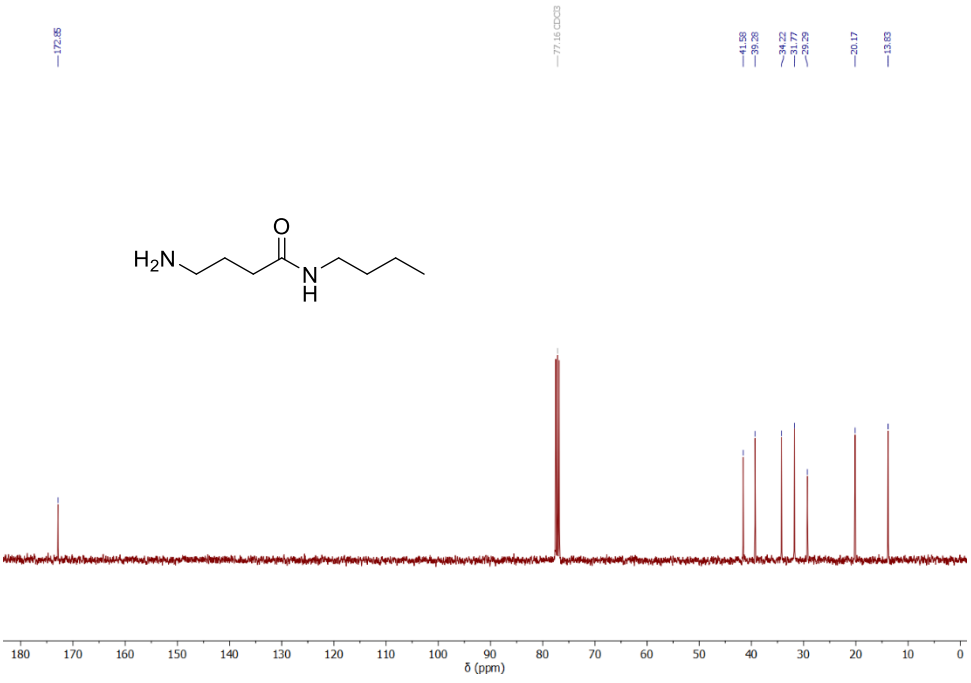

Figure S20. ^{13}C NMR spectrum of compound **6d** (100 MHz, $CDCl_3$, at 25 °C).

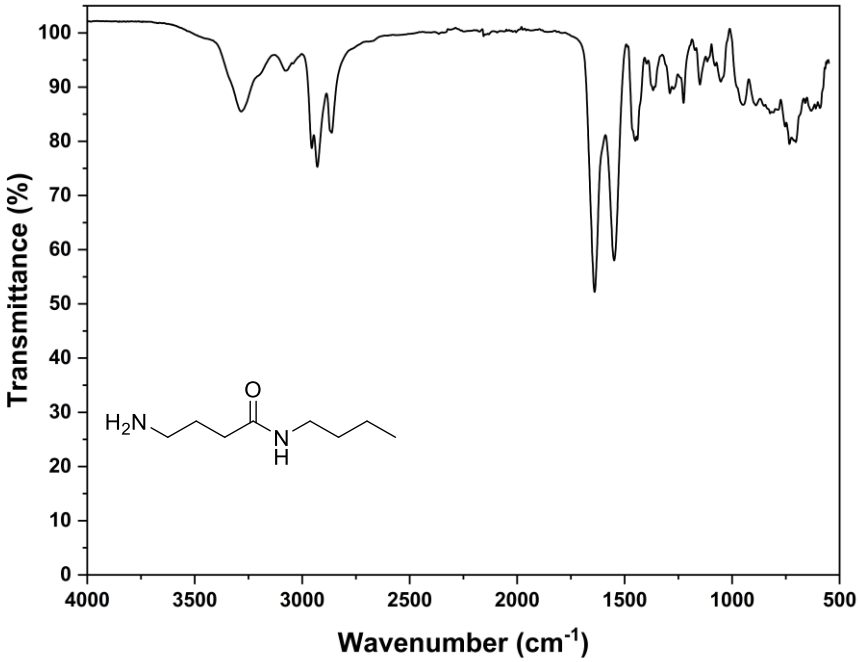

Figure S21. The FTIR spectrum of compound **6d**.

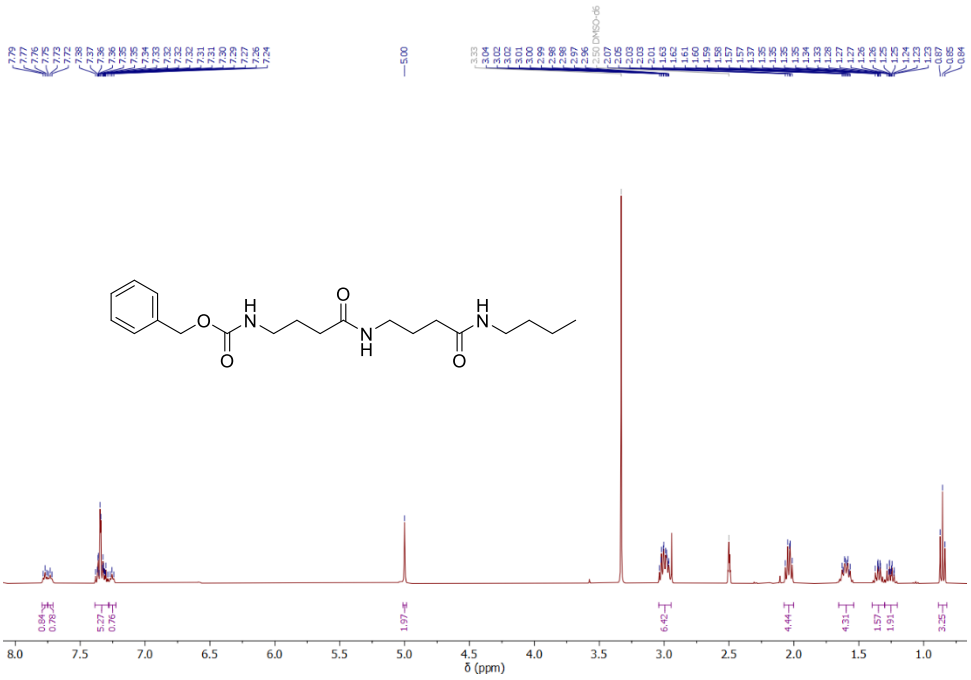

Figure S22. ^{1}H NMR spectrum of compound **5e** (400 MHz, DMSO-d_6, at 25 °C).

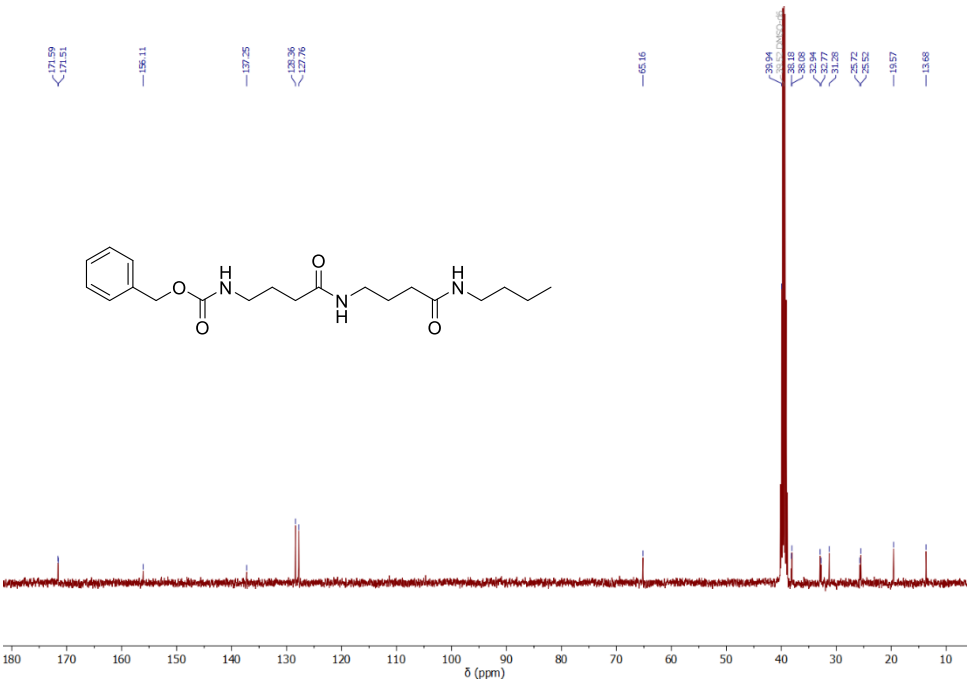

Figure S23. ^{13}C NMR spectrum of compound **5e** (100 MHz, DMSO-d_6, at 25 °C).

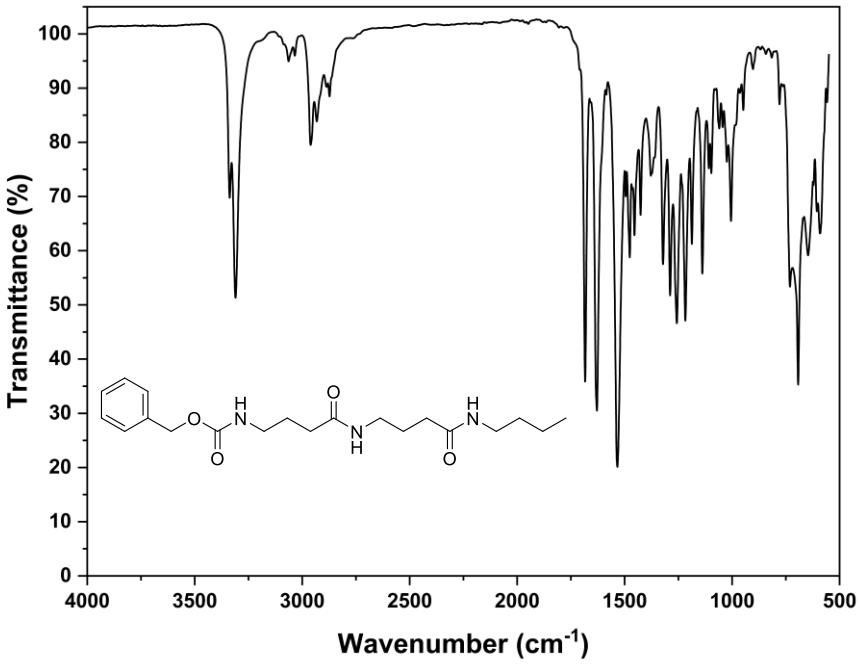

Figure S24. The FTIR spectrum of compound **5e**.

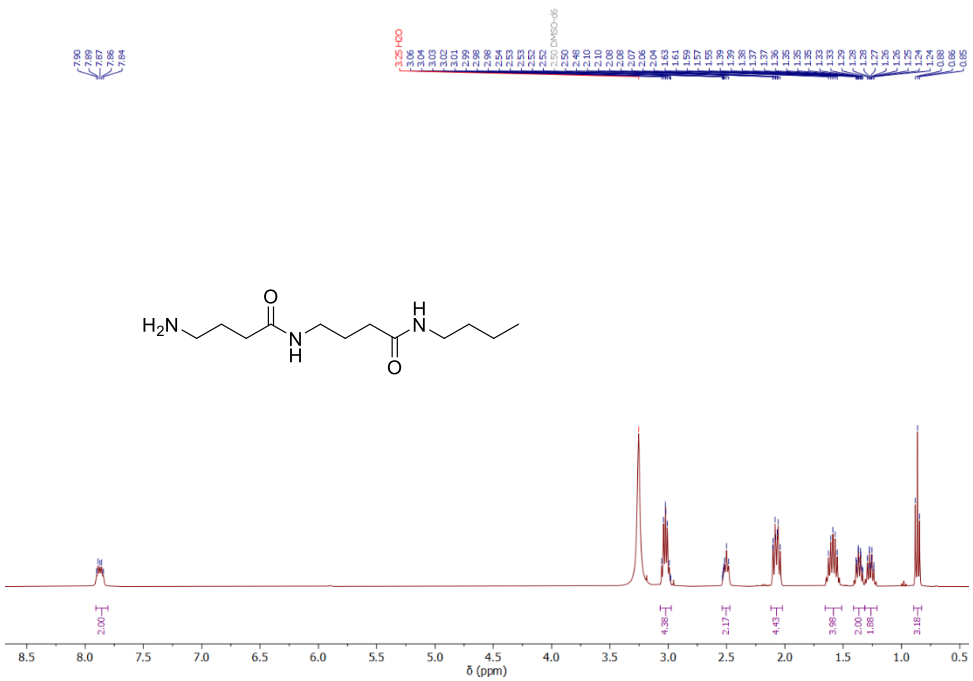

Figure S25. ^{1}H NMR spectrum of compound **6e** (400 MHz, DMSO-d_6, at 25 °C).

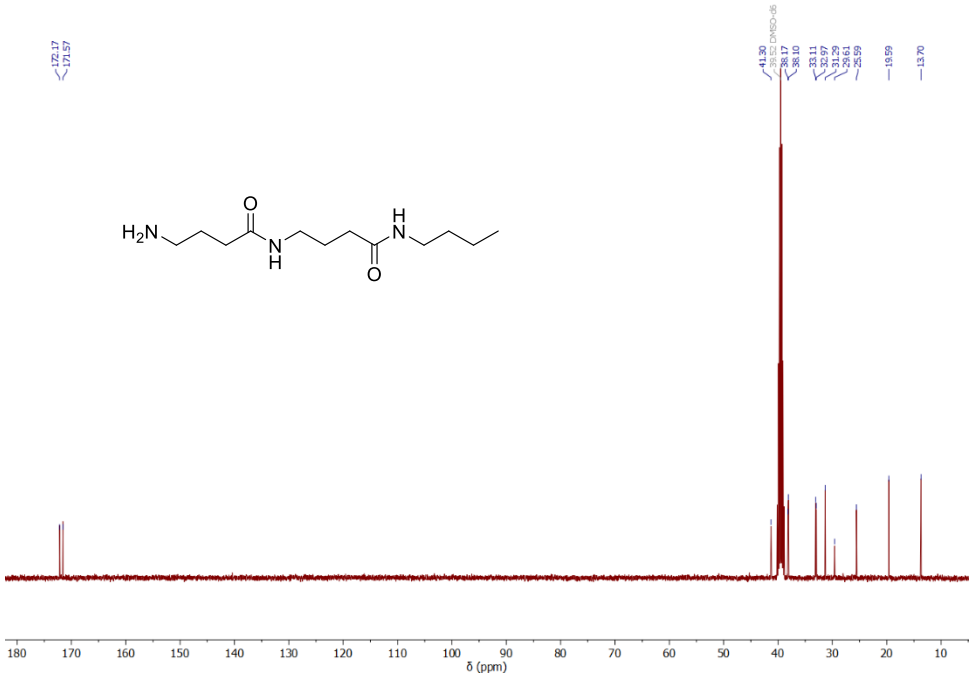

Figure S26. ^{13}C NMR spectrum of compound **6e** (100 MHz, DMSO-d_6, at 25 °C).

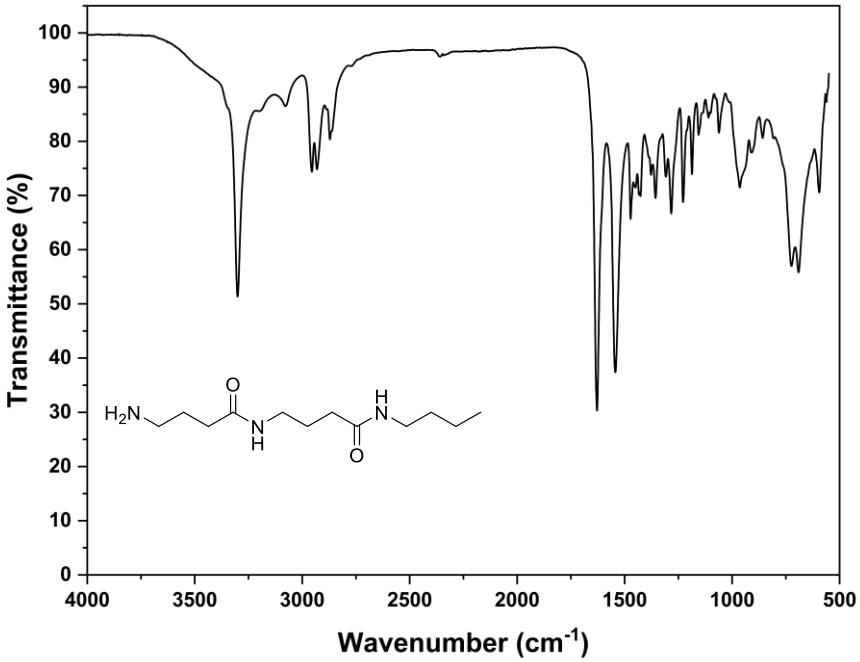

Figure S27. The FTIR spectrum of compound **6e**.

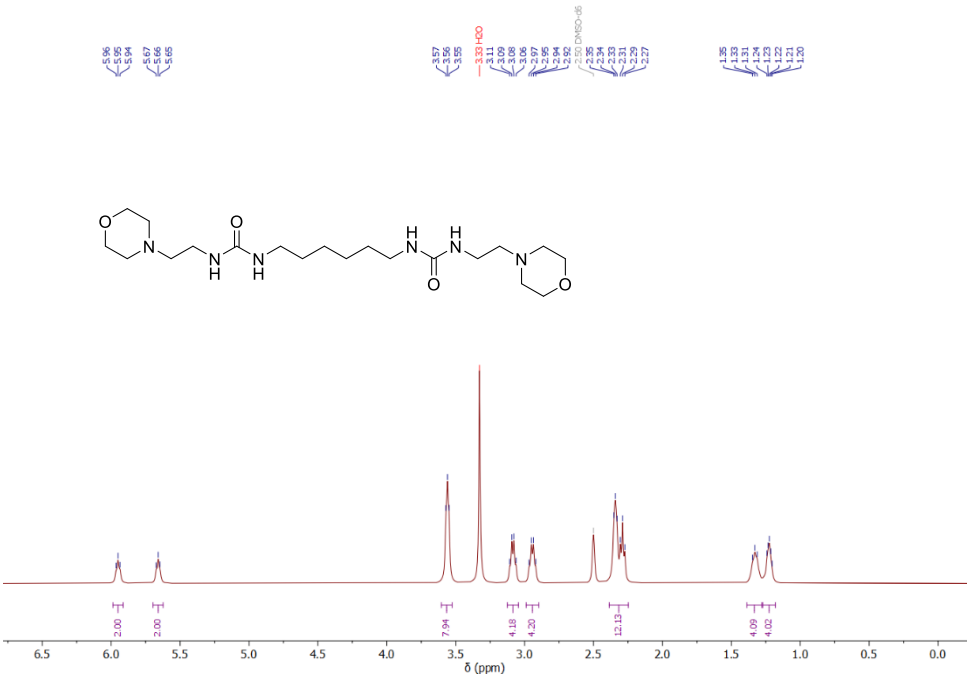

Figure S28. ^{1}H NMR spectrum of compound **1a** (400 MHz, DMSO-d_6, at 25 °C).

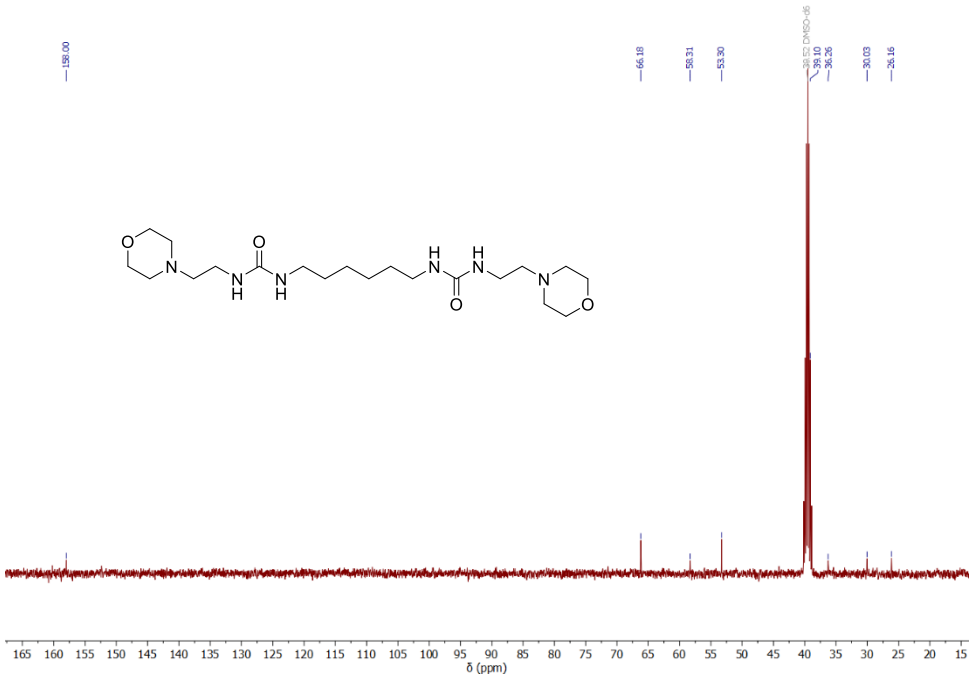

Figure S29. ^{13}C NMR spectrum of compound **1a** (100 MHz, DMSO-d_6, at 25 °C).

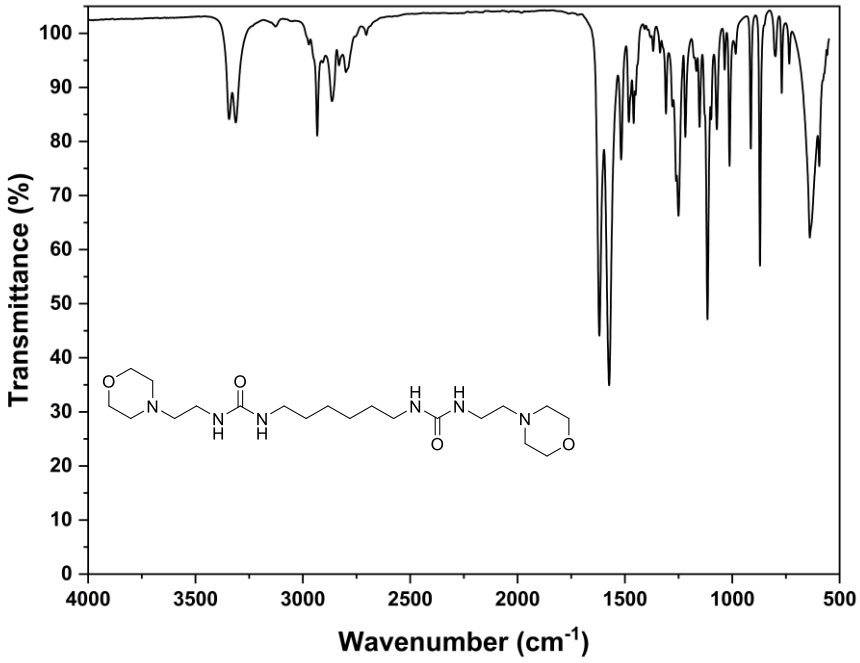

Figure S30. The FTIR spectrum of compound **1a**.

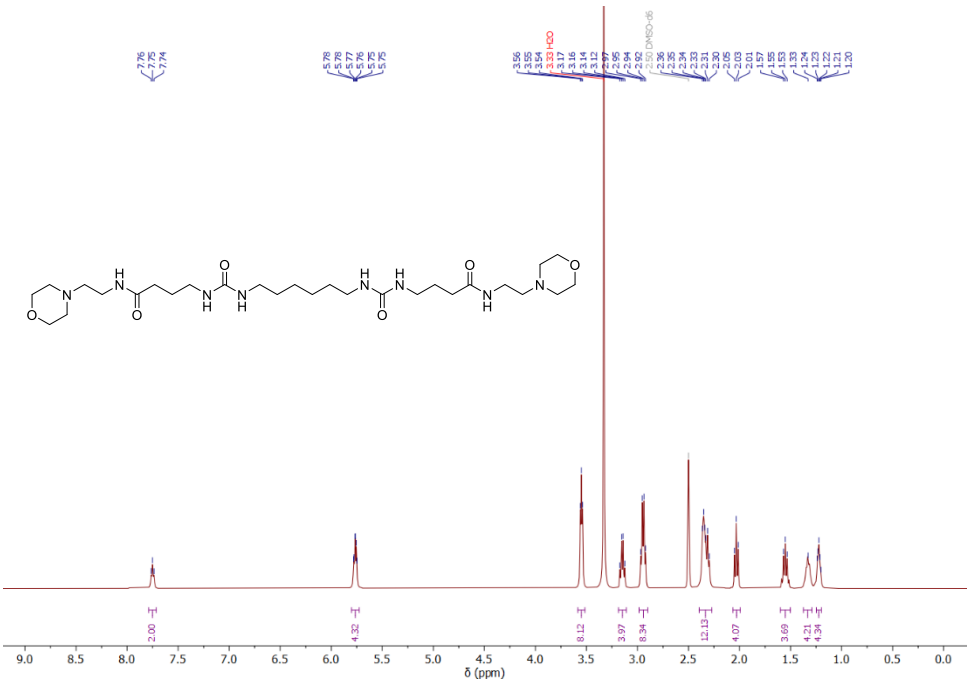

Figure S31. ^{1}H NMR spectrum of compound **1b** (400 MHz, DMSO-d_6, at 25 °C).

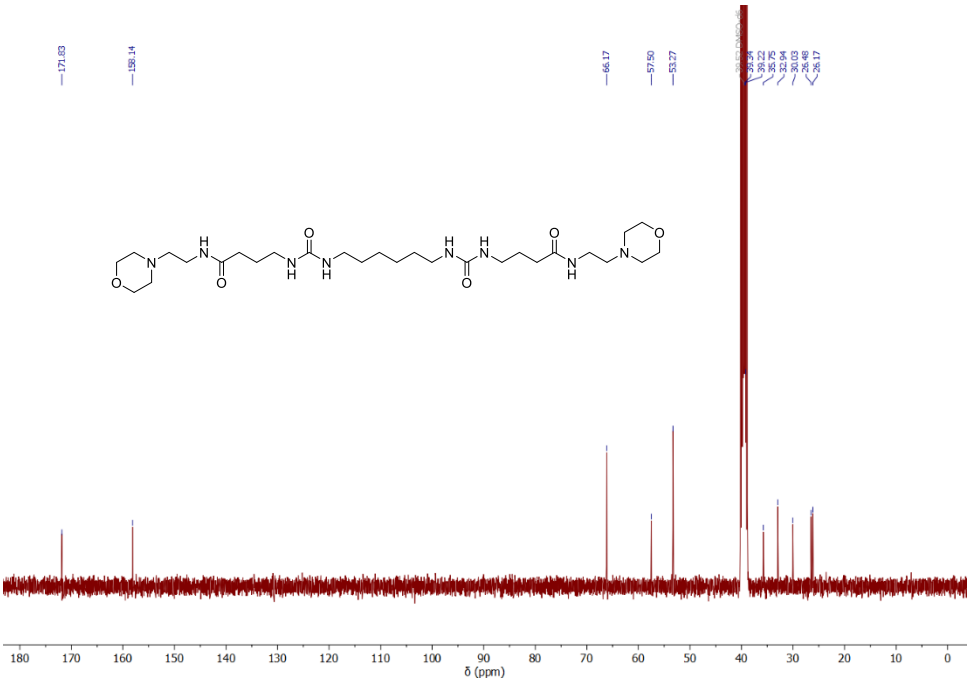

Figure S32. ^{13}C NMR spectrum of compound **1b** (100 MHz, DMSO-d_6, at 25 °C).

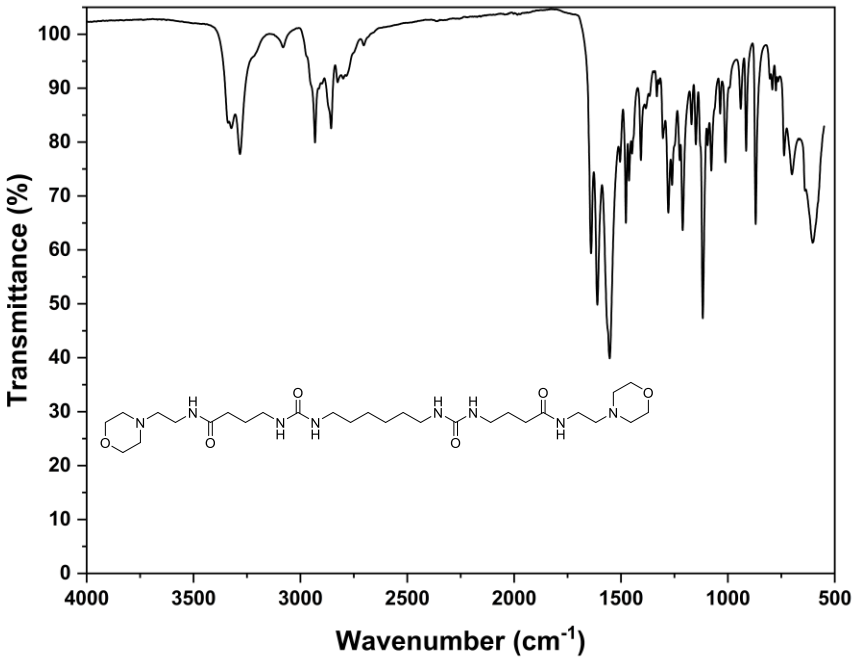

Figure S33. The FTIR spectrum of compound **1b**.

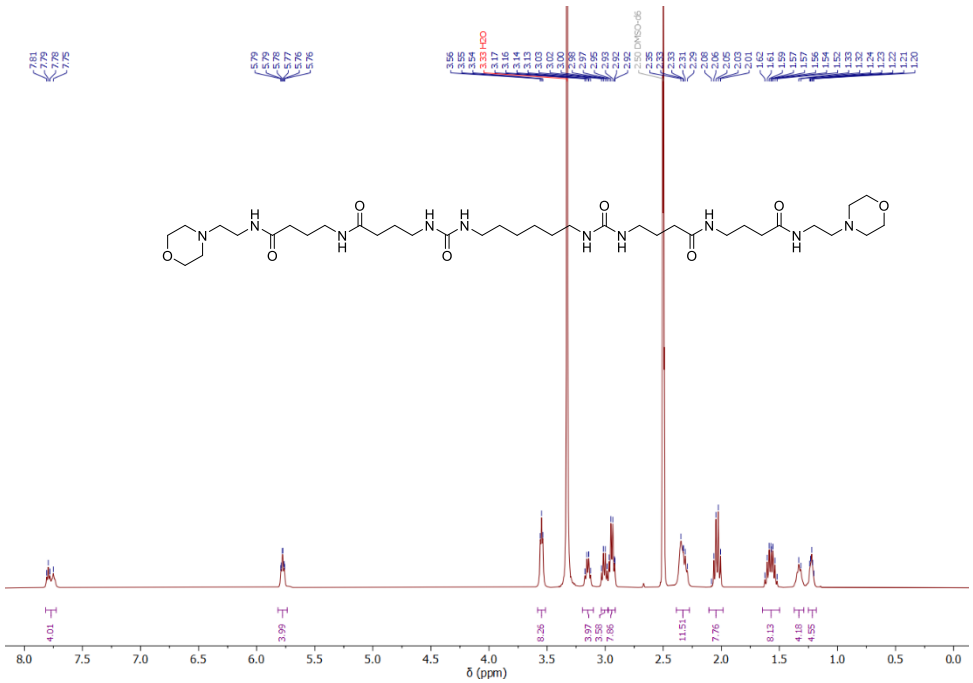

Figure S34. ^{1}H NMR spectrum of compound **1c** (400 MHz, DMSO-d_6, at 25 °C).

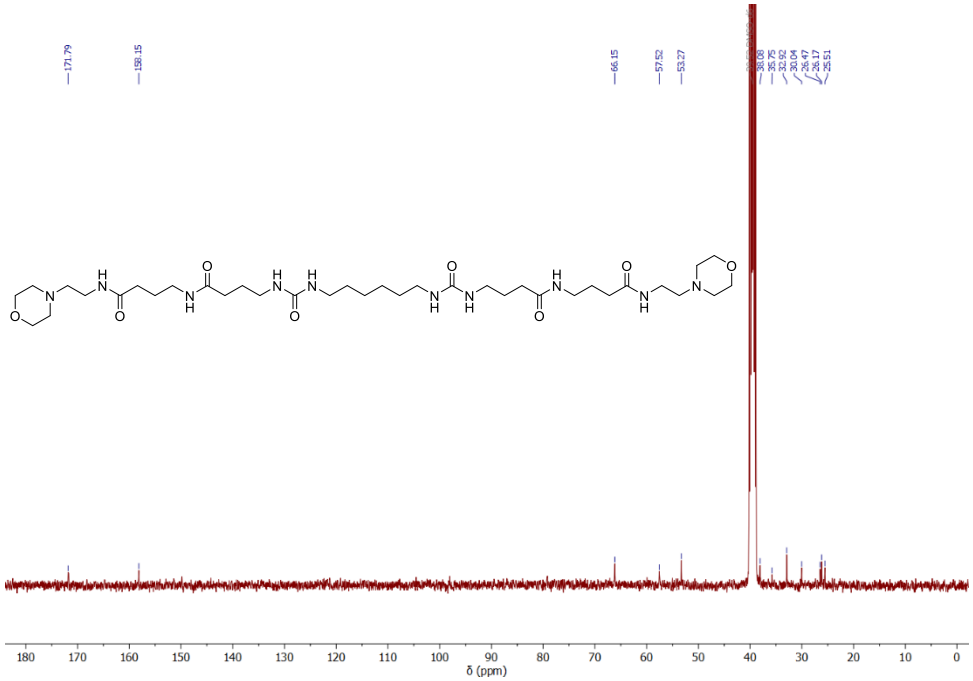

Figure S35. ^{13}C NMR spectrum of compound **1c** (100 MHz, DMSO-d_6, at 25 °C).

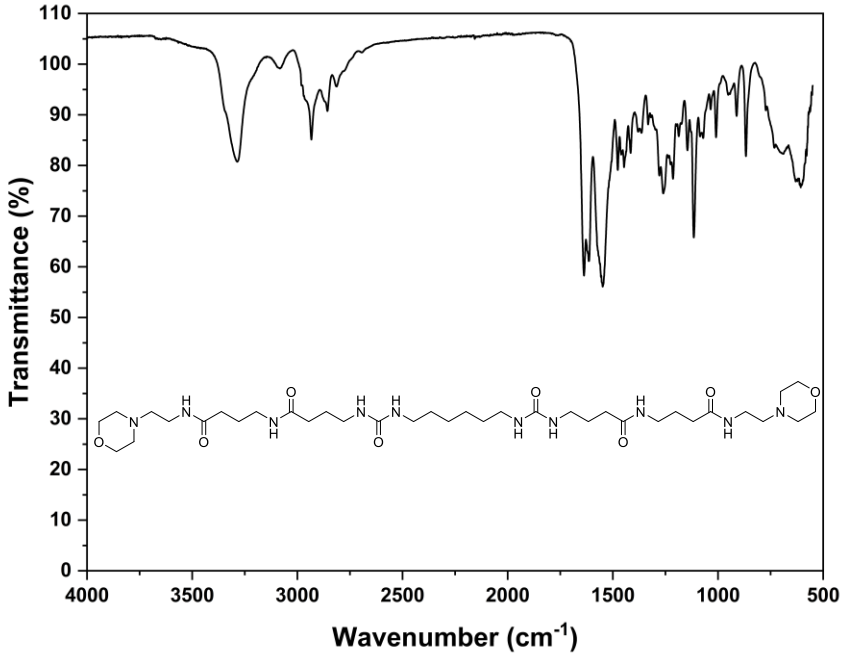

Figure S36. The FTIR spectrum of compound **1c**.

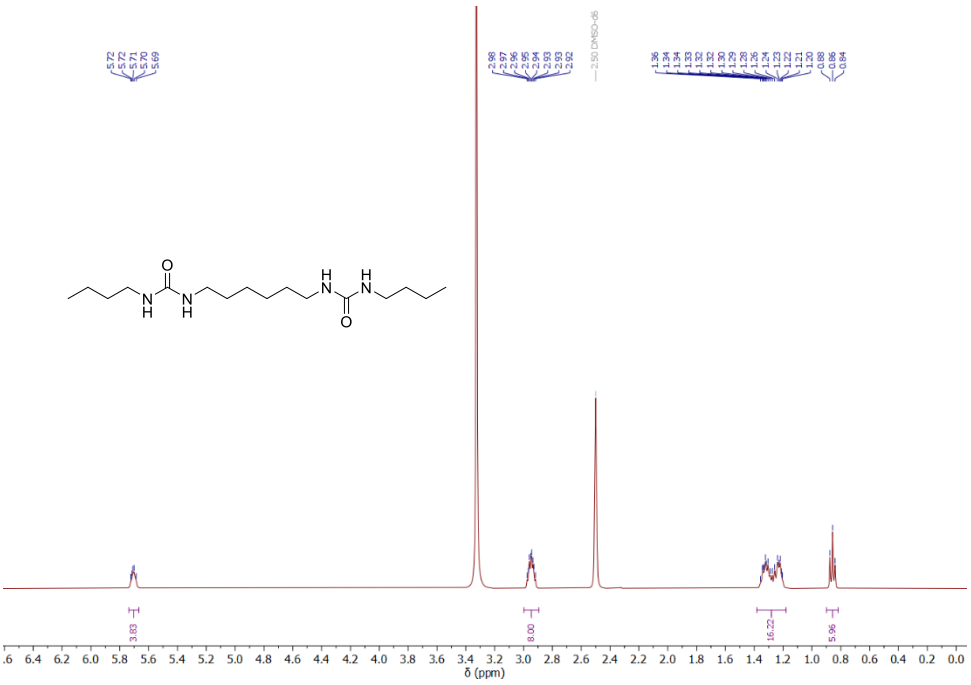

Figure S37. ^{1}H NMR spectrum of compound **1d** (400 MHz, DMSO-d_6, at 25 °C).

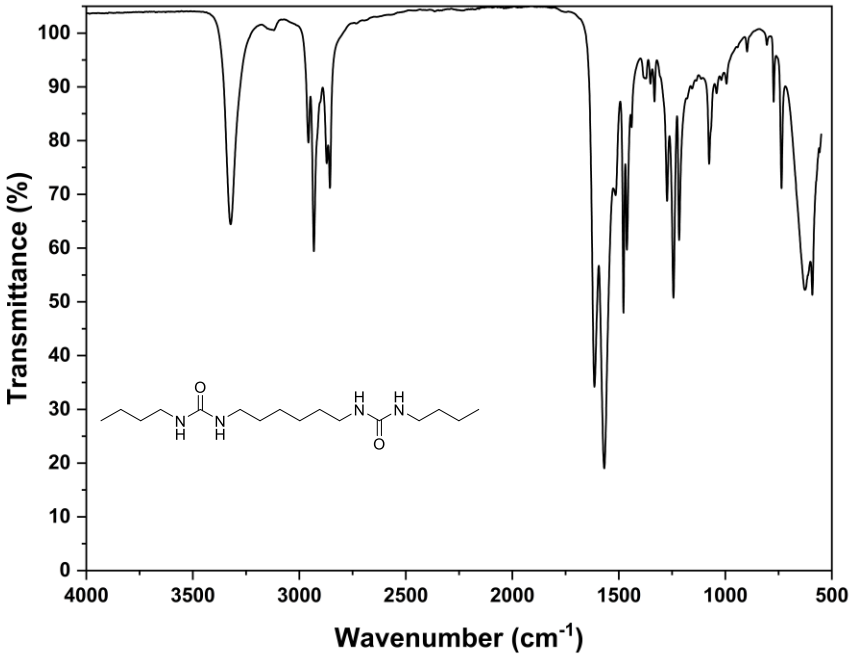

Figure S38. The FTIR spectrum of compound **1d**.

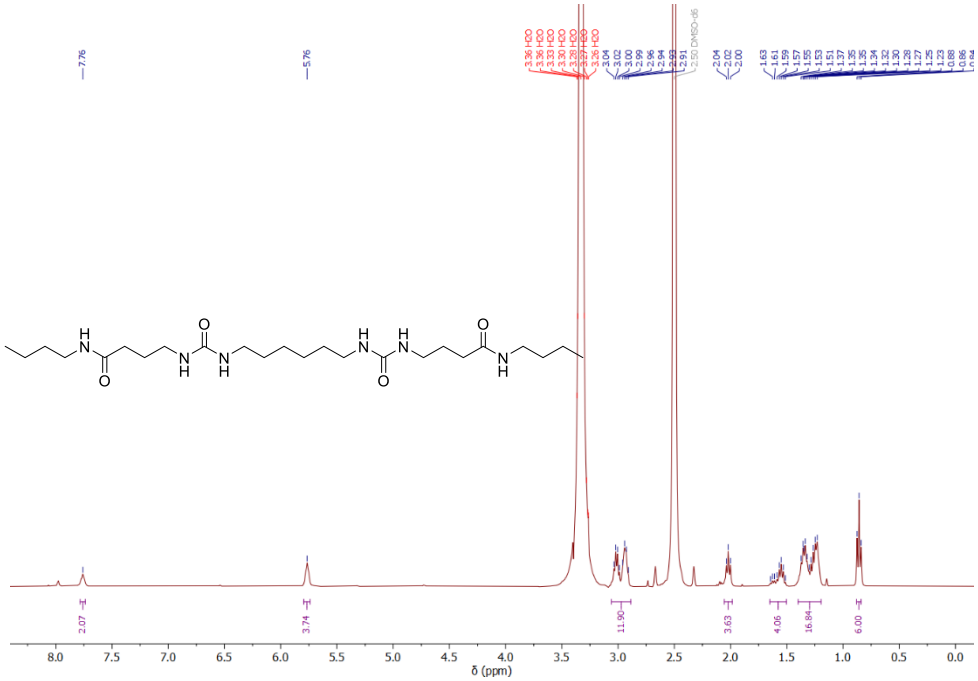

Figure S39. ^{1}H NMR spectrum of compound **1e** (400 MHz, DMSO-d_6, at 25 °C).

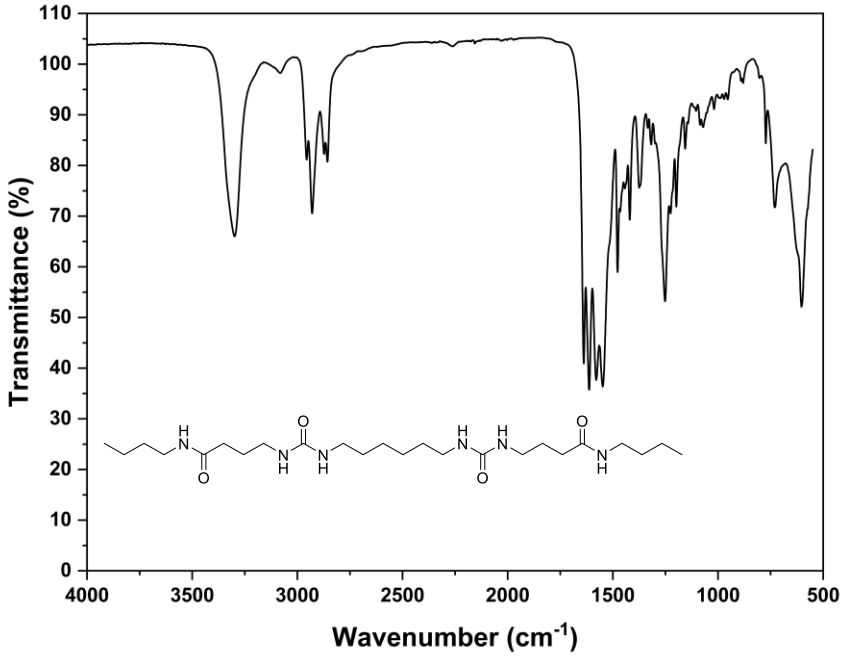

Figure S40. The FTIR spectrum of compound **1e**.

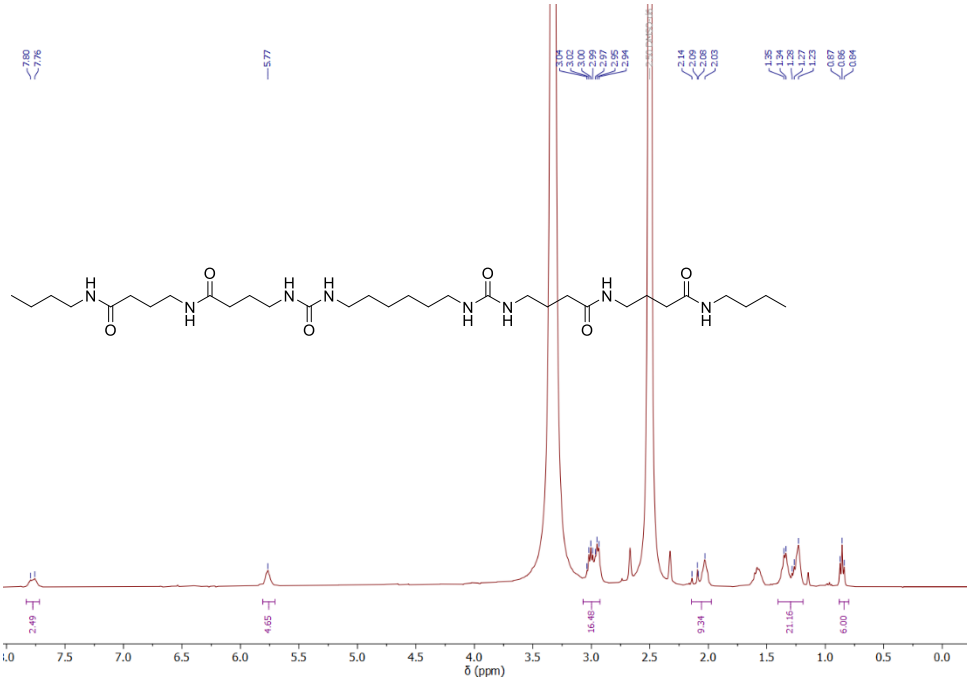

Figure S41. ^{1}H NMR spectrum of compound **1f** (400 MHz, DMSO-*d*$_6$, at 25 °C).

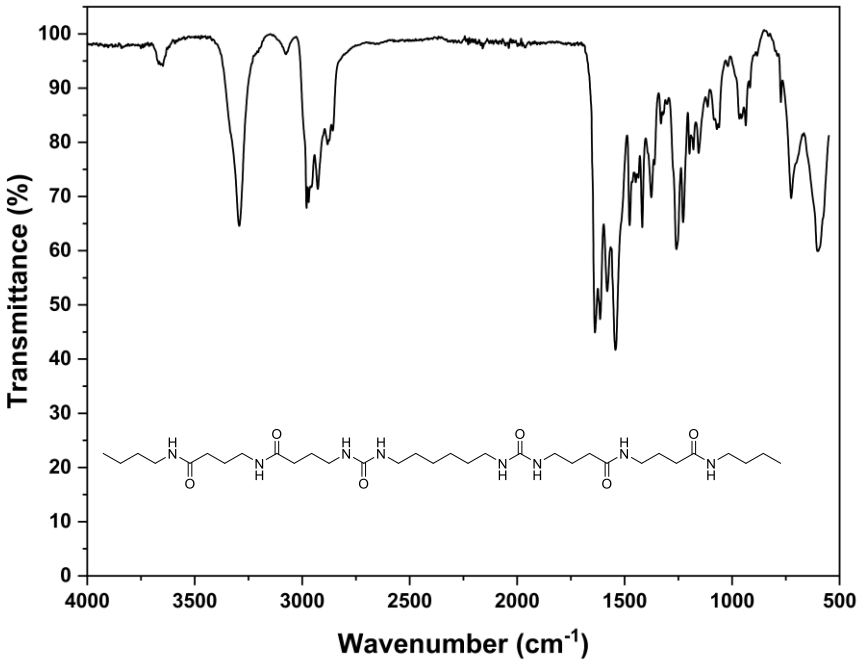

Figure S42. The FTIR spectrum of compound **1f**.

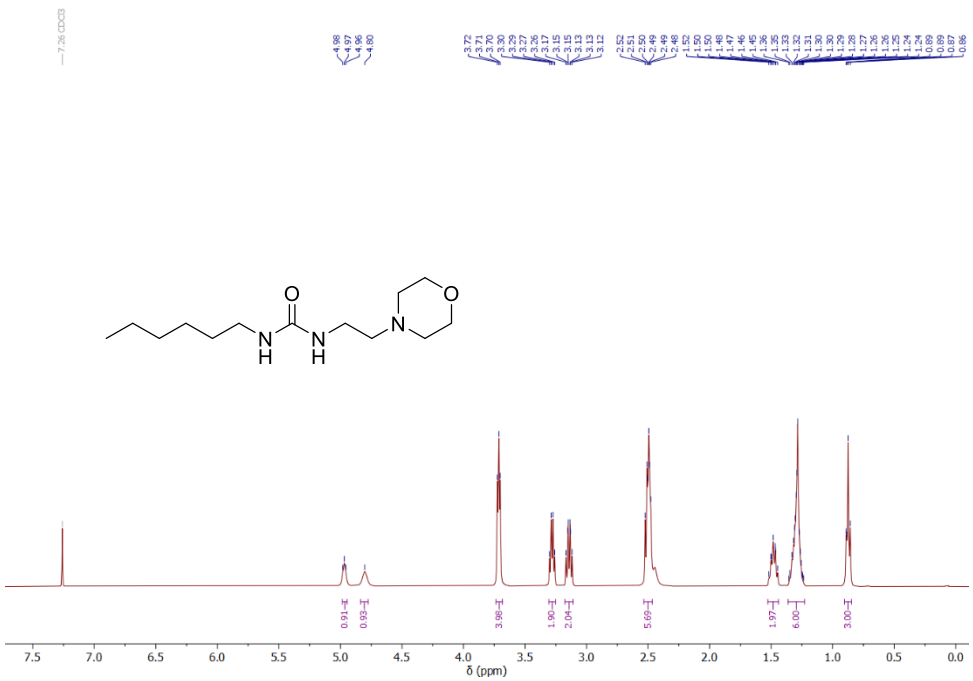

Figure S43. ^{1}H NMR spectrum of compound **2a** (400 MHz, $CDCl_3$, at 25 °C).

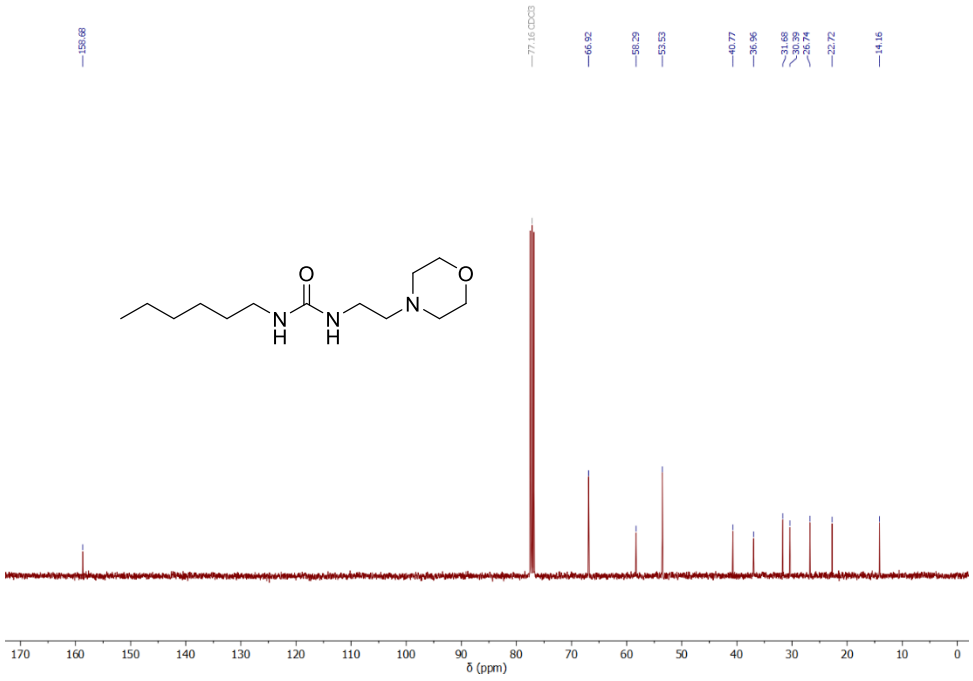

Figure S44. ^{13}C NMR spectrum of compound **2a** (100 MHz, $CDCl_3$, at 25 °C).

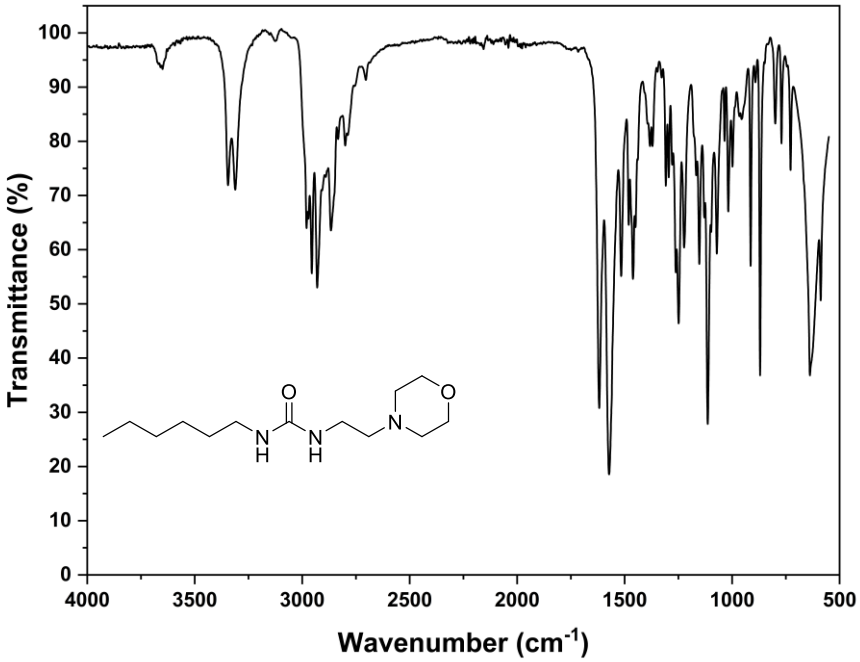

Figure S45. The FTIR spectrum of compound **2a**.

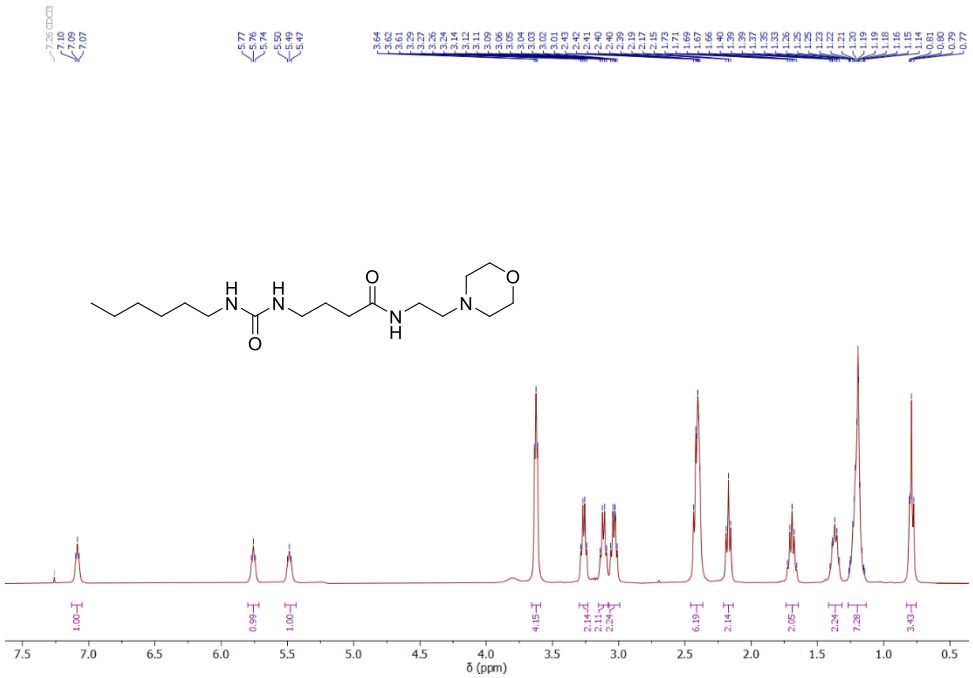

Figure S46. ^{1}H NMR spectrum of compound **2b** (400 MHz, $CDCl_3$, at 25 °C).

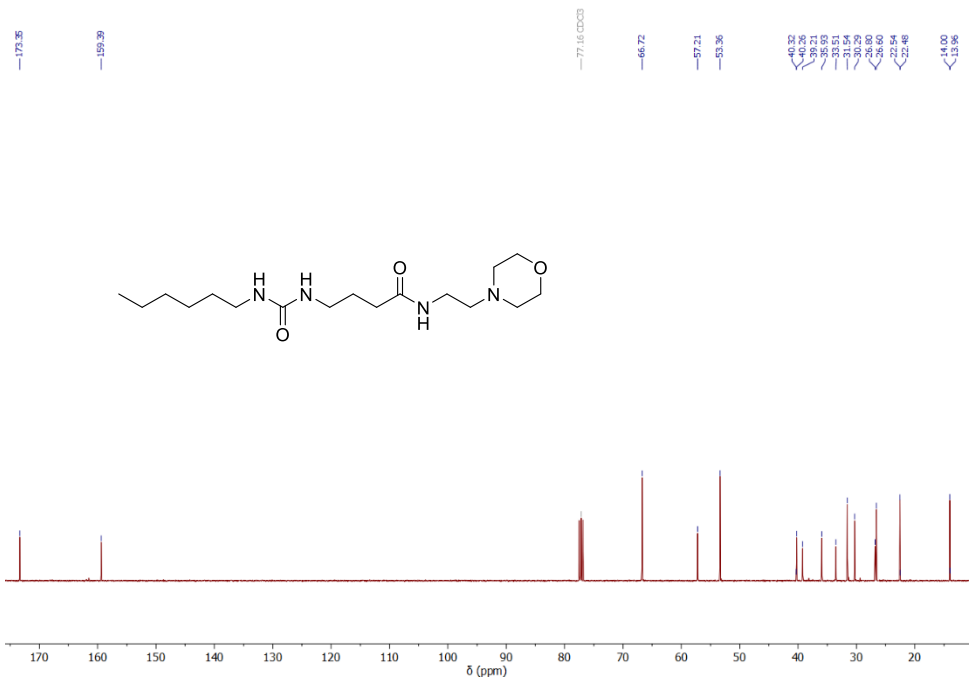

Figure S47. ^{13}C NMR spectrum of compound **2b** (100 MHz, $CDCl_3$, at 25 °C).

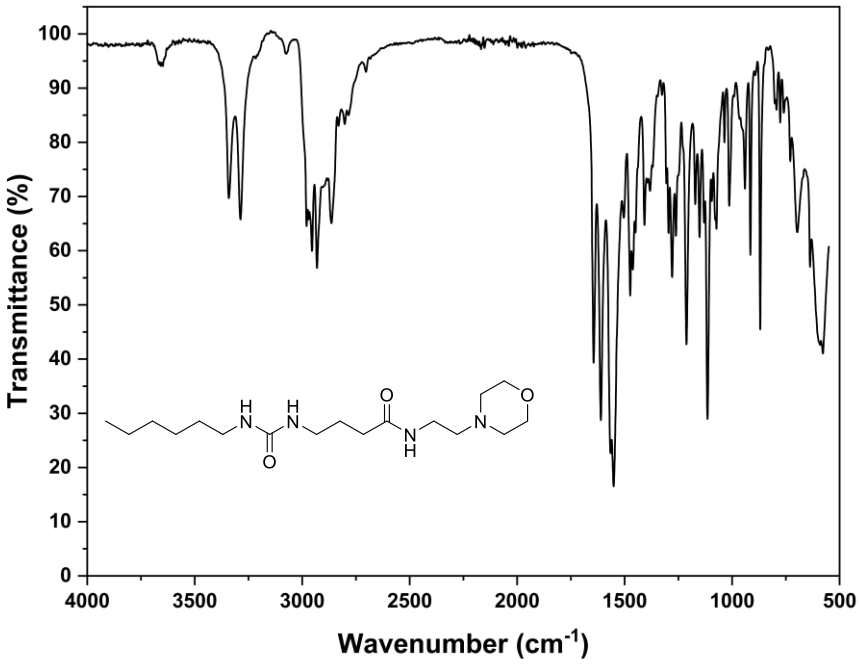

Figure S48. The FTIR spectrum of compound **2b**.

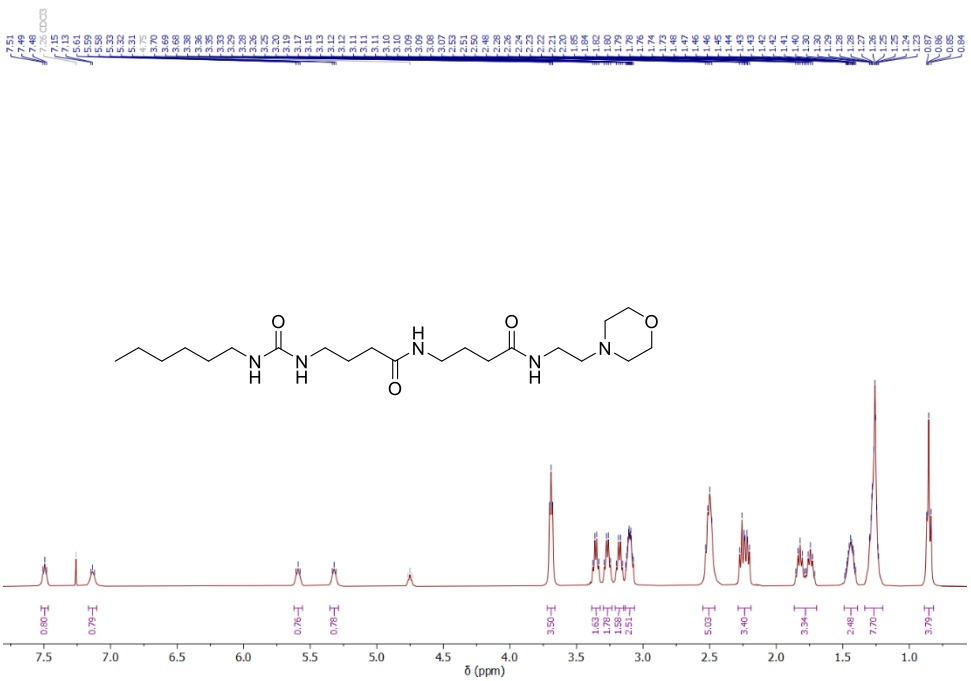

Figure S49. ^{1}H NMR spectrum of compound **2c** (400 MHz, $CDCl_3$, at 25 °C).

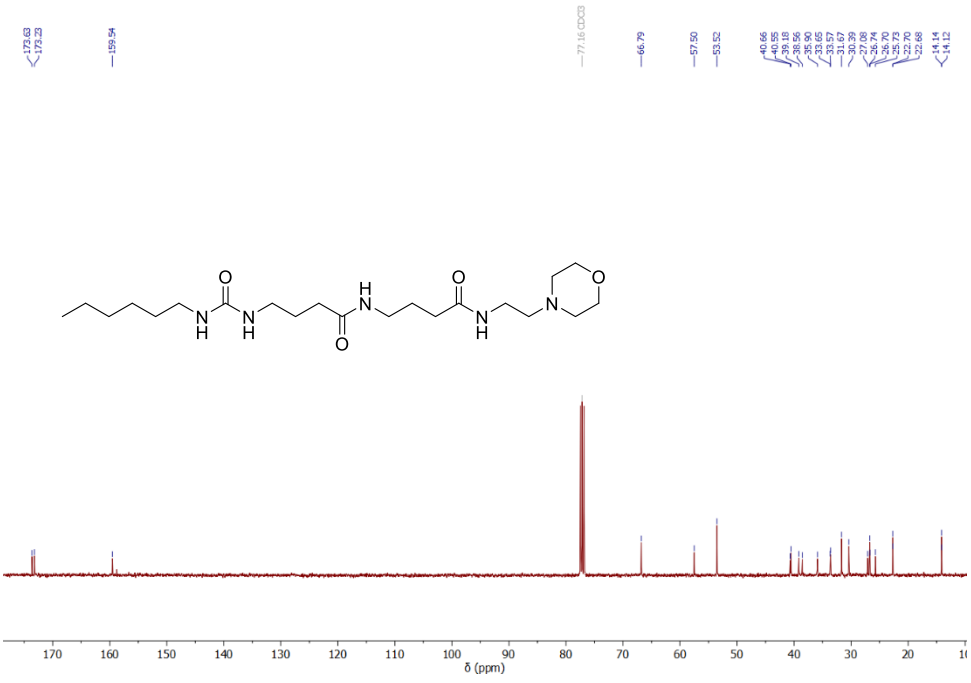

Figure S50. ^{13}C NMR spectrum of compound **2c** (100 MHz, $CDCl_3$, at 25 °C).

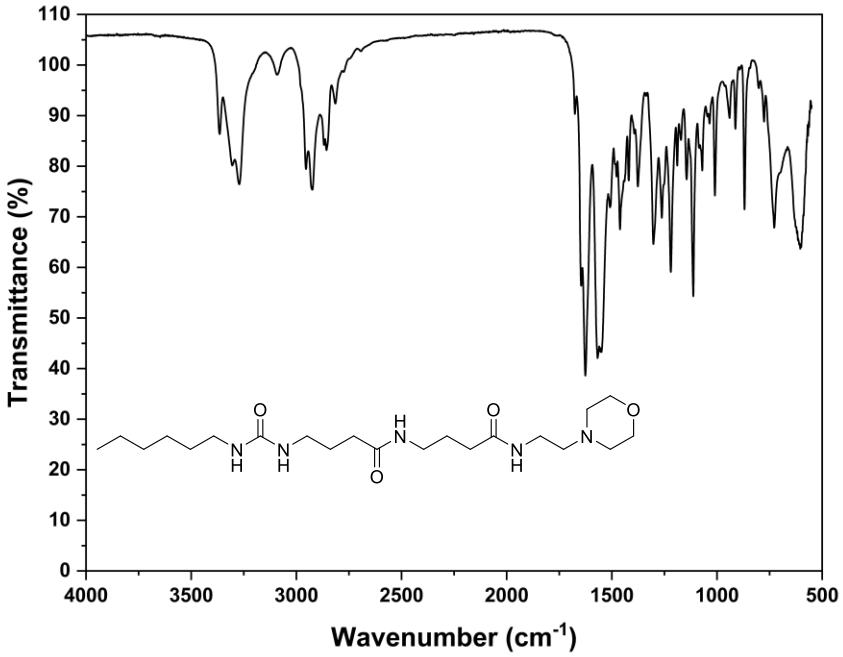

Figure S51. The FTIR spectrum of compound **2c**.

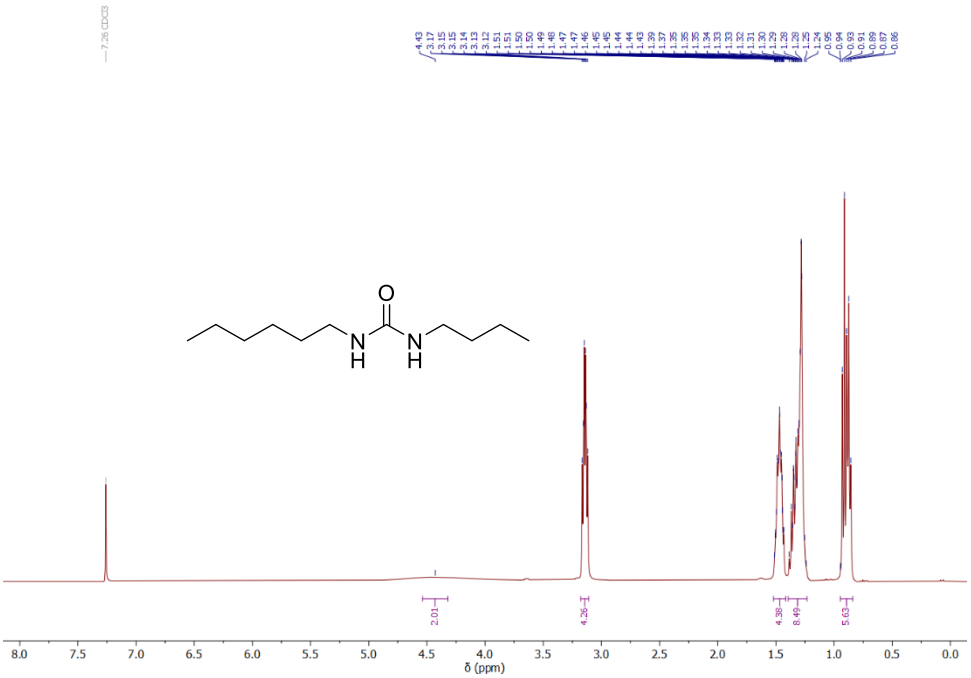

Figure S52. ^{1}H NMR spectrum of compound **2d** (400 MHz, $CDCl_3$, at 25 °C).

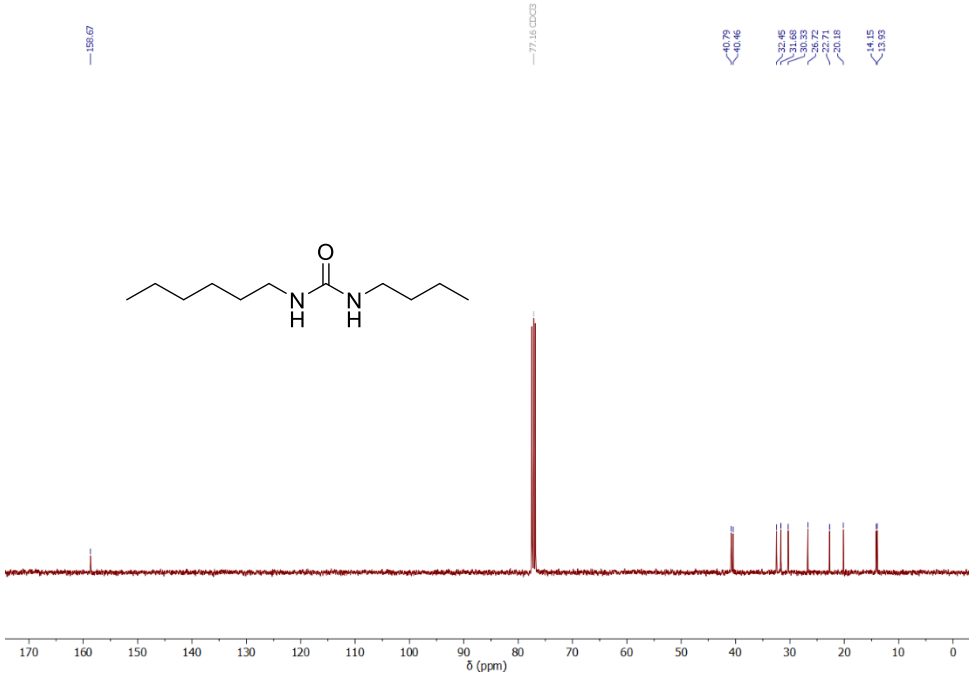

Figure S53. ^{13}C NMR spectrum of compound **2d** (100 MHz, $CDCl_3$, at 25 °C).

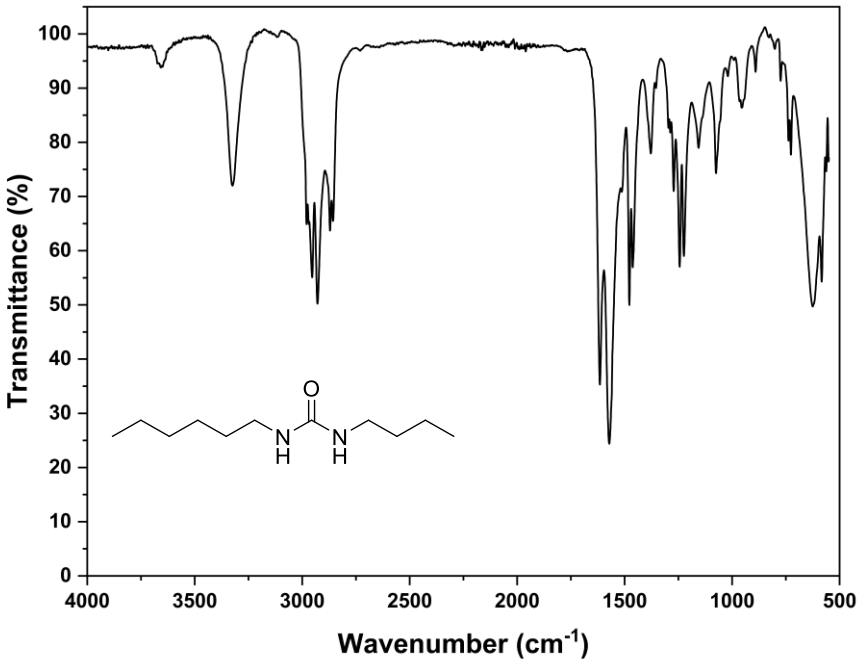

Figure S54. The FTIR spectrum of compound **2d**.

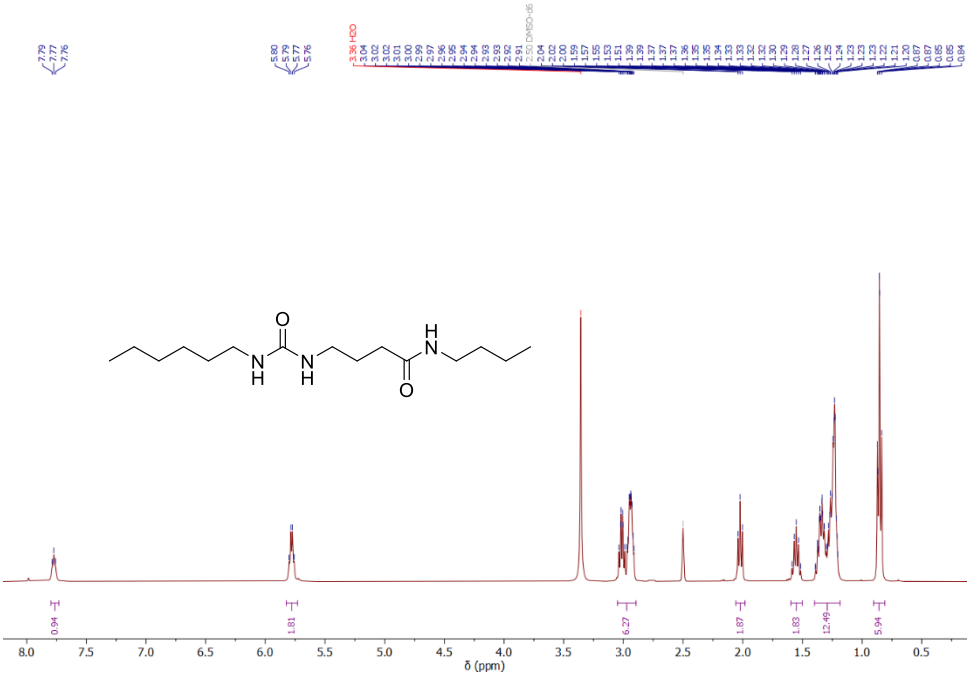

Figure S55. ^{1}H NMR spectrum of compound **2e** (400 MHz, DMSO-d_6, at 25 °C).

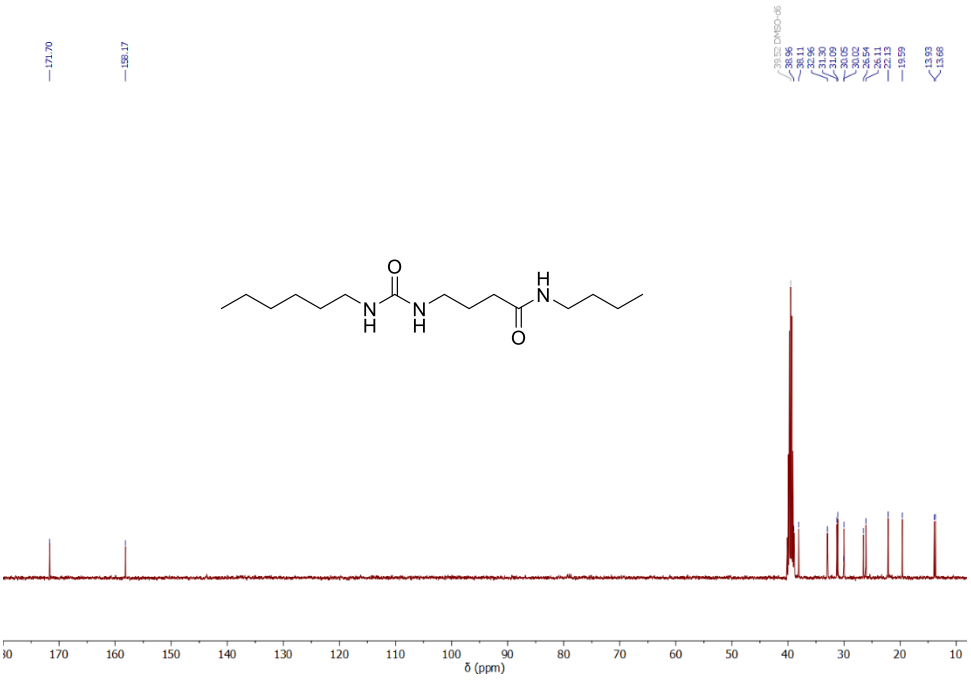

Figure S56. ^{13}C NMR spectrum of compound **2e** (100 MHz, DMSO-d_6, at 25 °C).

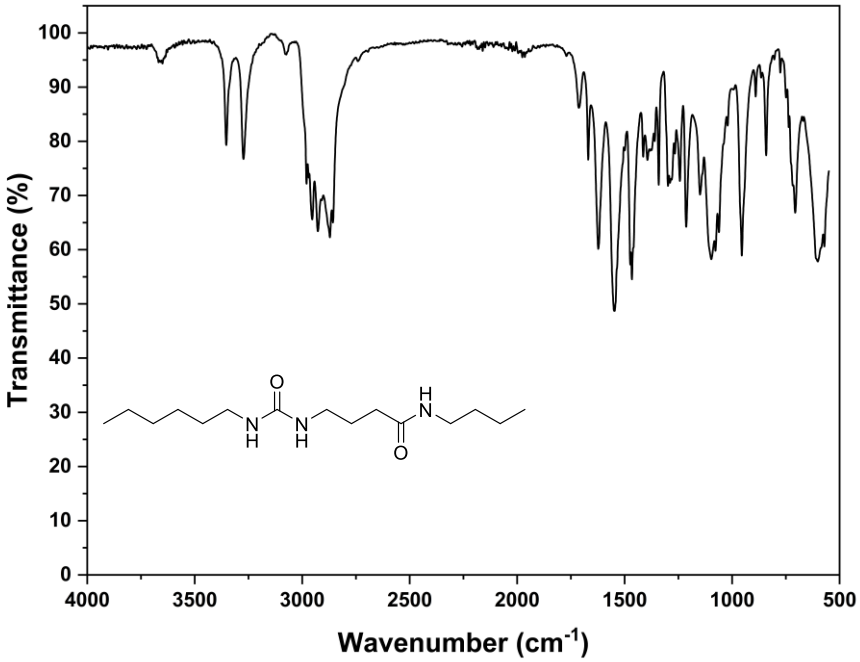

Figure S57. The FTIR spectrum of compound **2e**.

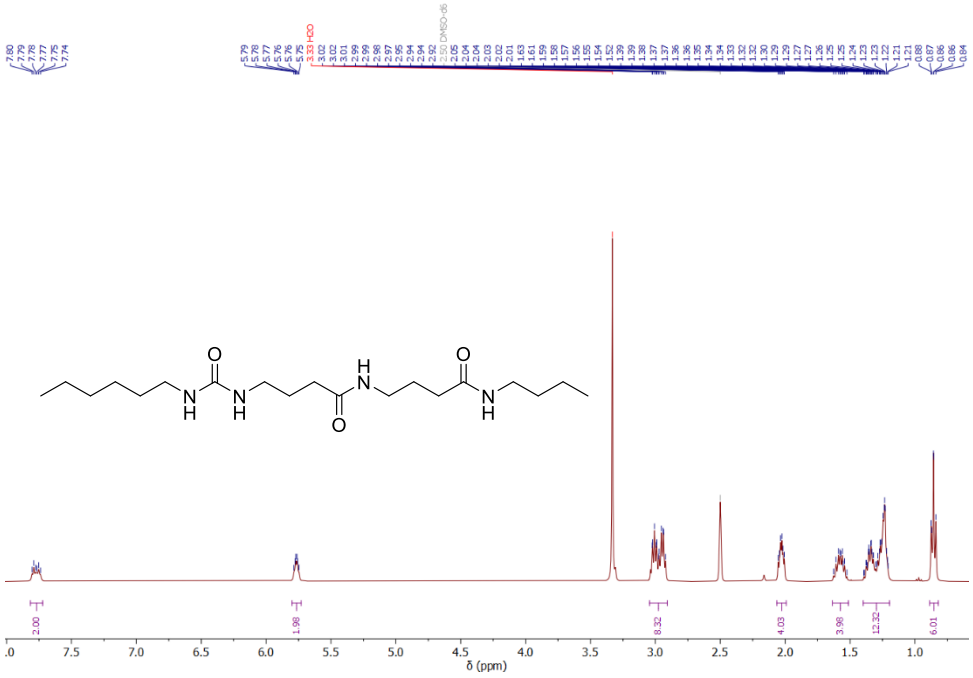

Figure S58. ^{1}H NMR spectrum of compound **2f** (400 MHz, DMSO-d_6, at 25 °C).

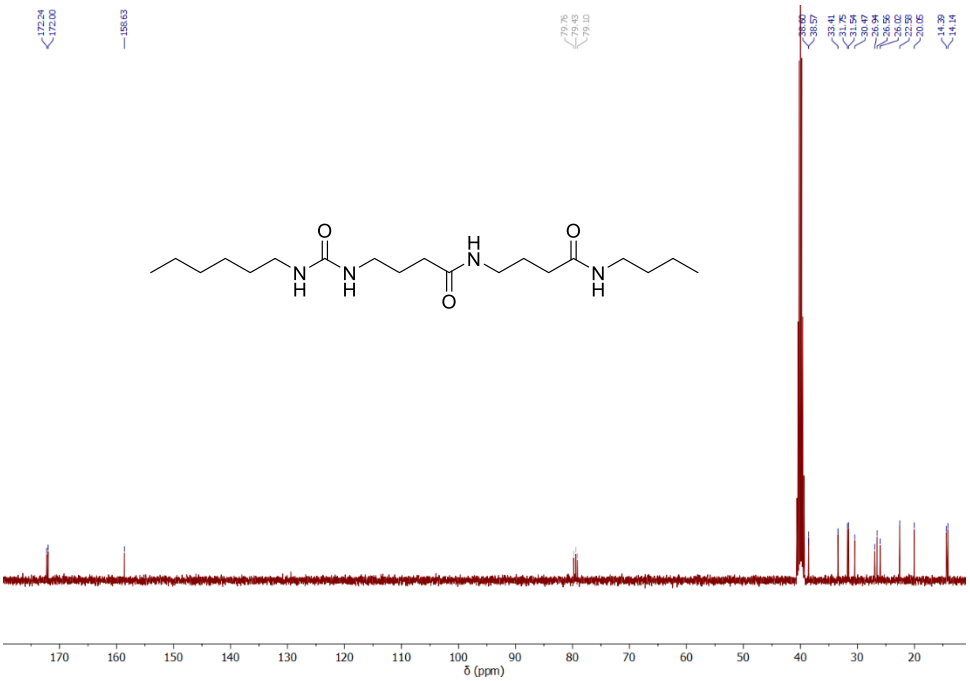

Figure S59. ^{13}C NMR spectrum of compound **2f** (100 MHz, DMSO-d_6, at 25 °C).

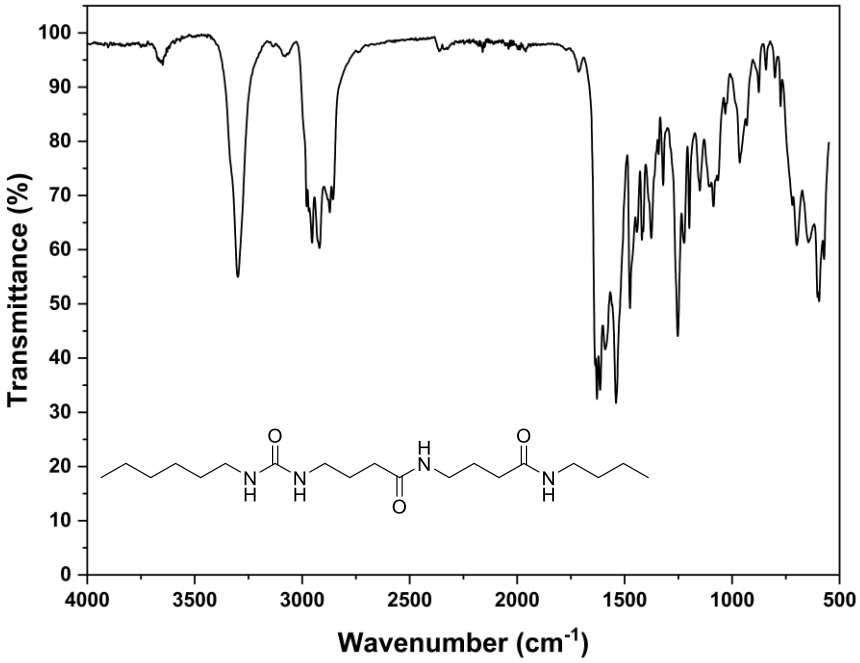

Figure S60. The FTIR spectrum of compound **2f**.

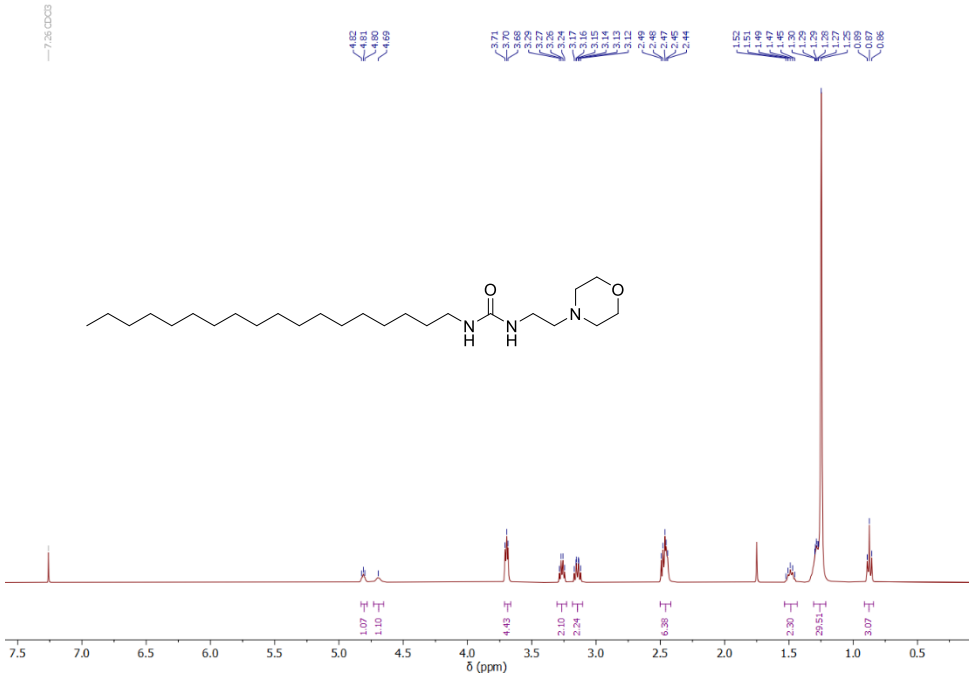

Figure S61. ^{1}H NMR spectrum of compound **3a** (400 MHz, $CDCl_3$, at 25 °C).

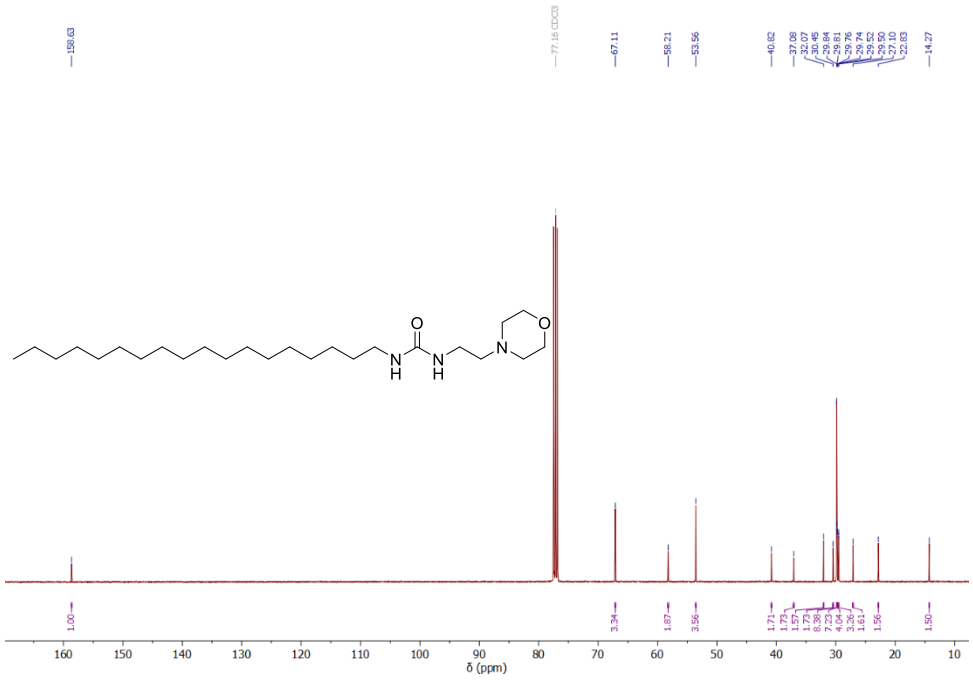

Figure S62. ^{13}C NMR spectrum of compound **3a** (100 MHz, $CDCl_3$, at 25 °C).

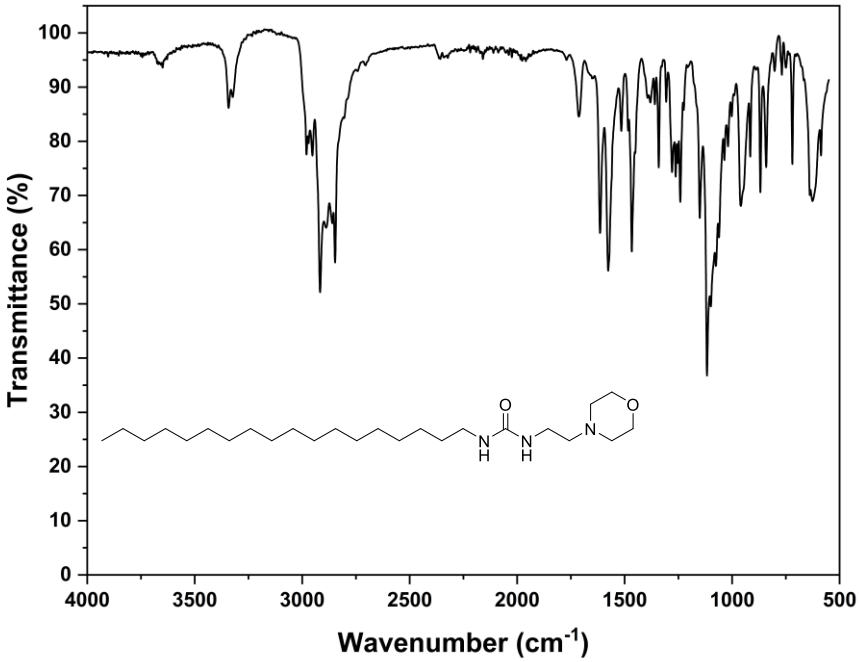

Figure S63. The FTIR spectrum of compound **3a**.

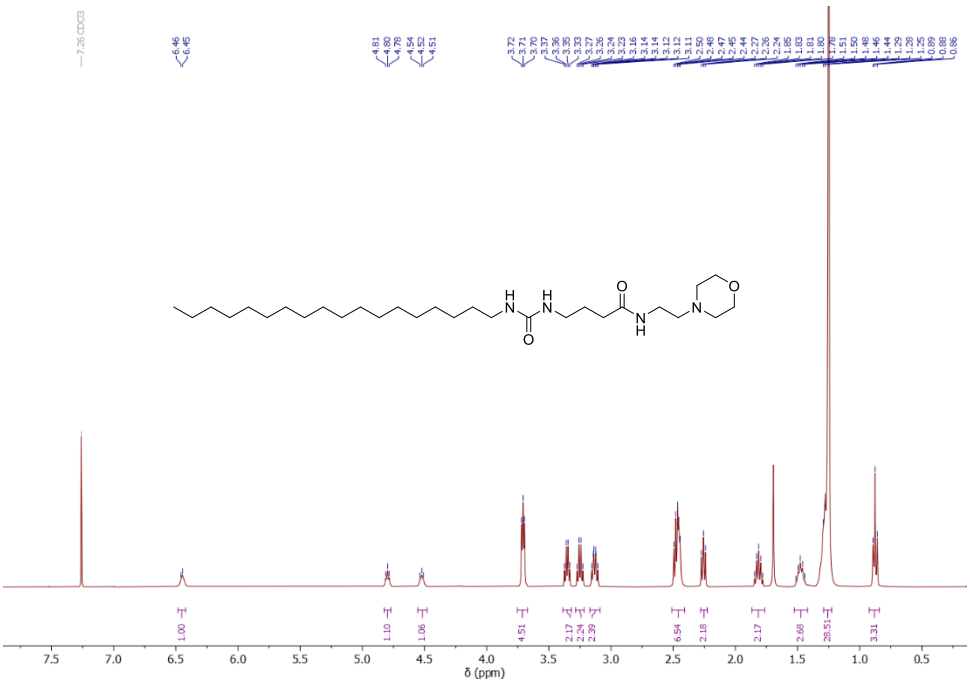

Figure S64. ^{1}H NMR spectrum of compound **3b** (400 MHz, $CDCl_3$, at 25 °C).

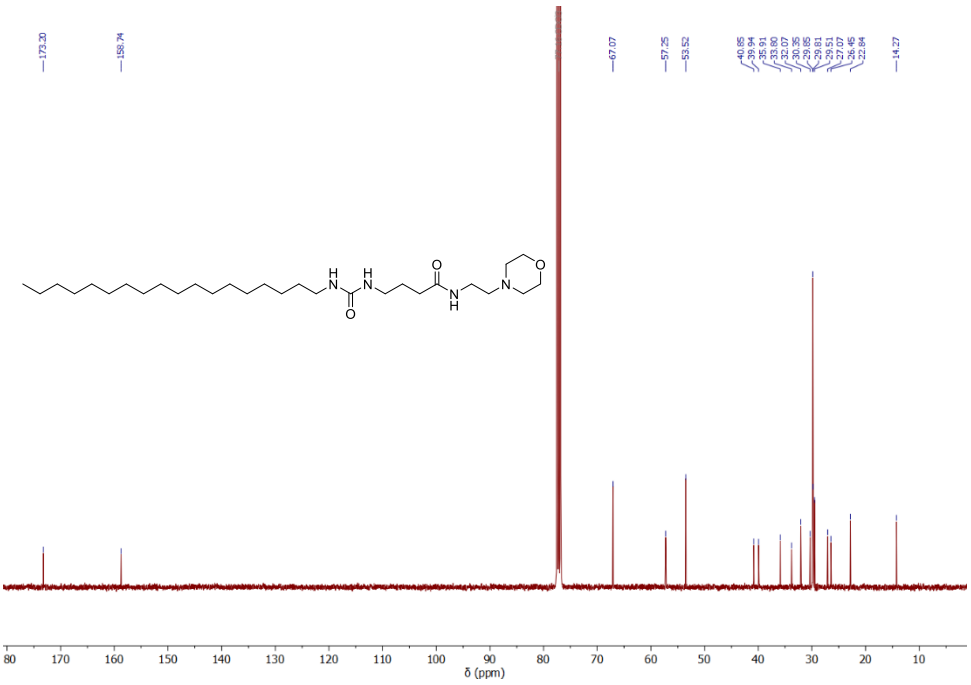

Figure S65. ^{13}C NMR spectrum of compound **3b** (100 MHz, $CDCl_3$, at 25 °C).

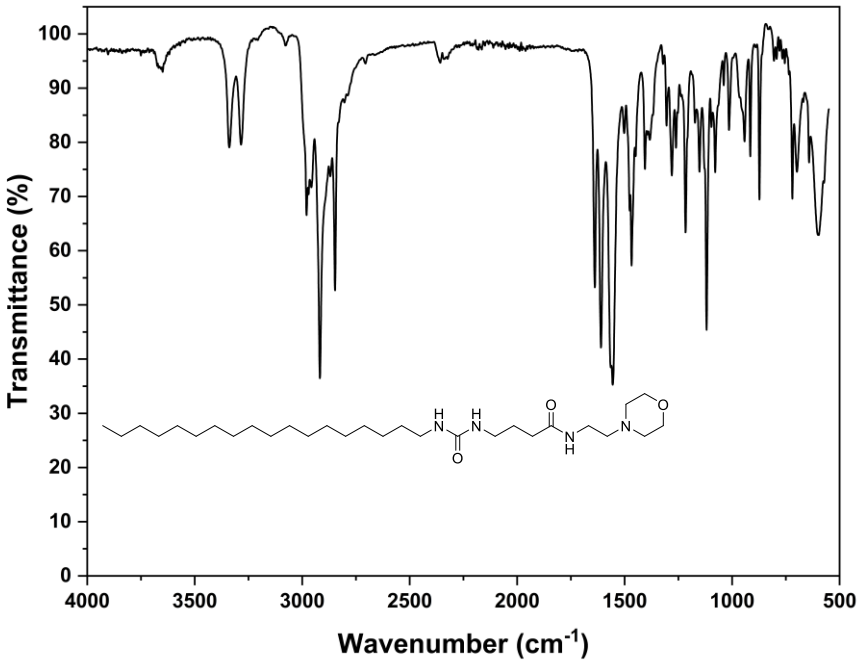

Figure S66. The FTIR spectrum of compound **3b**.

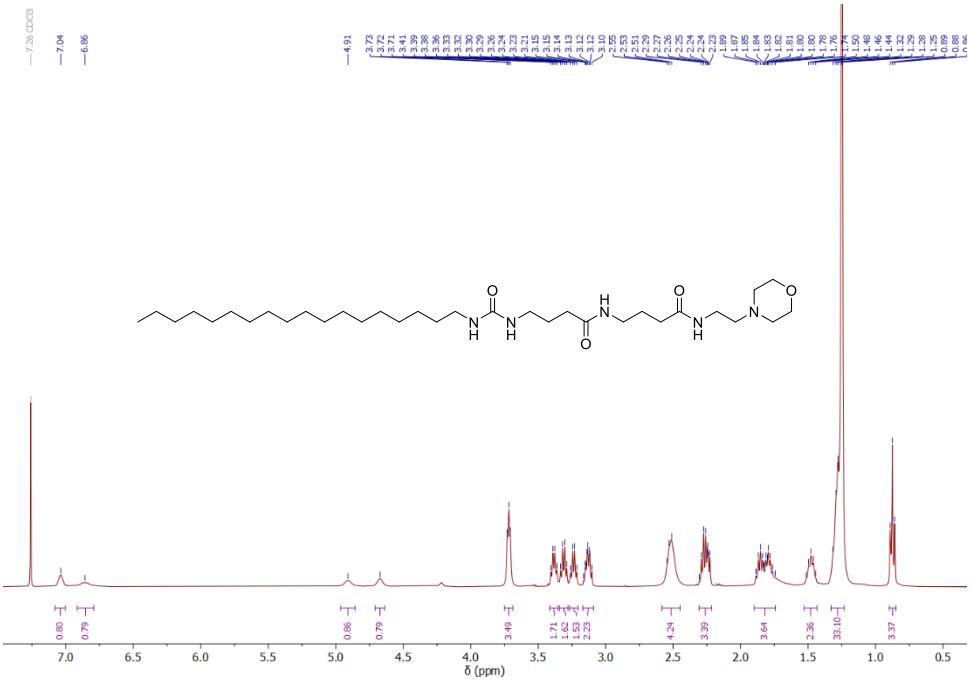

Figure S67. ^{1}H NMR spectrum of compound **3c** (400 MHz, CDCl3, at 25 °C).

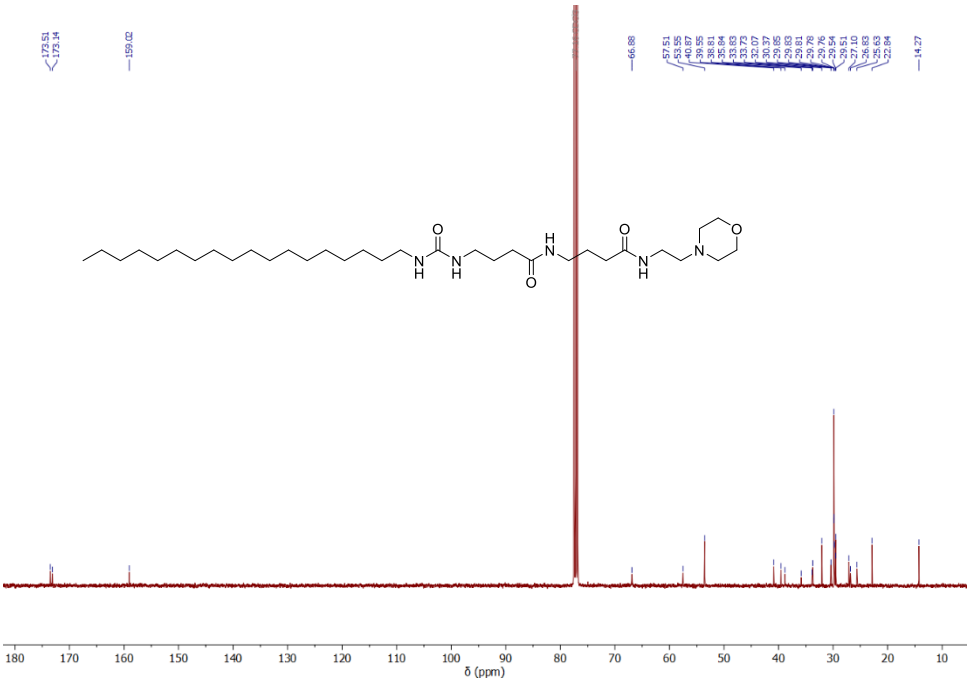

Figure S68. ^{13}C NMR spectrum of compound **3c** (100 MHz, CDCl3, at 25 °C).

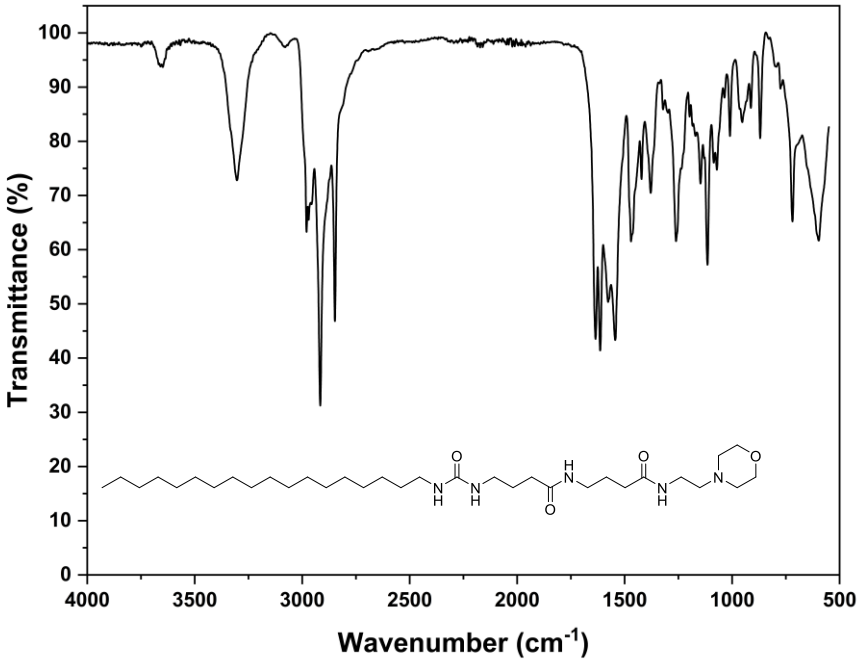

Figure S69. The FTIR spectrum of compound **3c**.

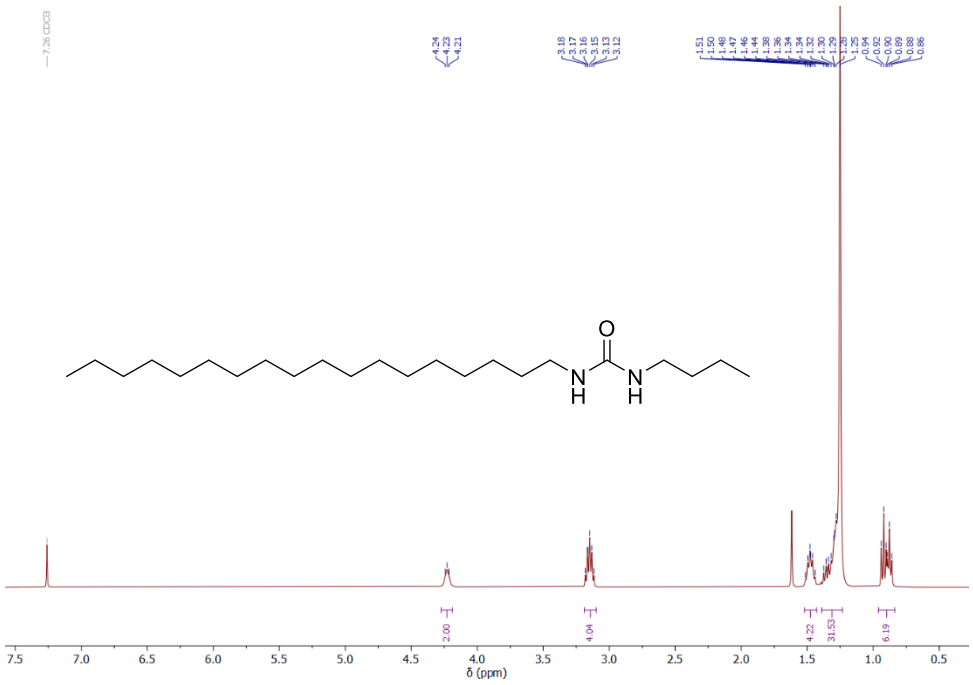

Figure S70. ^{1}H NMR spectrum of compound **3d** (400 MHz, CDCl3, at 25 °C).

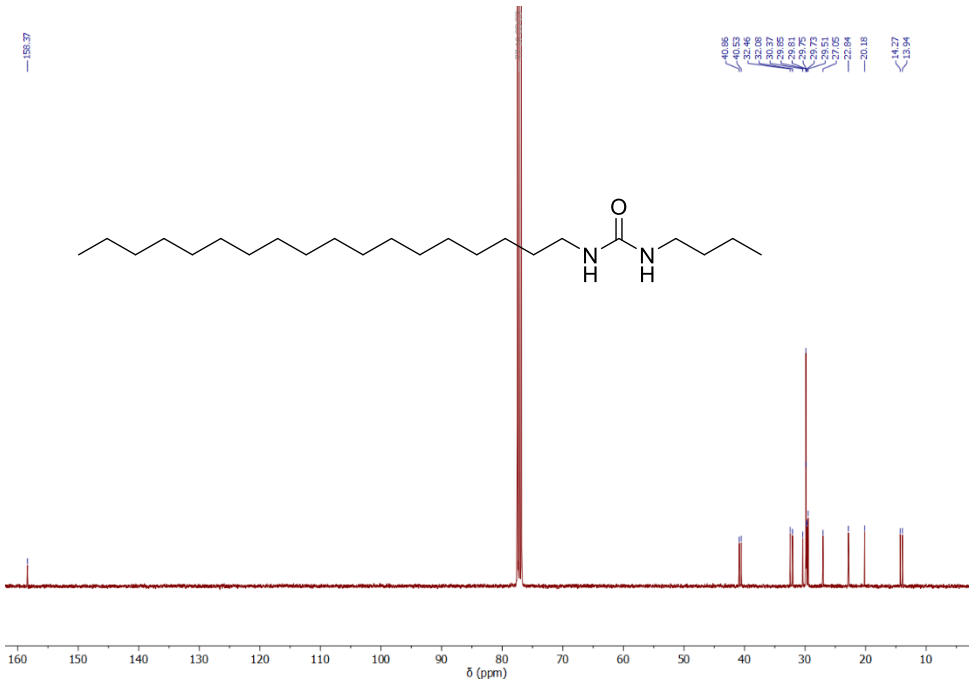

Figure S71. ^{13}C NMR spectrum of compound **3d** (100 MHz, $CDCl_3$, at 25 °C).

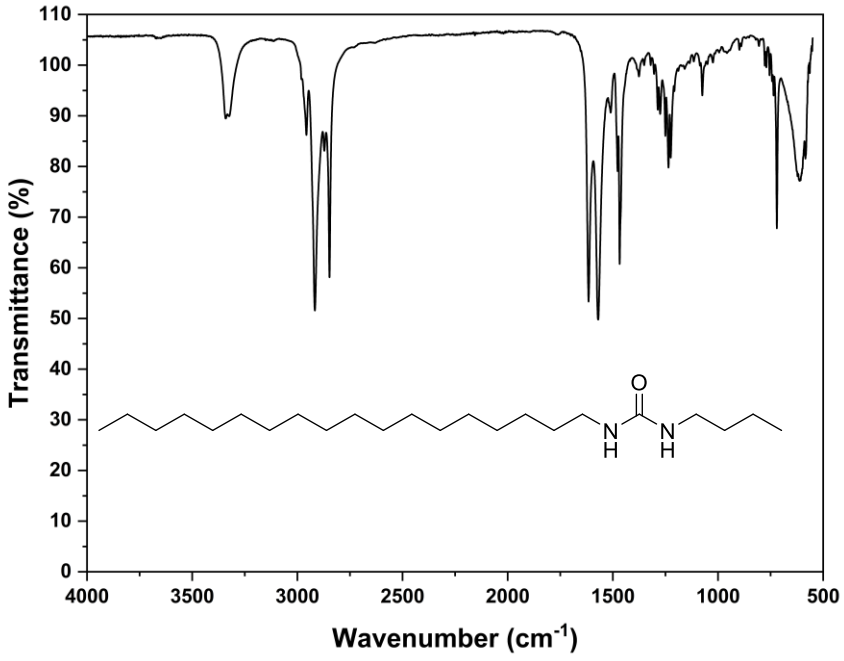

Figure S72. The FTIR spectrum of compound **3d**.

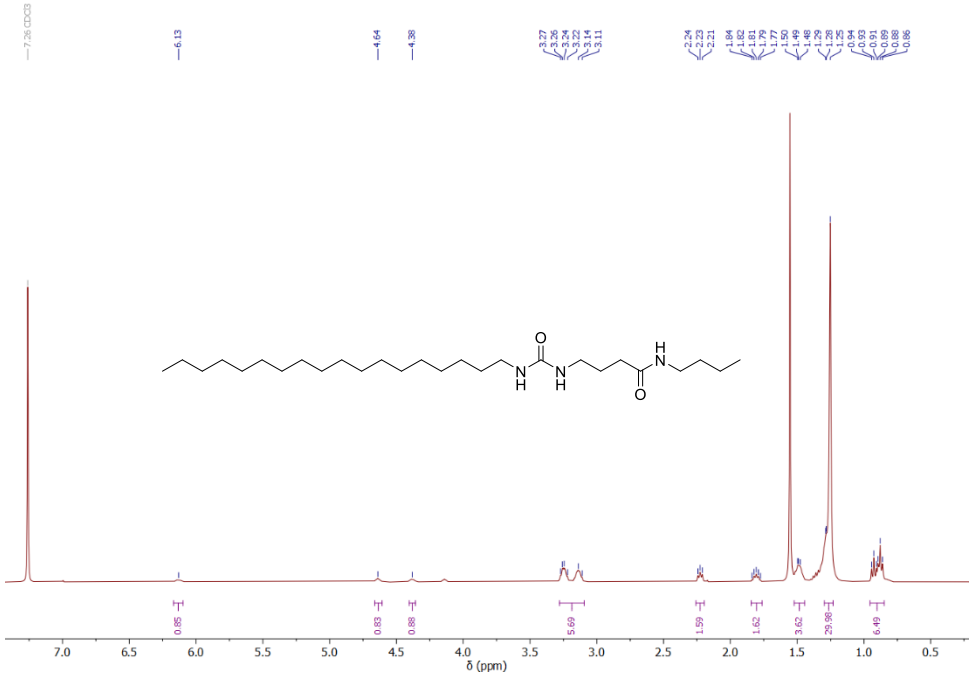

Figure S73. ^{1}H NMR spectrum of compound **3e** (400 MHz, $CDCl_3$, at 25 °C).

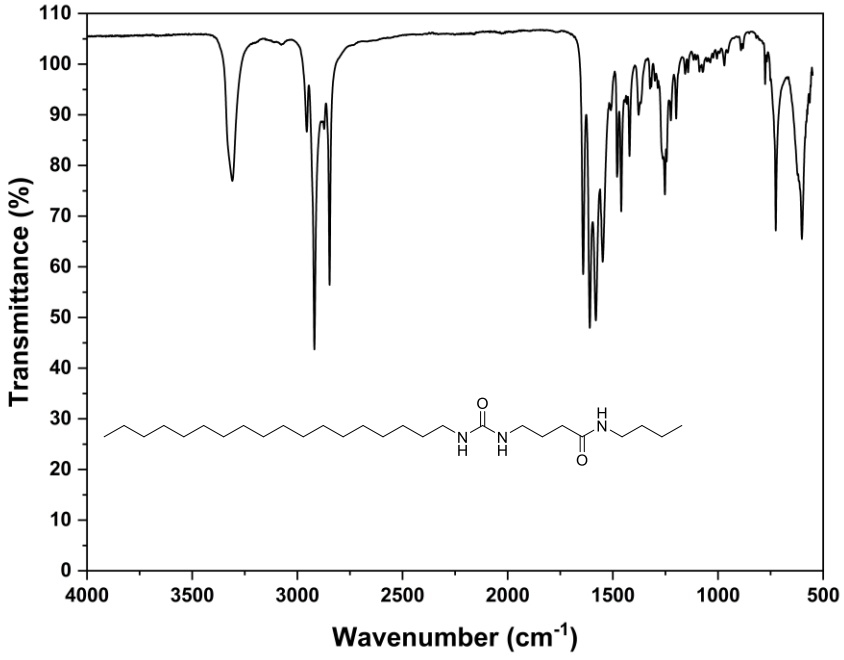

Figure S74. The FTIR spectrum of compound **3e**.

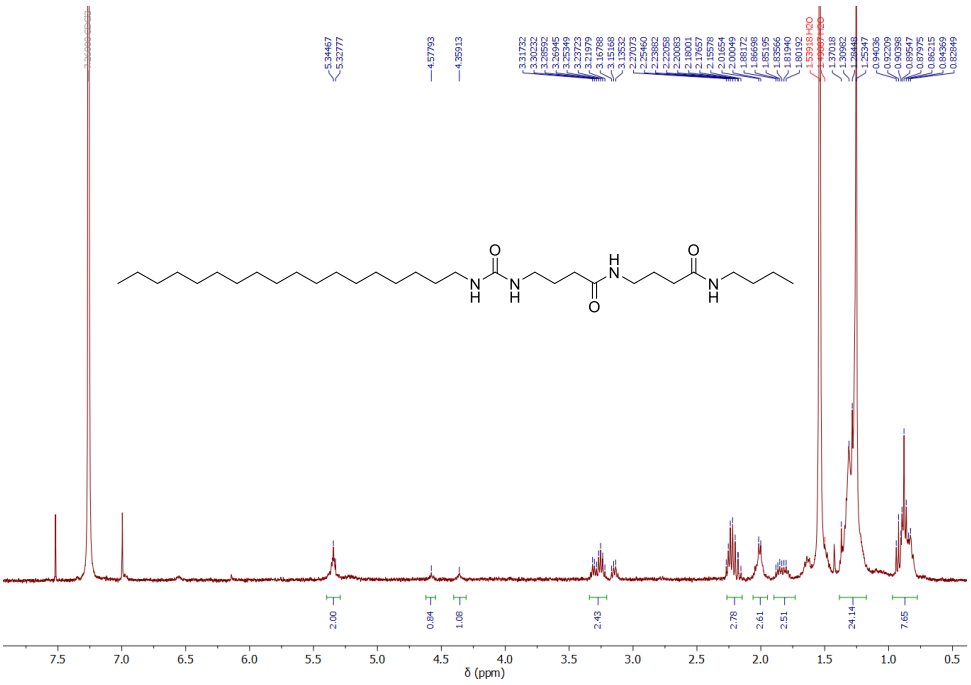

Figure S75. ^{1}H NMR spectrum of compound **3f** (400 MHz, DMSO-*d*$_6$, at 25 °C).

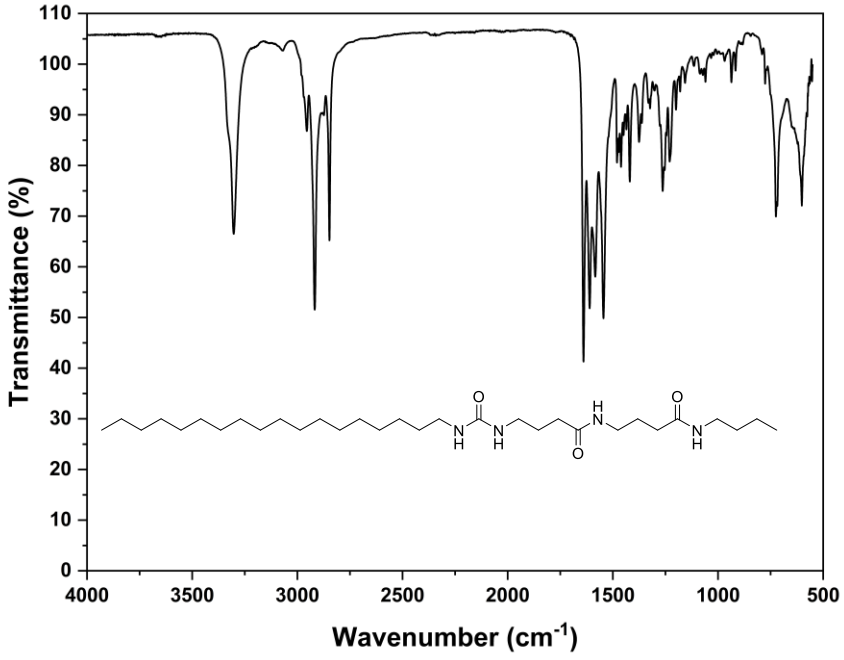

Figure S76. The FTIR spectrum of compound **3f**.

Table S1: Gel screening results of the bis-urea and mono-urea gelators.

Solvent	1a	1b	1c	1e	1f	2a	2b	2c	2d	2e	3c	3e
Hexane	IS	IS	P	IS	P	IS	IS	IS	S	P	P	P
Cyclohexane	P	IS	IS	P	IS	IS	IS	IS	S	P	PG	P
1,2,4-trichlorobenzene	PG	IS	IS	IS	IS	IS	IS	IS	S	VL	PG	PG
Toluene	P	SI	IS	P	IS	S	P	P	S	P	S	P
Benzene	VL	P	P	IS	S	S	S	P	S	P	S	S
THF	IS	IS	IS	IS	IS	P	IS	P	S	P	P	PG
$CHCl_3$	S	IS	IS	IS	P	S	S	S	S	S	S	P
Nitrobenzene	IS	IS	IS	IS	P	S	S	S	S	PG	S	PG
Dioxane	P	IS	VL	IS	IS	IS	IS	P	S	P	PG	S
DMSO	VS	P	P	IS	P	IS	VL	S	S	S	PG	PG
MeOH	S	IS	P	IS	P	IS	IS	IS	S	S	P	P
EtOH	P	IS	IS	IS	IS	IS	IS	IS	S	P	PG	PG
Water	IS	IS	IS	IS	IS	IS	IS	IS	IS	IS	IS	IS

[a] Abbreviations used: (IS = insoluble in the solvent under reflux, G= gel (concentration of 10 mg mL^{-1}, unless specified), P = precipitation, VL = viscous liquid, S= solution, PG = partial gel, G^o= opaque gel, G^T= translucent gel, G^C= transparent/clear gel).

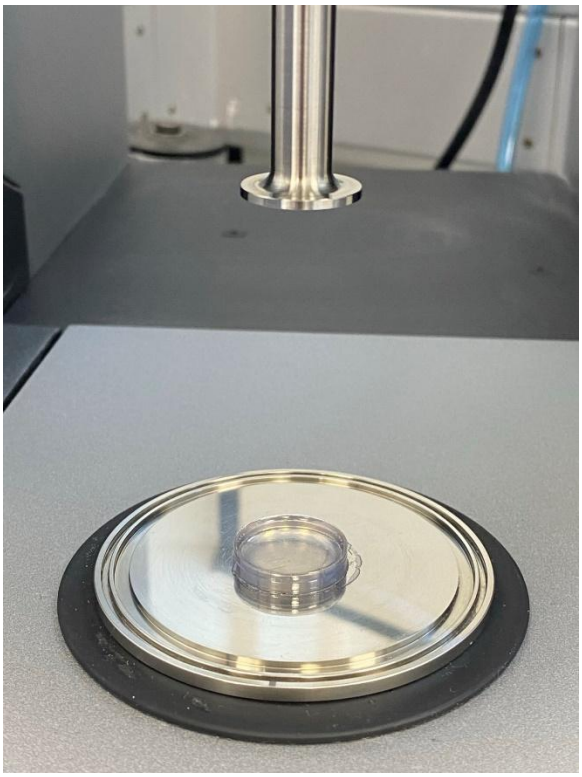

Figure S77. Organogel disk-shape sample (**LMWG3a**) with a diameter and thickness of 10 mm and 1 mm for rheological experiments.

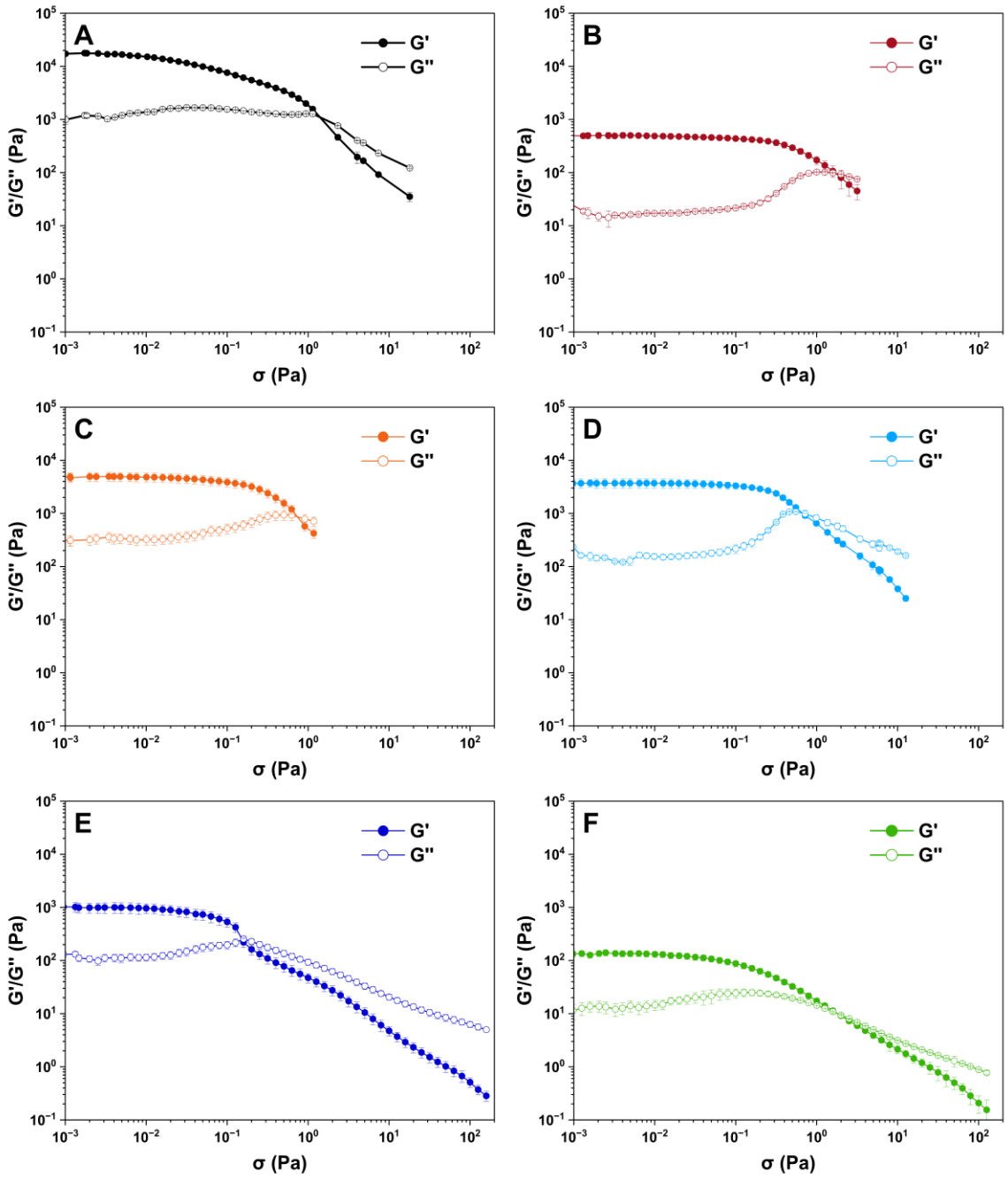

Figure S78. Dynamic rheological property (G' and G'') evaluation of **LMWG1d** (**A**), **LMWG2f** (**B**), **LMWG3a** (**C**), **LMWG3b** (**D**), **LMWG3d** (**E**), **and LMWG3e** (**F**) as a function of the applied shear stress; standard deviation error bars were calculated from three separate measurements.

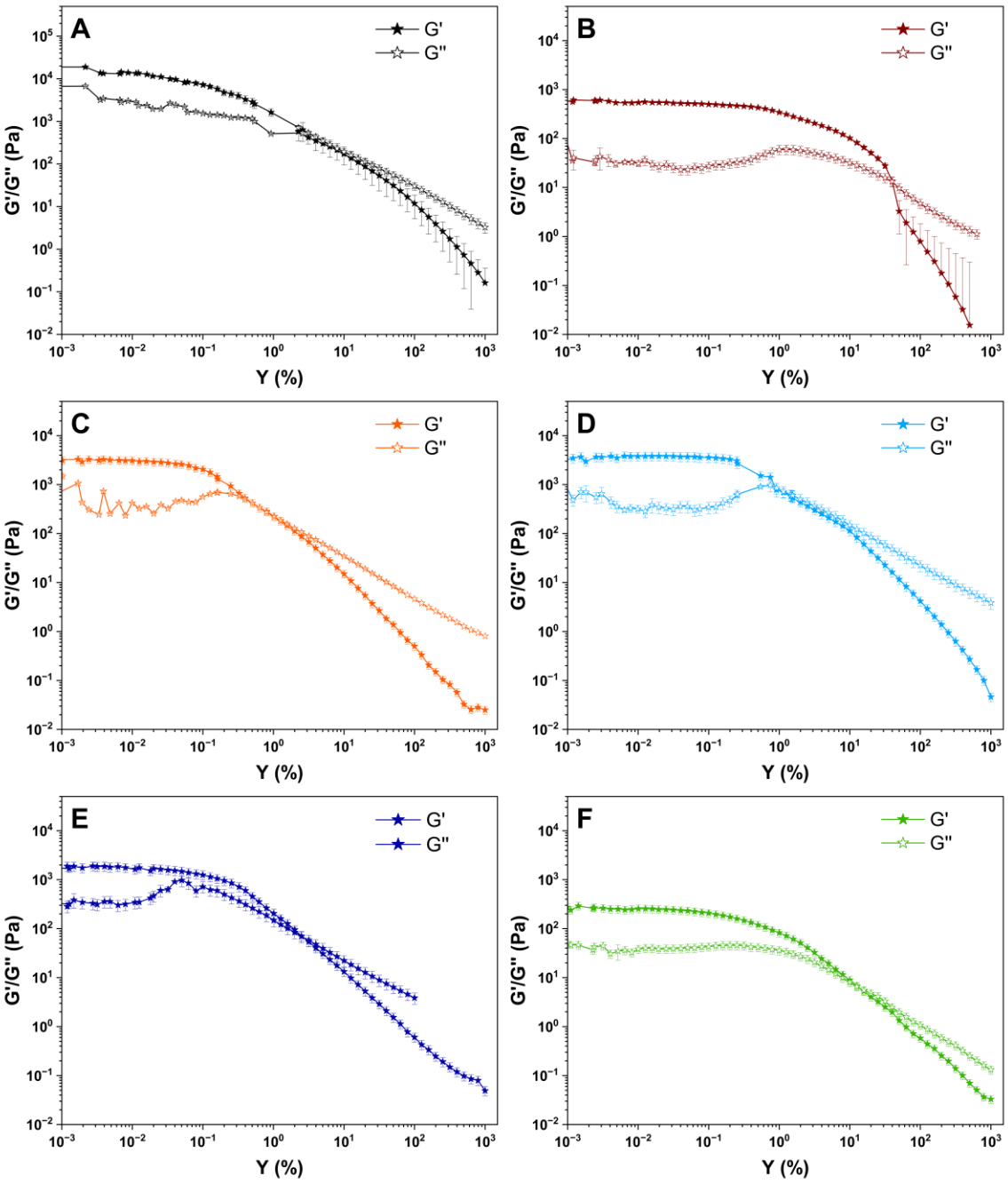

Figure S79. Dynamic rheological property (G' and G'') evaluation of **LMWG1d** (**A**), **LMWG2f** (**B**), **LMWG3a** (**C**), **LMWG3b** (**D**), **LMWG3d** (**E**), **and LMWG3e** (**F**) as a function of the applied shear strain; standard deviation error bars were calculated from three separate measurements.

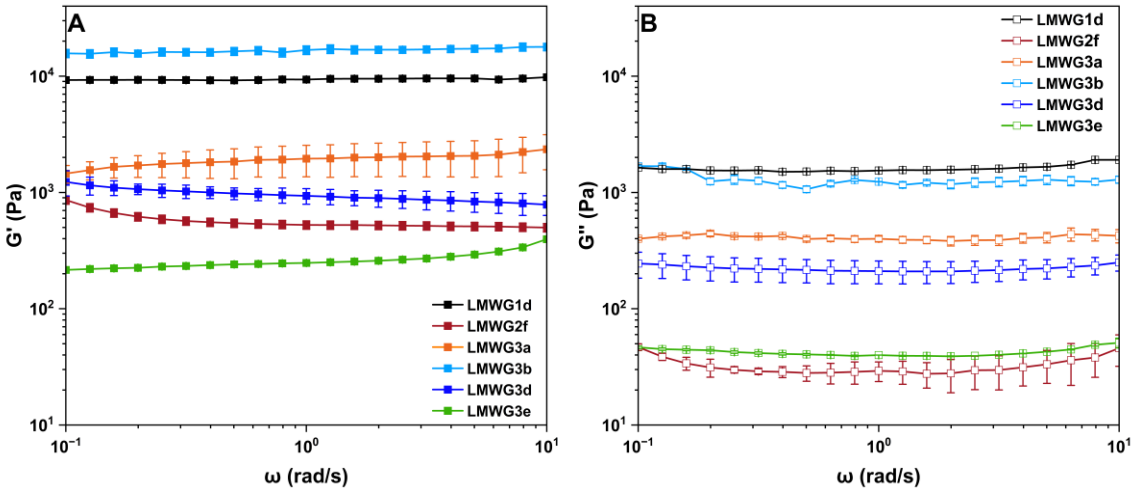

Figure S80. Frequency sweep experiments showing evaluation of the dynamic rheological properties, G' (**A**) and G'' (**B**) of LMWGs; standard deviation error bars were calculated from three separate measurements.

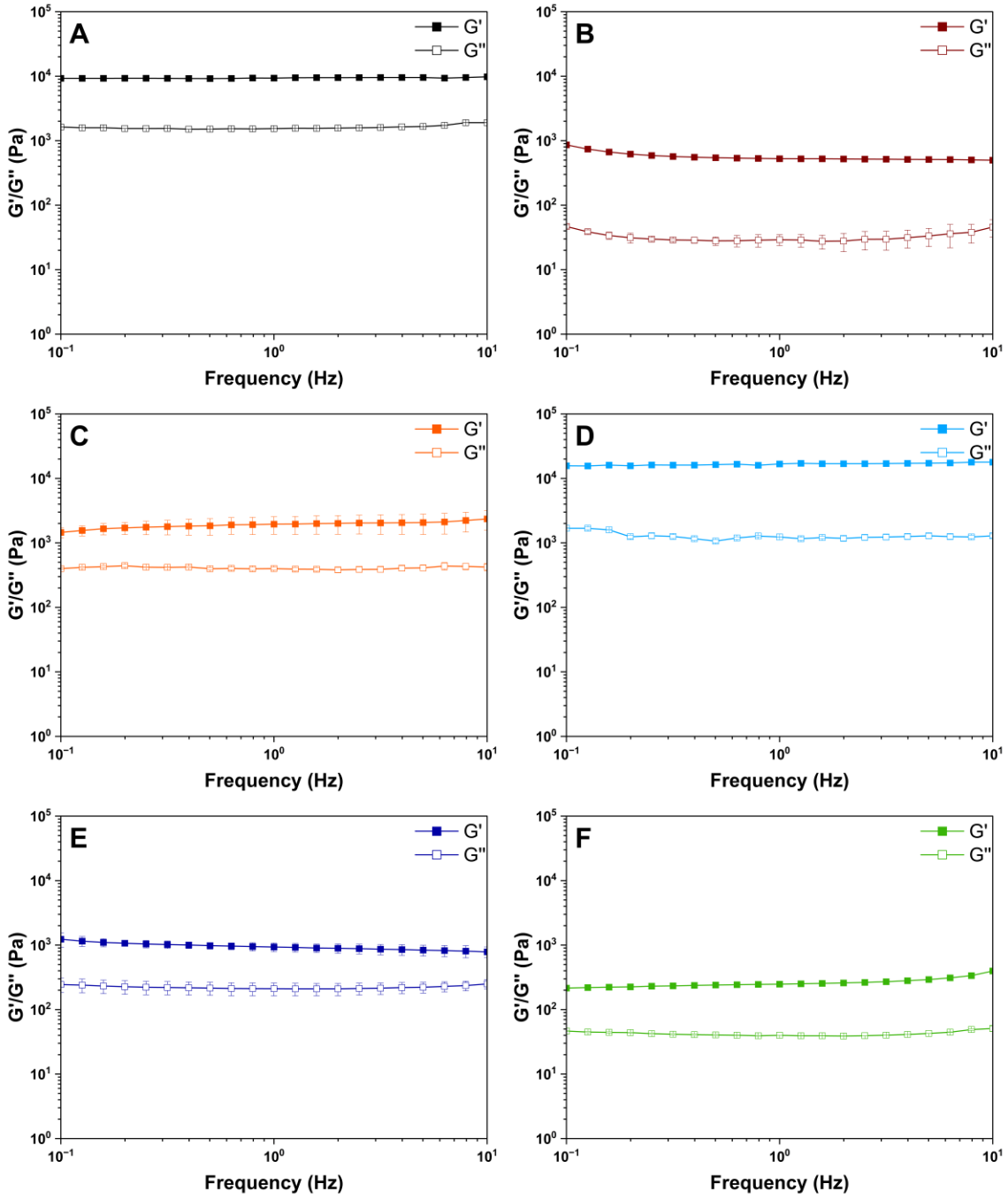

Figure S81. Frequency sweep experiments showing evaluation of the dynamic rheological properties of **LMWG1d** (**A**)**, LMWG2f** (**B**)**, LMWG3a** (**C**)**, LMWG3b** (**D**)**, LMWG3d** (**E**)**, and LMWG3e** (**F**); standard deviation error bars were calculated from three separate measurements.

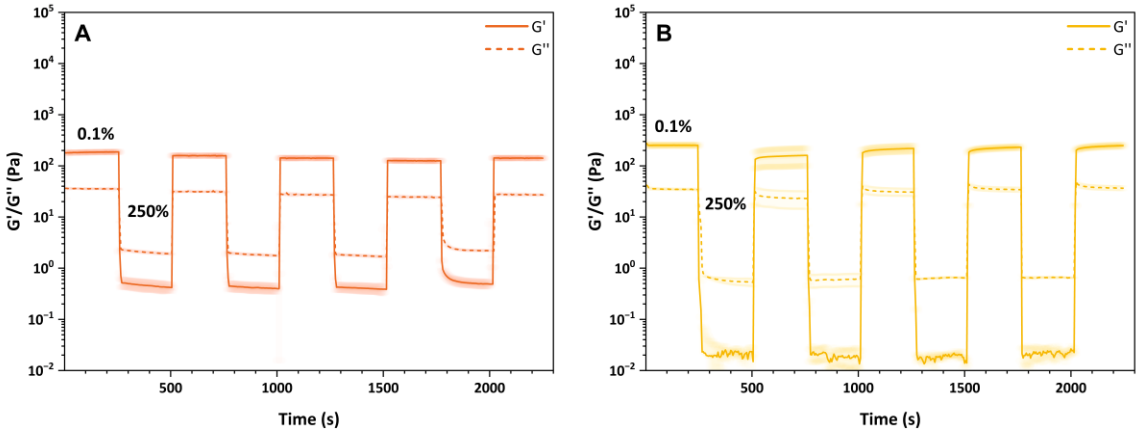

Figure S82. Continuous step-strain measurements (thixotropic recovery) of **LMWG3d** (**A**), and **LMWG3e** (**B**), LMWG3a at 25 °C (high-amplitude oscillatory parameters: strain γ = 250%, frequency = 1 Hz, low-amplitude oscillatory parameters: strain γ = 0.1%, frequency = 1 Hz). Shaded regions are standard deviation error bars calculated from three separate measurements.

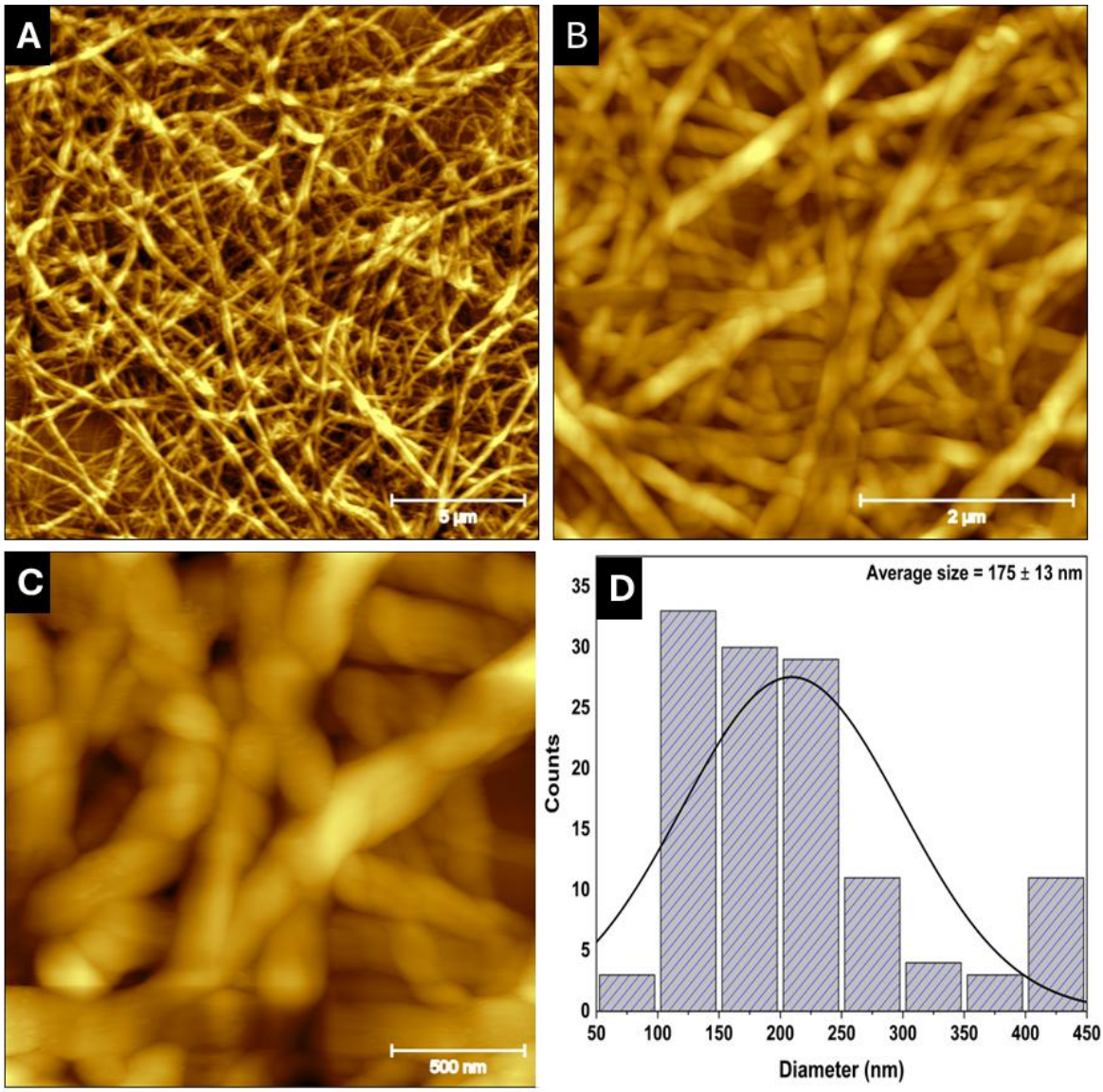

Figure S83. AFM tapping mode height images of xerogel **LMWG1d** at scale bars 5 *µ*m (**A**), 2 *µ*m (**B**), 500 nm (**C**), and (**D**) calculated average fibres diameter distributions were observed around 175 nm.

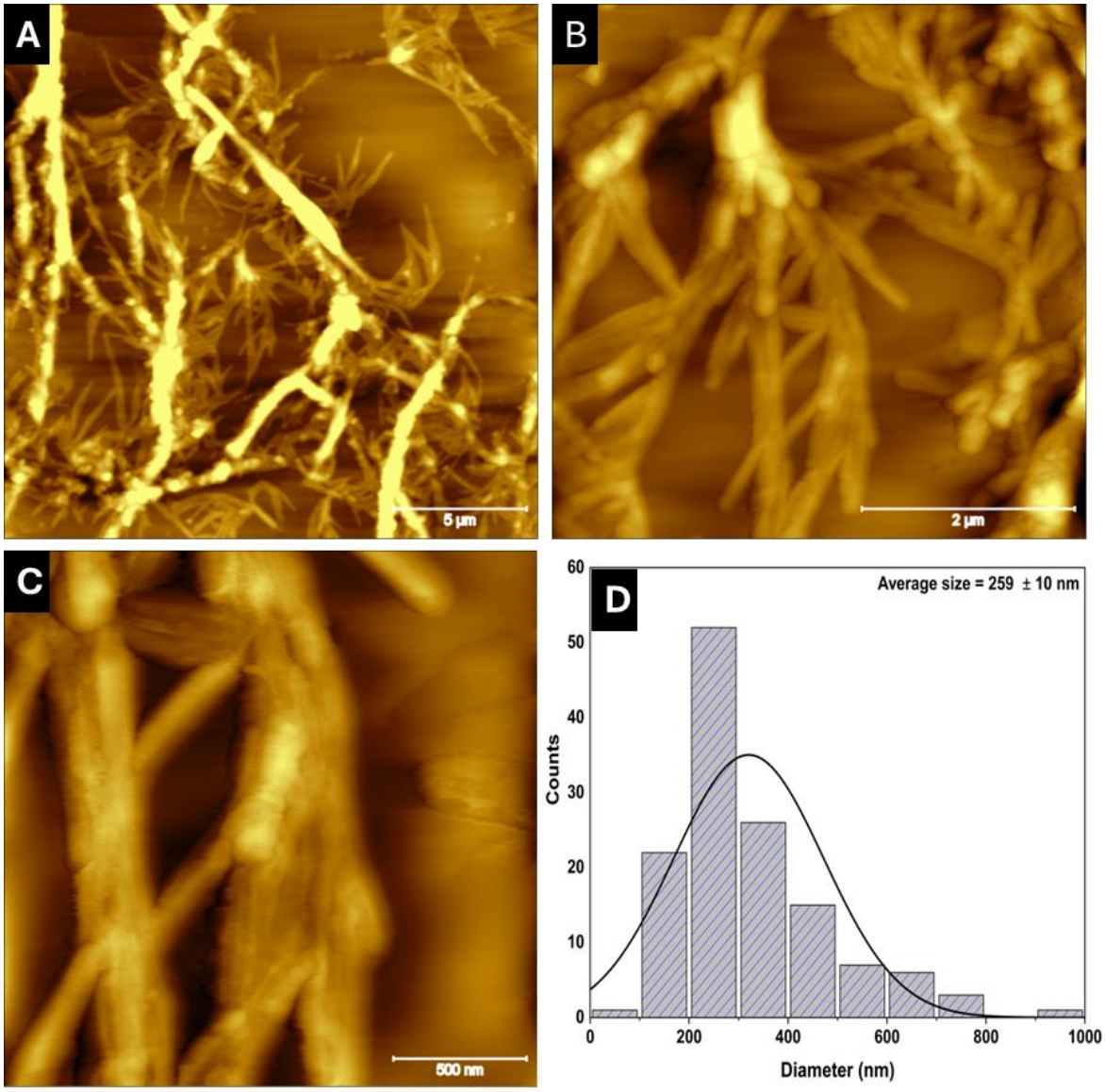

Figure S84. AFM tapping mode height images of xerogel **LMWG2f** at scale bars 5 *µ*m (**A**), 2 *µ*m (**B**), 500 nm (**C**), and (**D**) calculated average fibres diameter distributions were observed around 259 nm.

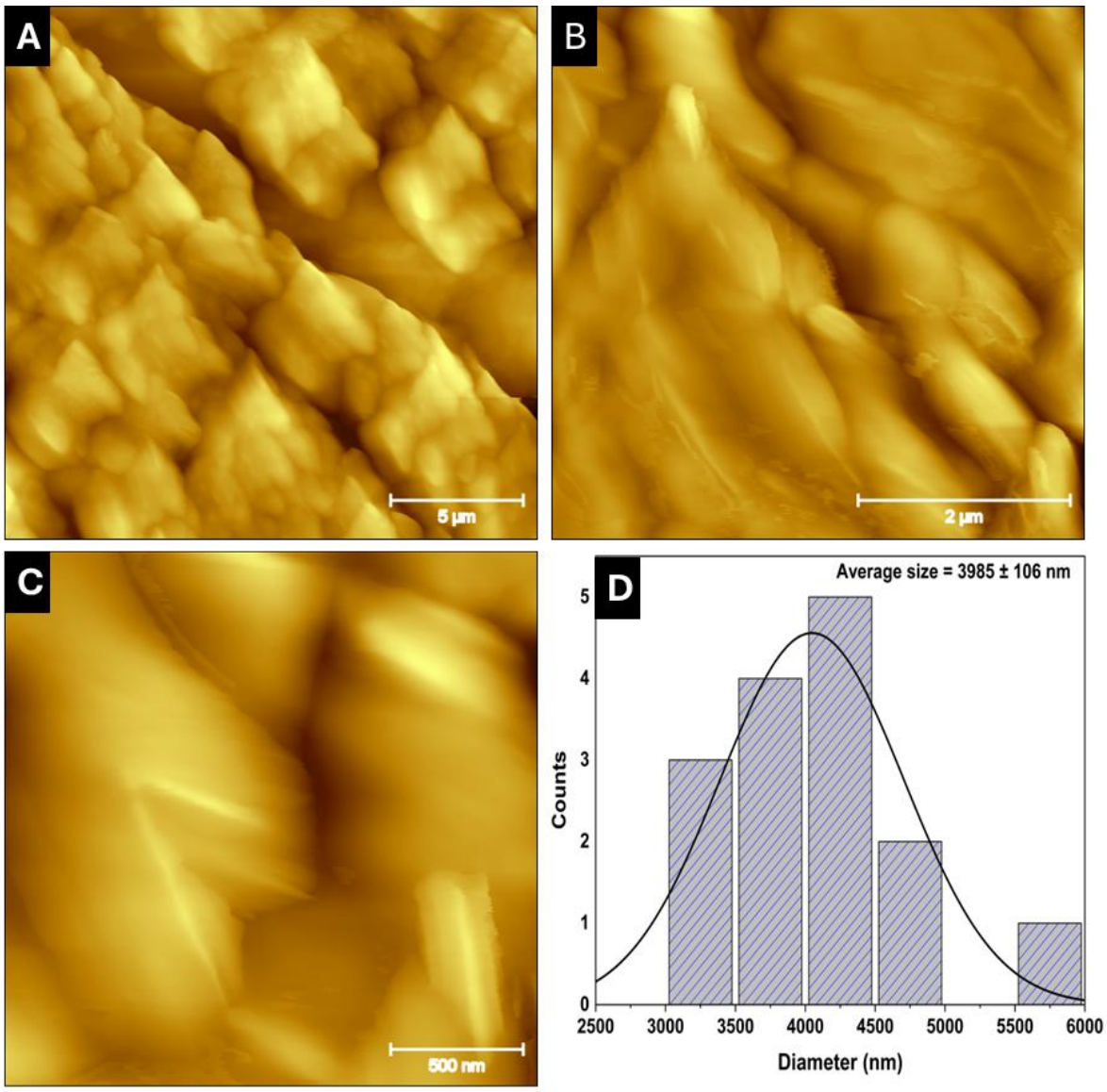

Figure S85. AFM tapping mode height images of xerogel **LMWG3a** at scale bars 5 *µ*m (**A**), 2 *µ*m (**B**), 500 nm (**C**), and (**D**) calculated average sheets diameter distributions were observed around 3985 nm.

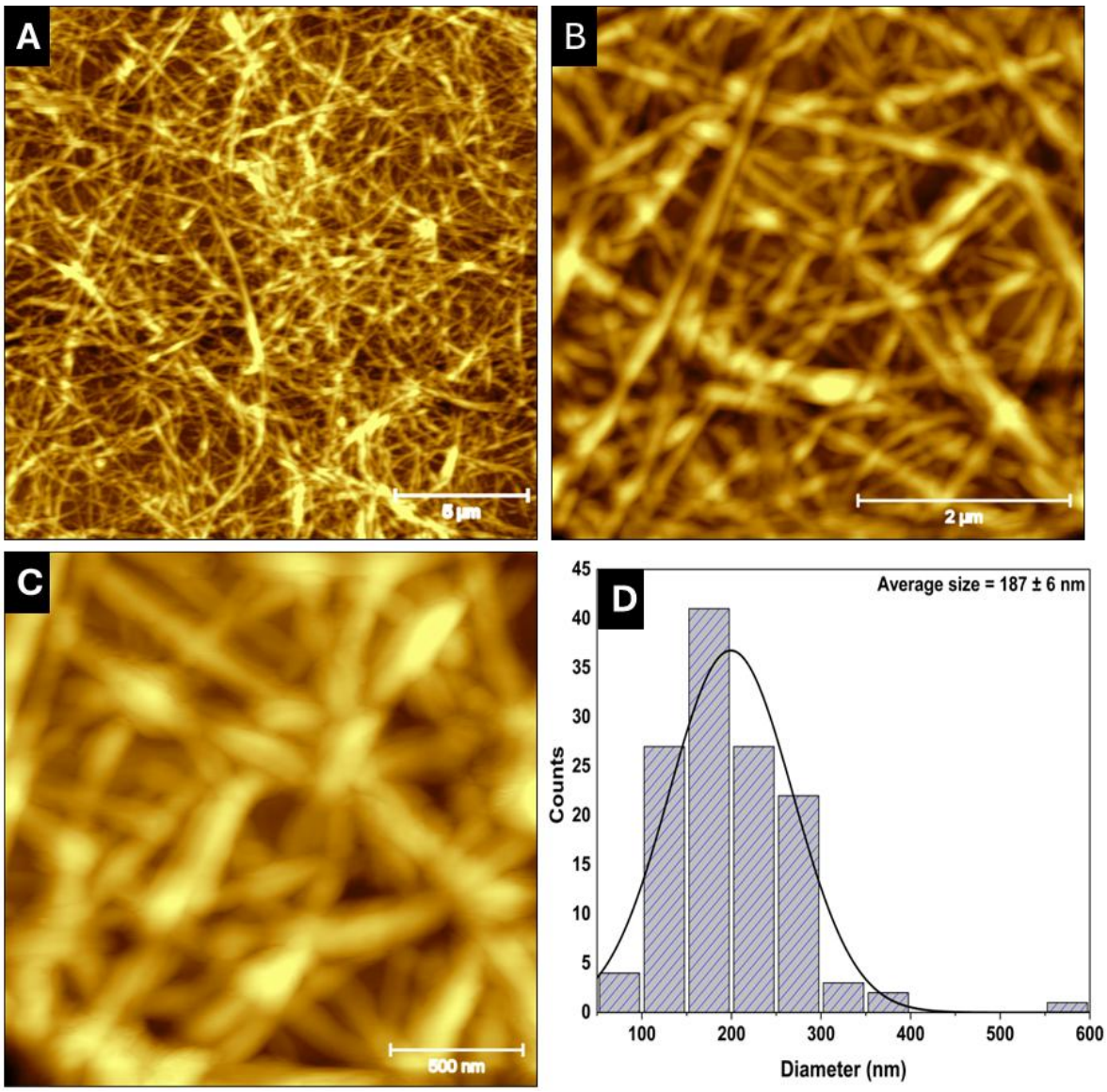

Figure S86. AFM tapping mode height images of xerogel **LMWG3b** at scale bars 5 *µ*m (**A**), 2 *µ*m (**B**), 500 nm (**C**), and (**D**) calculated average fibres diameter distributions were observed around 187 nm.

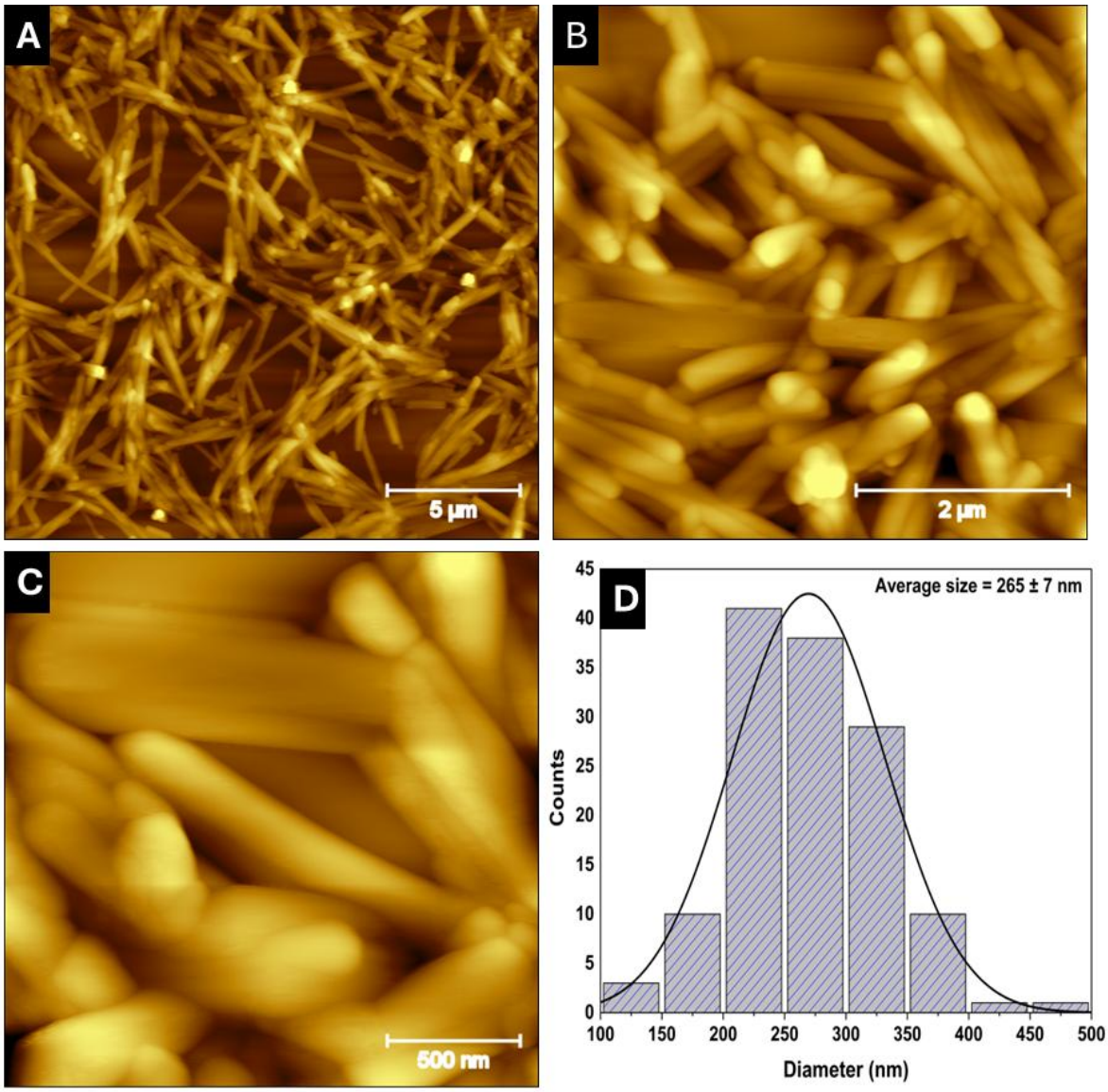

Figure S87. AFM tapping mode height images of xerogel **LMWG3d** at scale bars 5 *µ*m (**A**), 2 *µ*m (**B**), 500 nm (**C**), and (**D**) calculated average like-rods diameter distributions were observed around 265 nm.

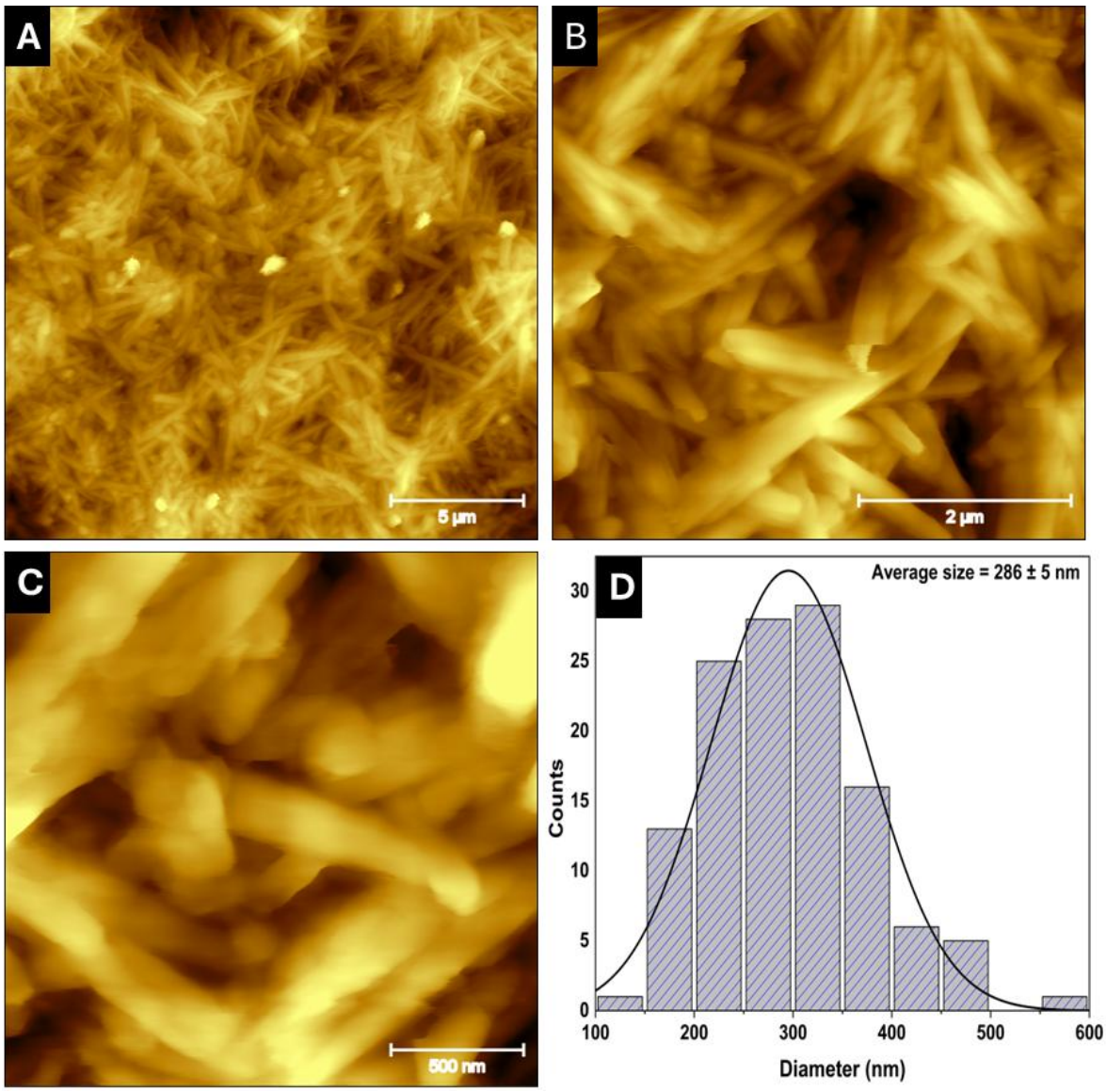

Figure S88. AFM tapping mode height images of xerogel **LMWG3e** at scale bars 5 *µ*m (**A**), 2 *µ*m (**B**), 500 nm (**C**), and (**D**) calculated average like-rods diameter distributions were observed around 286 nm.

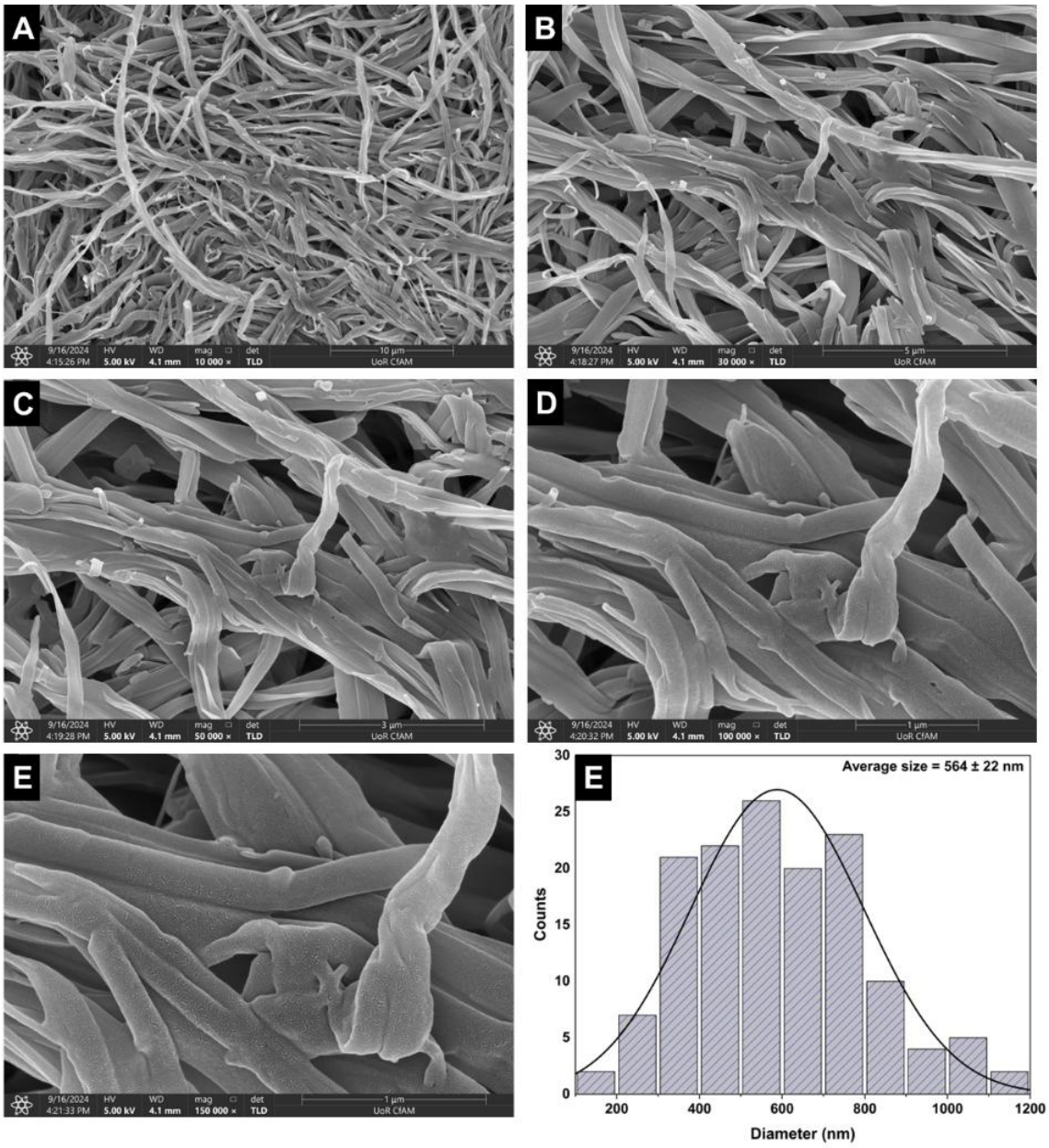

Figure S89. SEM images of xerogel **LMWG1d** at scale bars 10 *μ*m (**A**), 5 *μ*m (**B**), 3 *μ*m (**C**), 1 *μ*m (**D**, **E**), and (**E**) calculated average fibres diameter distributions were observed around 564 nm.

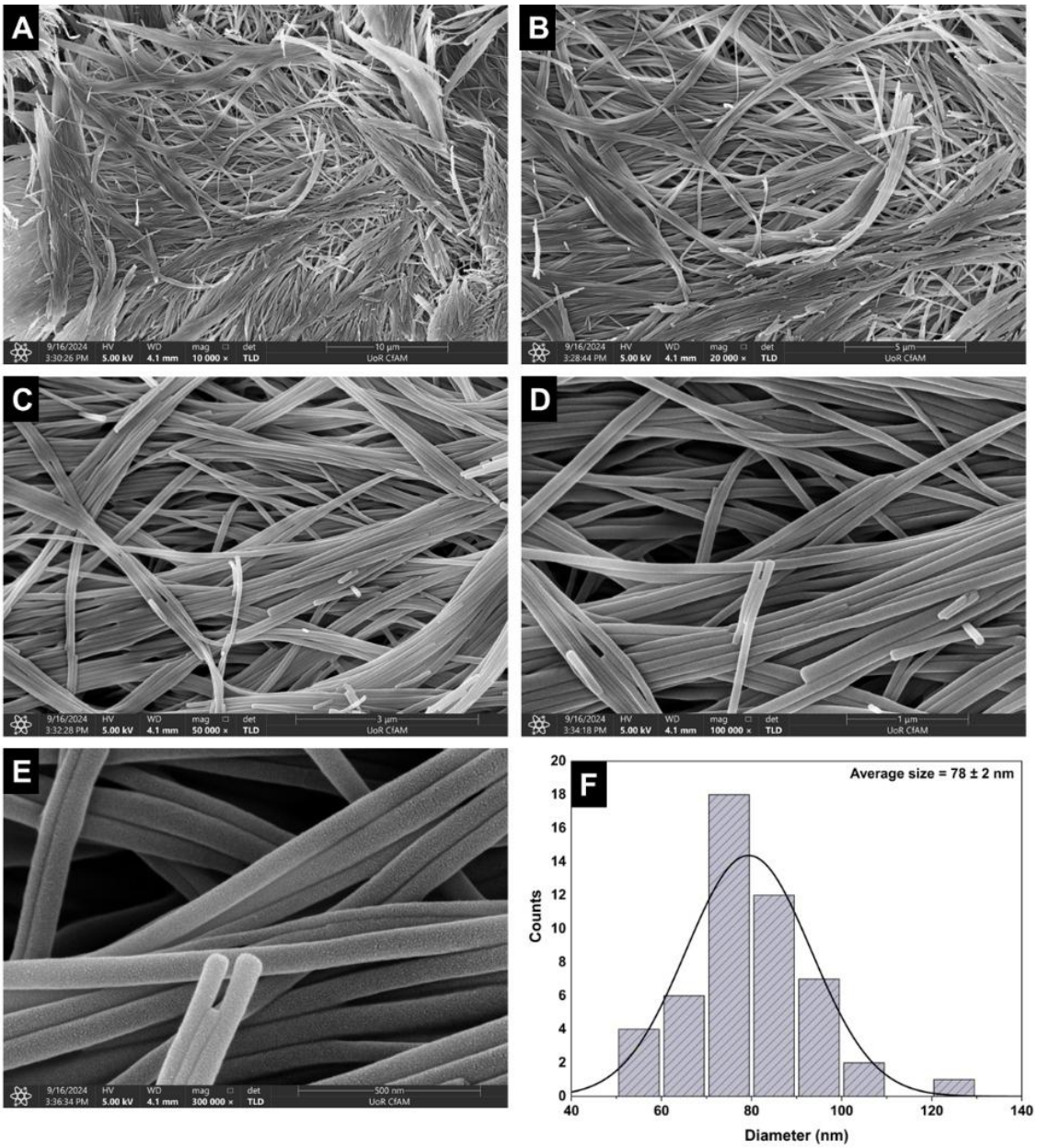

Figure S90. SEM images of xerogel **LMWG2f** at scale bars 10 *μ*m (**A**), 5 *μ*m (**B**), 3 *μ*m (**C**), 1 *μ*m (**D**), 500 nm (**E**), and (**F**) calculated average fibres diameter distributions were observed around 78 nm.

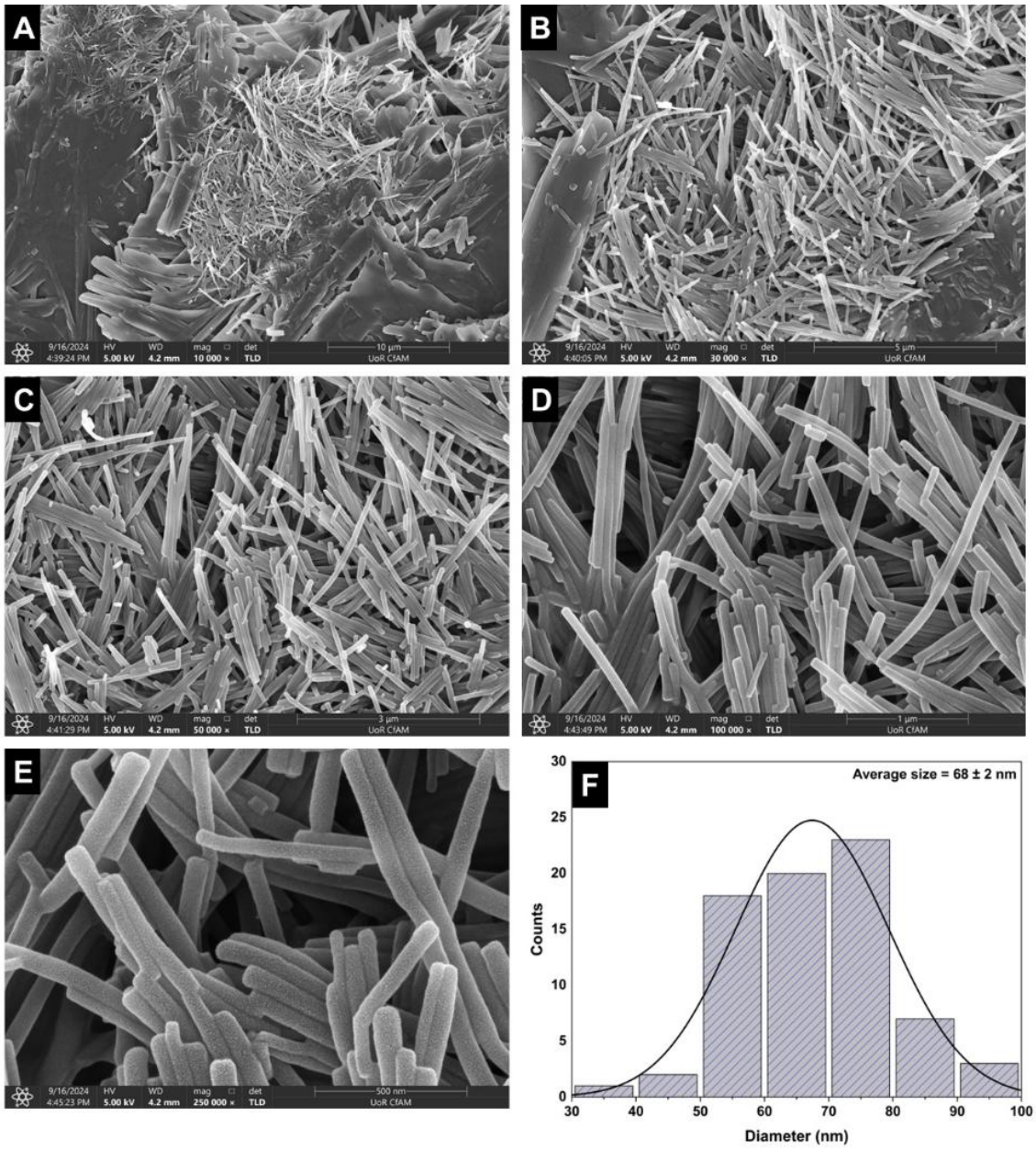

Figure S91. SEM images of xerogel **LMWG3a** at scale bars 10 *μ*m (**A**), 5 *μ*m (**B**), 3 *μ*m (**C**), and 1 *μ*m (**D**), 500 nm (**E**), and (**F**) calculated average fibres diameter distributions were observed around 68 nm.

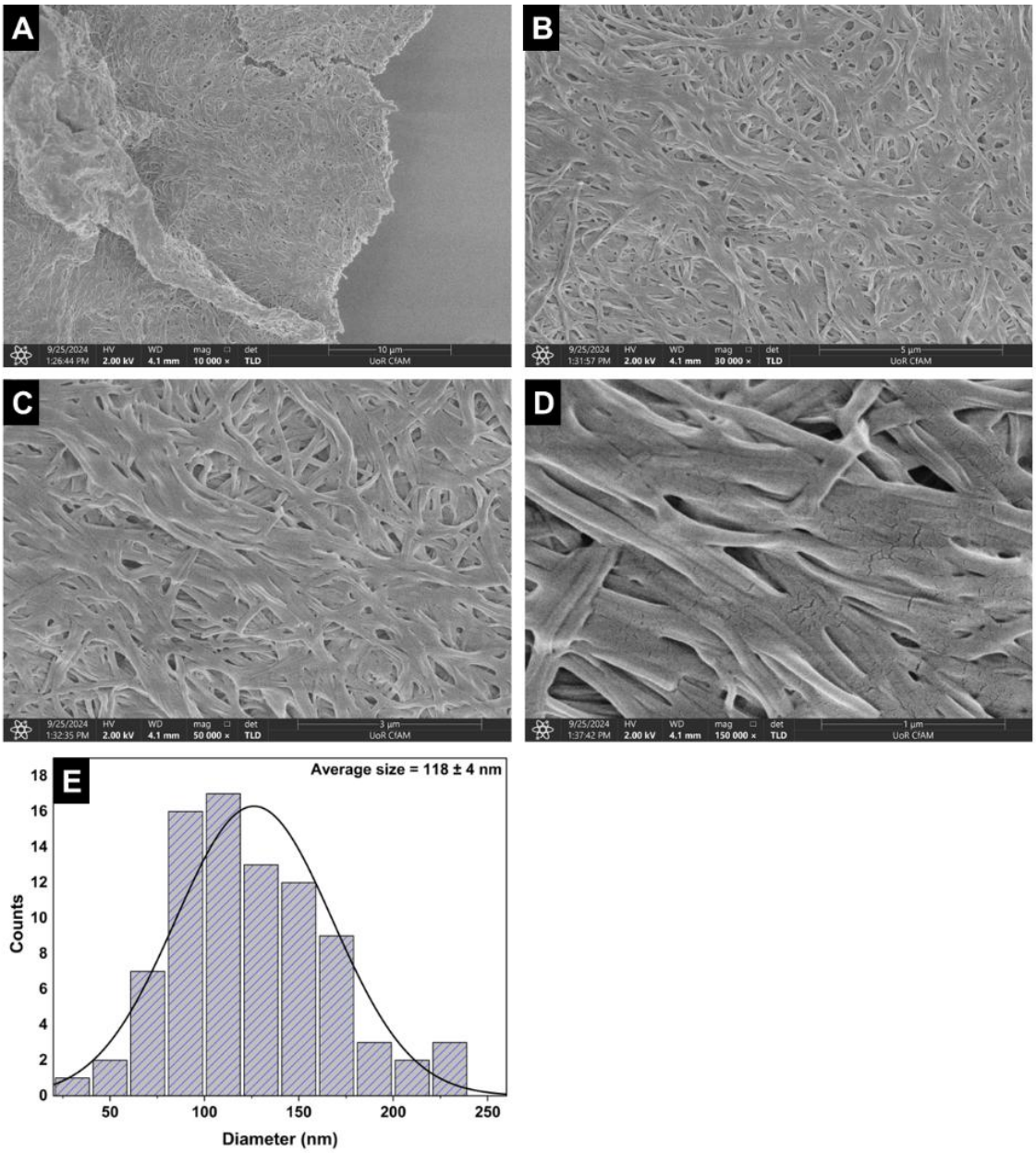

Figure S92. SEM images of xerogel **LMWG3b** at scale bars 10 *μ*m (**A**), 5 *μ*m (**B**), 3 *μ*m (**C**), 1 *μ*m (**D**), and (**E**) calculated average fibres diameter distributions were observed around 118 nm. Lots of nano-fibres with a diameter of ca. 118 nm which are crosslinked and intertwined into 3D networks. It should be noted that a high degree of knots is evident, and it is reasonable to attribute the robust mechanical and rheological properties to this.

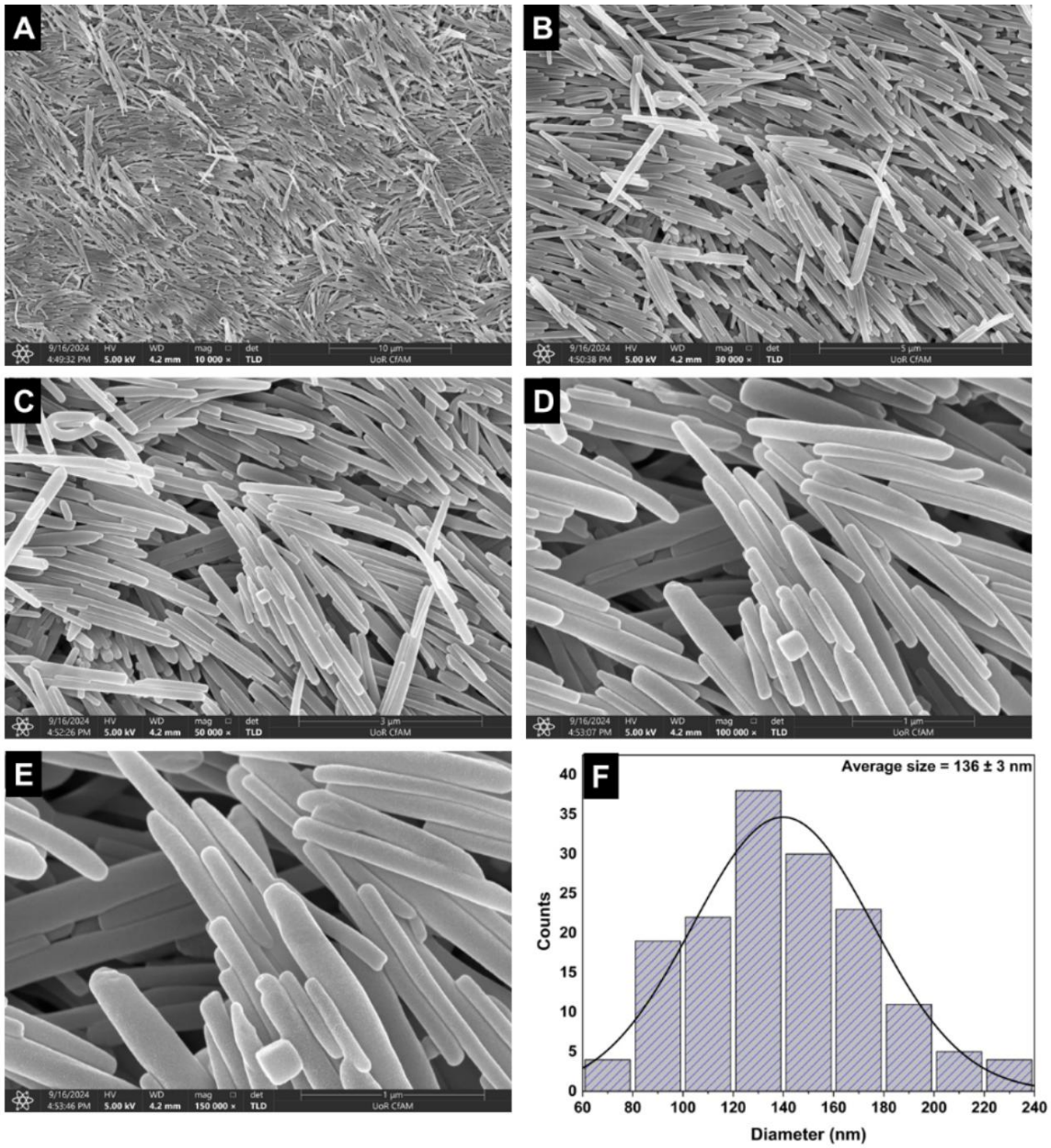

Figure S93. SEM images of xerogel **LMWG3d** at scale bars 10 *μ*m (**A**), 5 *μ*m (**B**), 3 *μ*m (**C**), 1 *μ*m (**D**, **E**), and (**F**) calculated average fibres diameter distributions were observed around 136 nm.

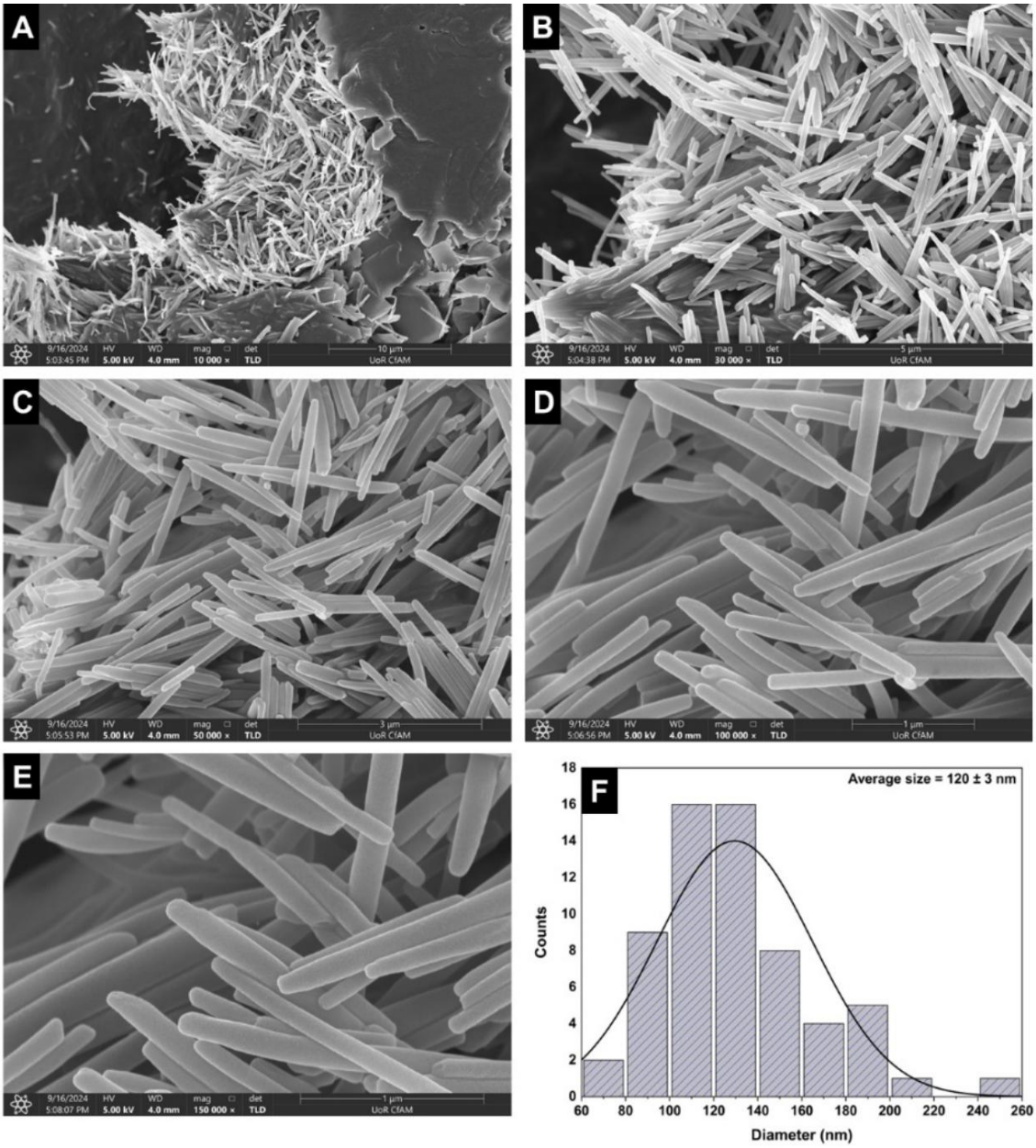

Figure S94. SEM images of xerogel **LMWG3e** at scale bars 10 *μ*m (**A**), 5 *μ*m (**B**), 3 *μ*m (**C**), and 1 *μ*m (**D**, **E**), and (**F**) calculated average fibres diameter distributions were observed around 120 nm.

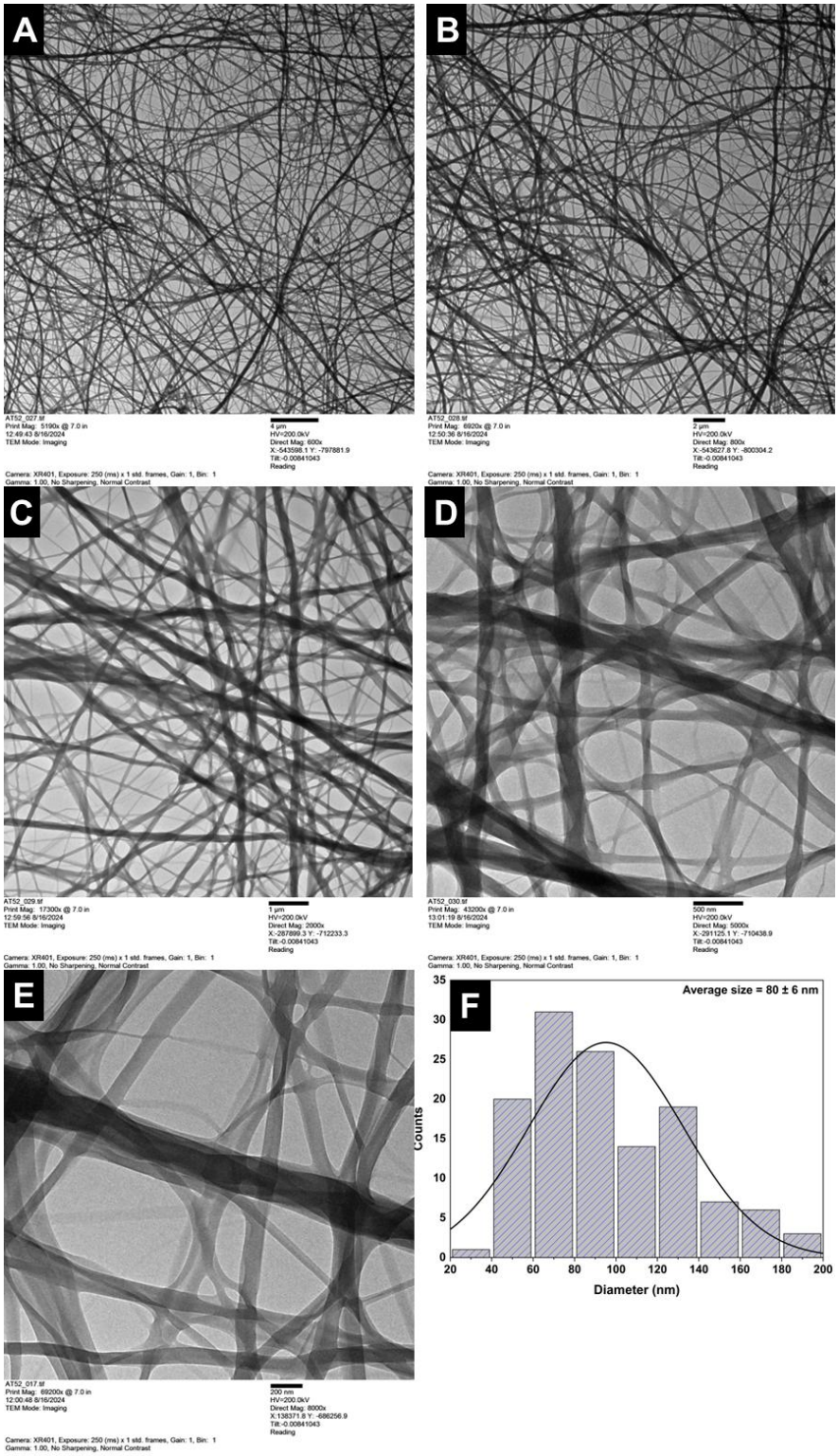

Figure S95. TEM images of xerogel **LMWG1d** at scale bars 4 *μ*m (**A**), 2 *μ*m (**B**), 1 *μ*m (**C**), 500 nm (**D**), 200 nm (**E**), and (**F**) calculated average fibres diameter distributions were observed around 80 nm.

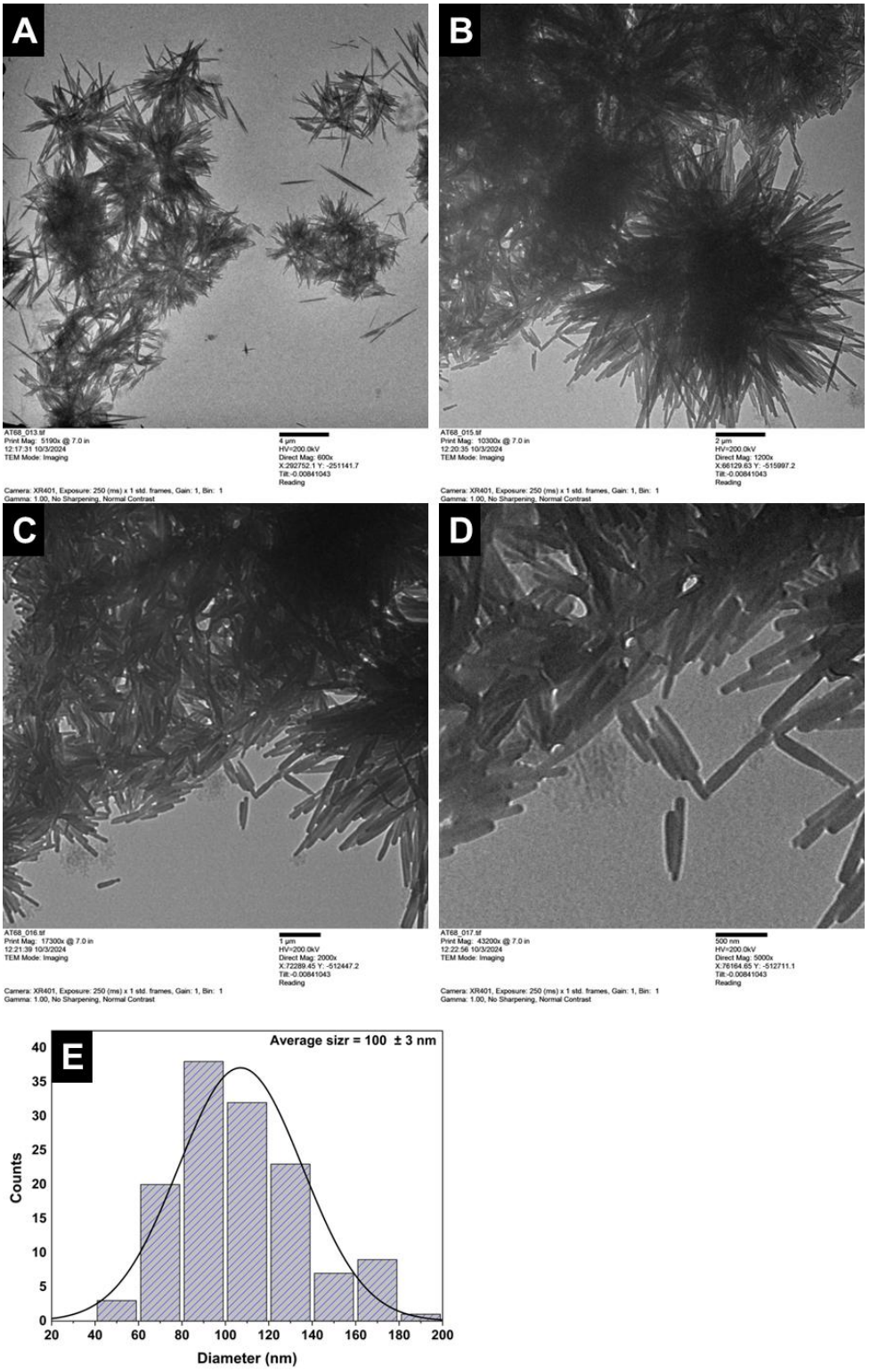

Figure S96. TEM images of xerogel **LMWG2f** at scale bars 4 *μ*m (**A**), 2 *μ*m (**B**), 1 *μ*m (**C**), 500 nm (**D**), and (**E**) calculated average like-rods diameter distributions were observed around 100 nm.

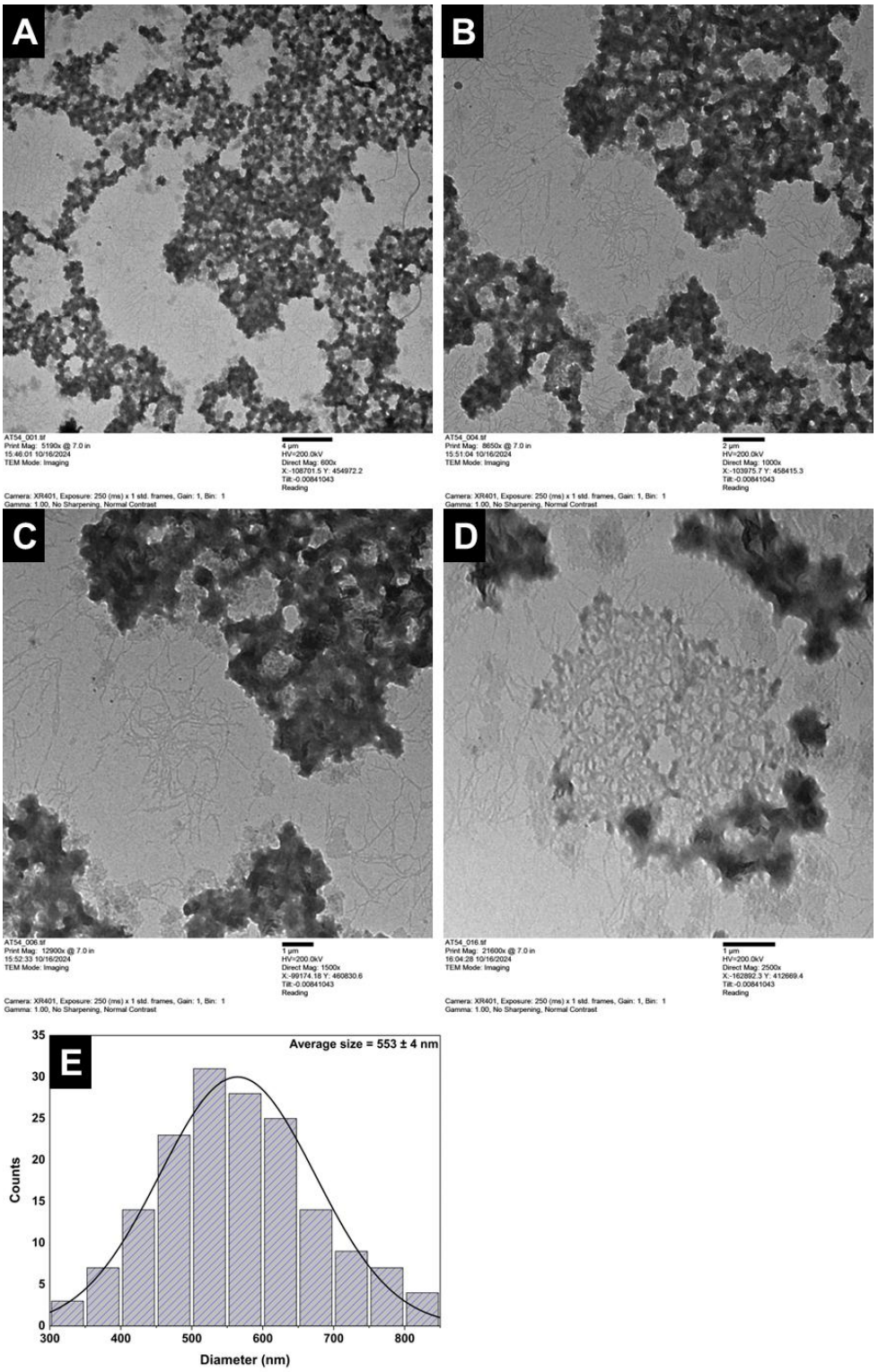

Figure S97. TEM images of xerogel **LMWG3a** at scale bars 4 *μ*m (**A**), 2 *μ*m (**B**), and 1 *μ*m (**C, D**), and (**F**) calculated average spheres/sheets diameter distributions were observed around 553 nm.

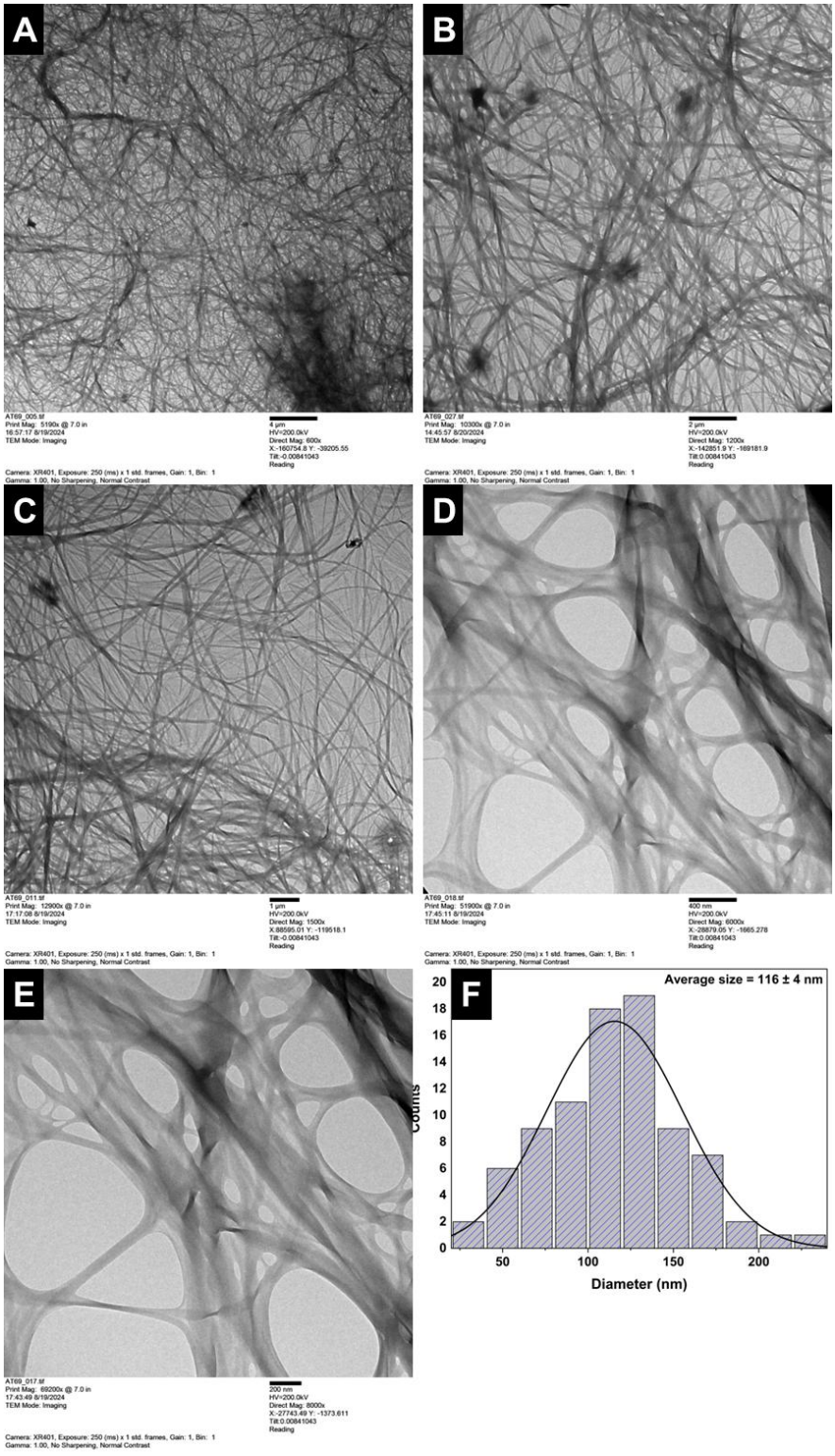

Figure S98. TEM images of xerogel **LMWG3b** at scale bars 4 *μ*m (**A**), 2 *μ*m (**B**), 1 *μ*m (**C**), 400 nm (**D**), 200 nm (**E**), and (**F**) calculated average fibres diameter distributions were observed around 116 nm.

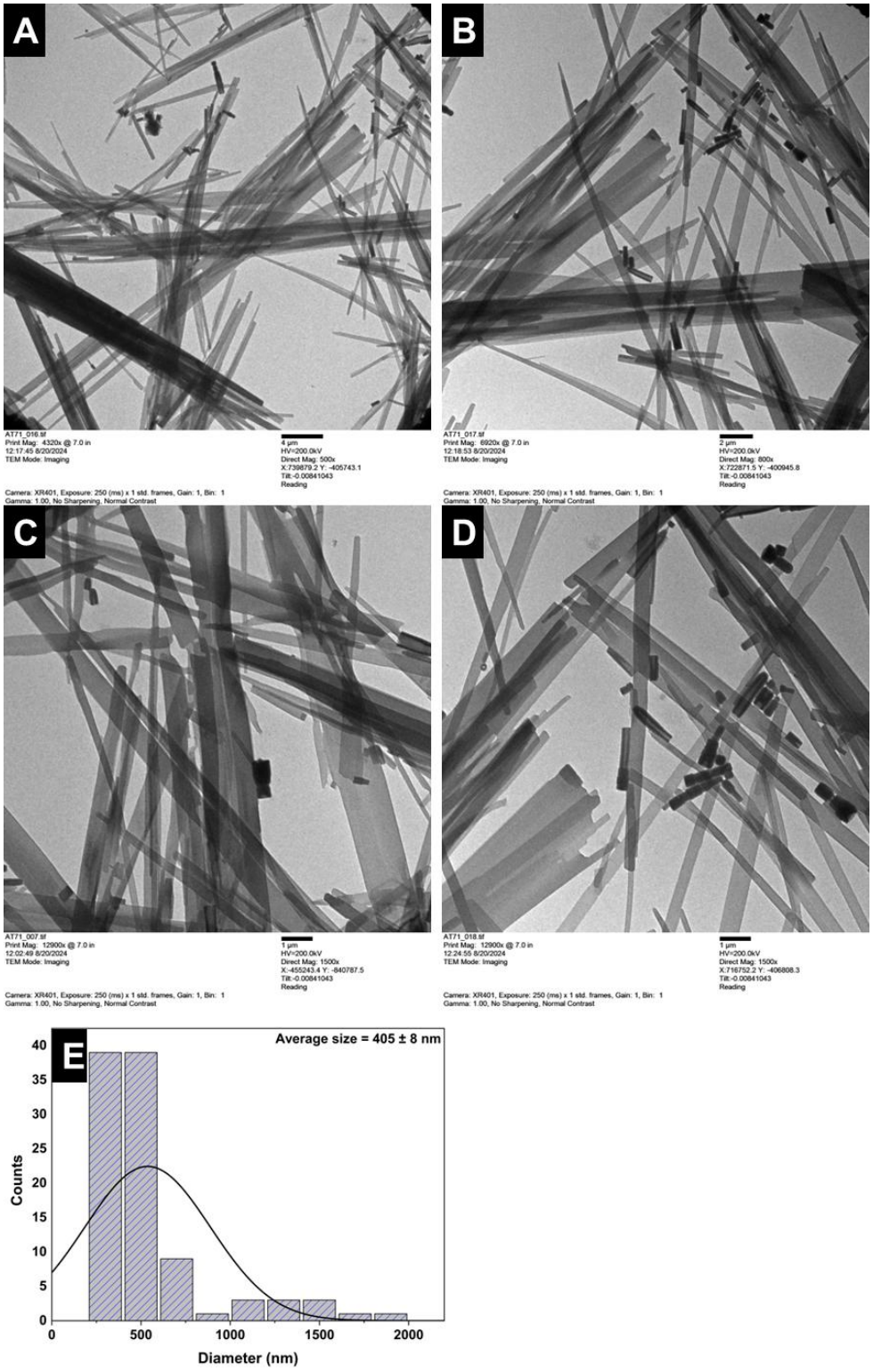

Figure S99. TEM images of xerogel **LMWG3d** at scale bars 4 *μ*m (**A**), 2 *μ*m (**B**), 1 *μ*m (**C, D**), and (**F**) calculated average like-rods diameter distributions were observed around 405 nm.

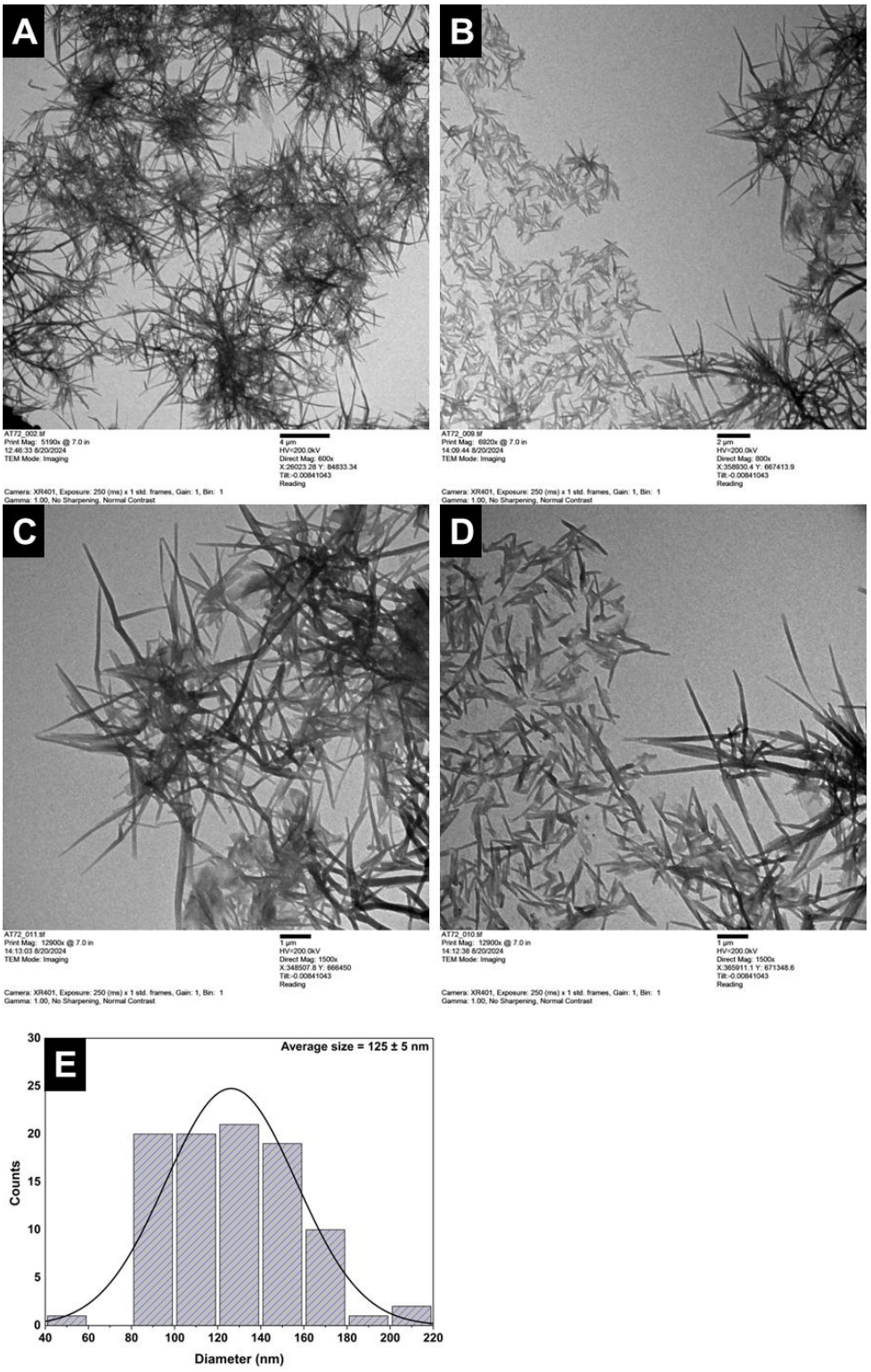

Figure S100. TEM images of xerogel **LMWG3e** at scale bars 4 *μ*m (**A**), 2 *μ*m (**B**), 1 *μ*m (**C, D**), and (**F**) calculated average fibres diameter distributions were observed around 125 nm.

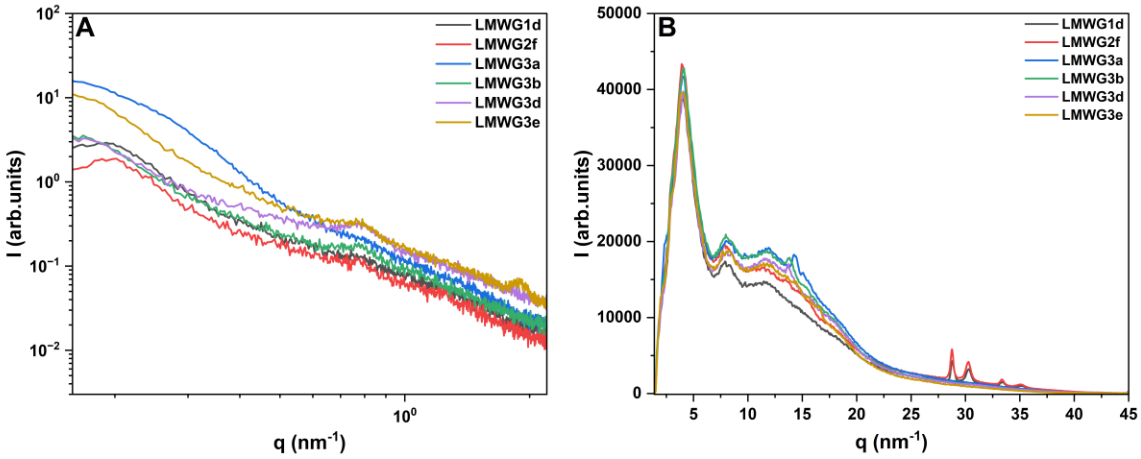

Figure S101: (**A**) SAXS and (**B**) WAXS profiles for xerogels of **LMWG1d-LMWG3e** at 25 °C.

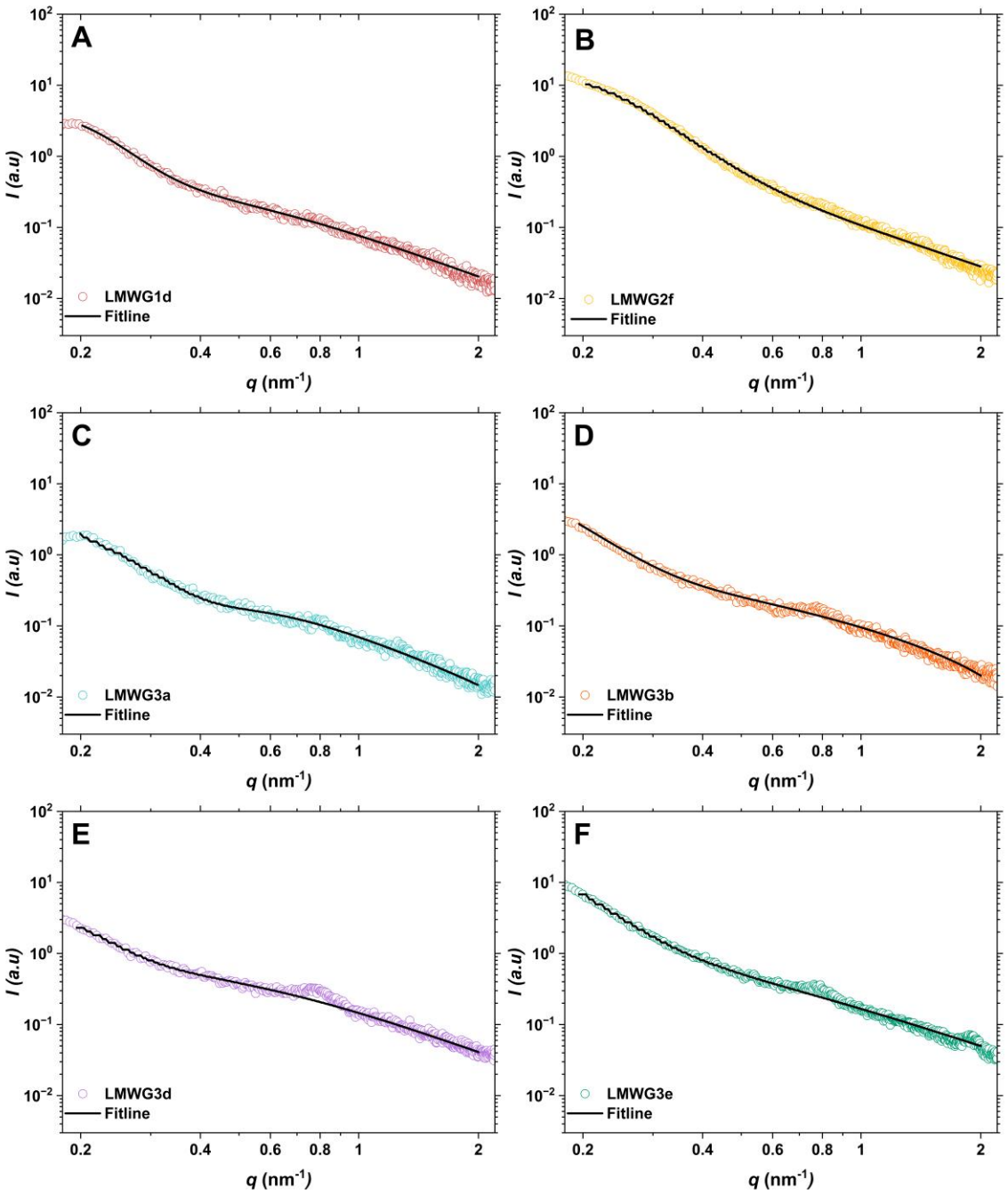

Figure S102: SAXS profiles (**A**-**F**) for xerogels of **LMWG1d**-**LMWG3e** and corresponding fitlines at 25 °C.

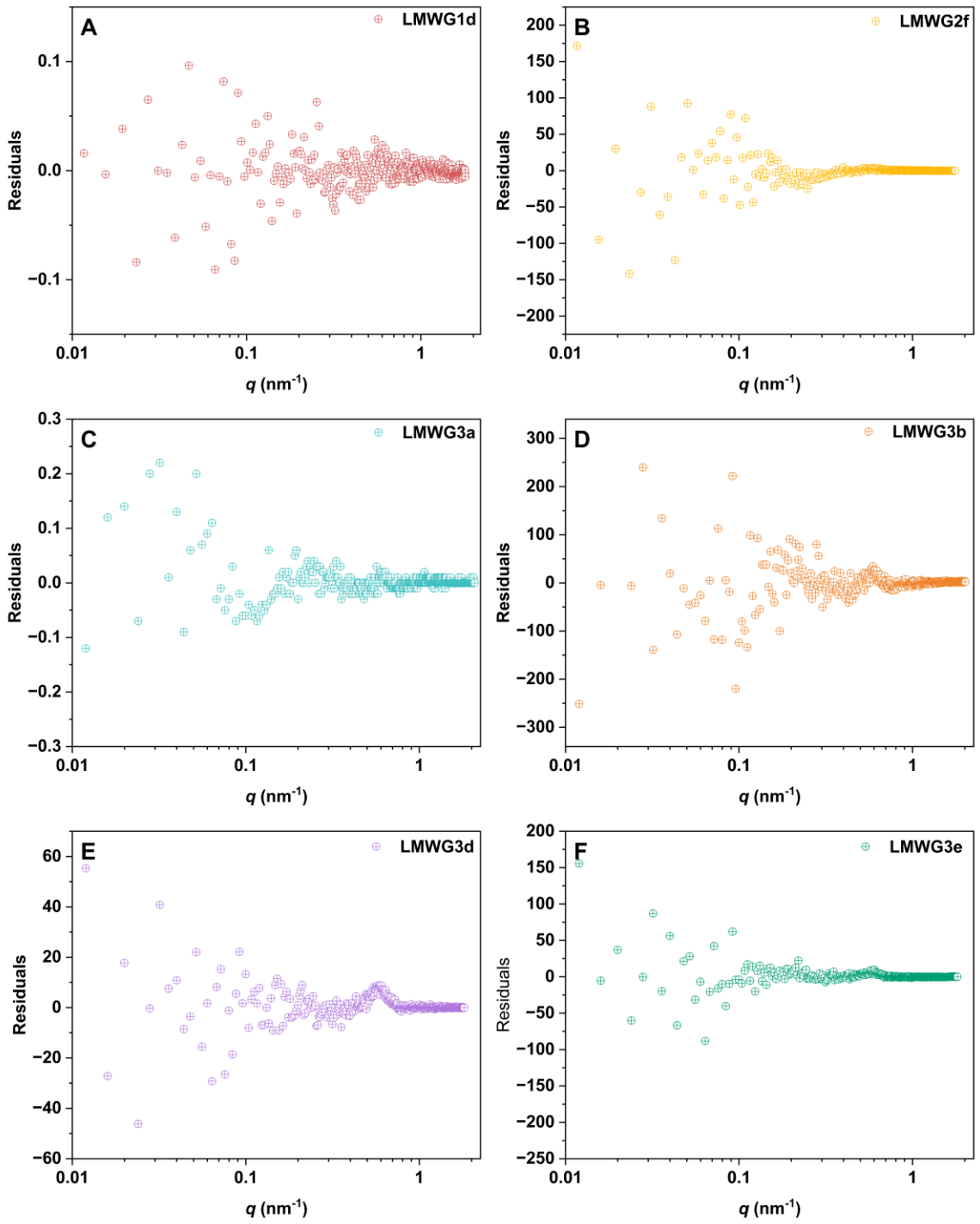

Figure S103: SAXS fitting residuals (**A-F**) for xerogels of **LMWG1d-LMWG3e** at 25 °C.

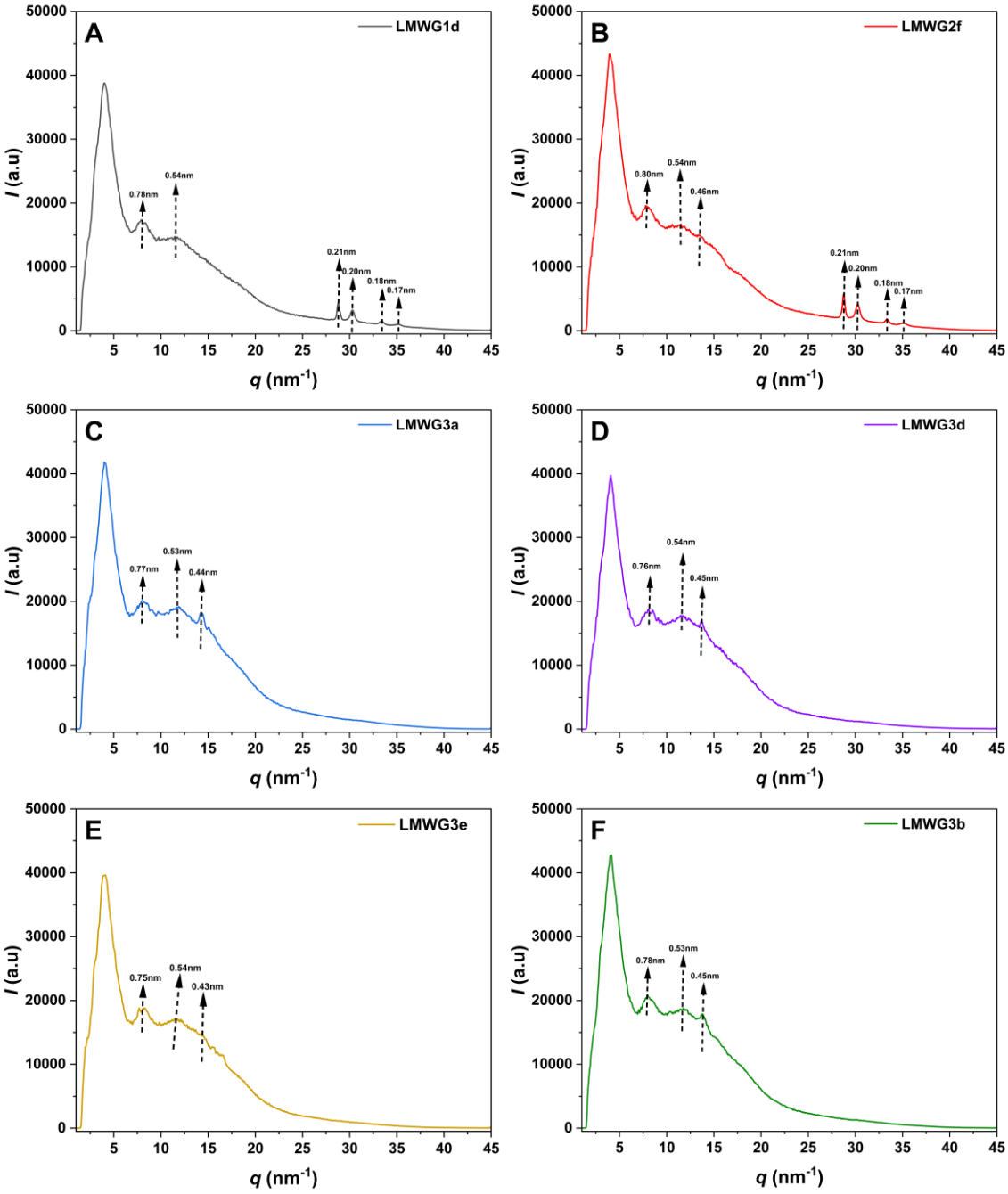

Figure S104: WAXS profiles (**A-F**) for xerogels of **LMWG1d-LMWG3e** at 25 °C.

Table S2. Summary of the parameters obtained from the fits of all the LMWGs.

Model (two_lorentzian)	LMWG1d	LMWG2f	LMWG3a	LMWG3b	LMWG3d	LMWG3e
lorentz_scale_1	3.99	16.25	2.46	10.17	3.50	15.13
lorentz_length_1(nm)	46.73 ± 21.06	43.40 ± 0.01	46.43 ± 0.16	65.66 ± 0.04	50.66 ± 0.17	55.12 ± 0.03
lorentz_exp_1	6.26	4.77	6.98	5.19	6.01	4.83
lorentz_scale_2	0.39	0.50	0.39	0.50	0.70	0.90
lorentz_length_2(nm)	19.00 ± 1.05	21.00 ± 0.06	22.51 ± 2.06	20.01 ± 0.01	19.00 ± 0.03	22.01 ± 0.01
lorentz_exp_2	2.19	2.00	2.03	2.10	2.10	1.93

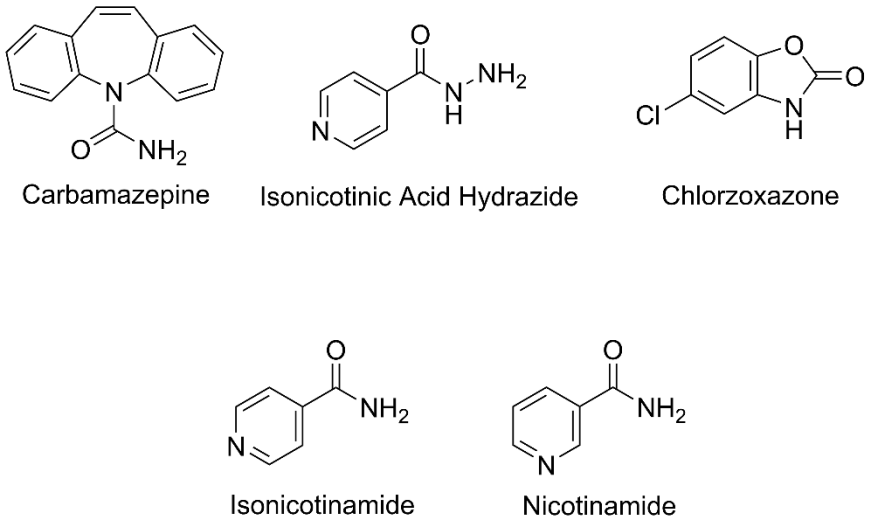

Figure S105: Chemical structures of the representative API's demonstrated for crystallization in LMWGs media.

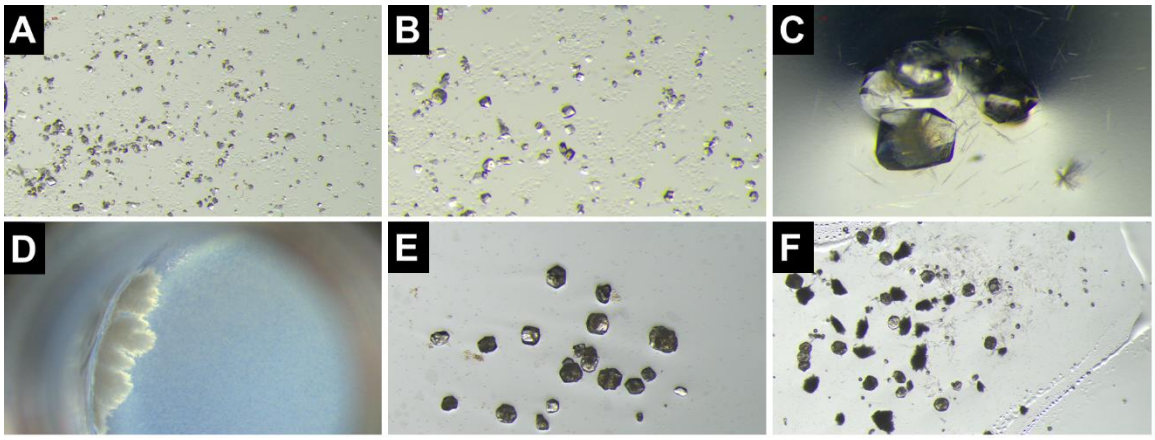

Figure S106: Morphology of the Carbamazepine (CBZ) crystals in 1 wt.% gelator, (**A**, **D**) 40 mg and 80 mg in **LMWG2f** (1,2,4-trichlorobenzene) ×7.5 magnification, (**B**, **E**) 40 mg and 80 mg in **LMWG3b** (1,2,4-trichlorobenzene) ×7.5 and ×15 magnification, respectively, and (**C**, **F**) 40 mg and 80 mg in **LMWG3d** (1,2,4-trichlorobenzene) ×30 and ×7.5 magnification, respectively.

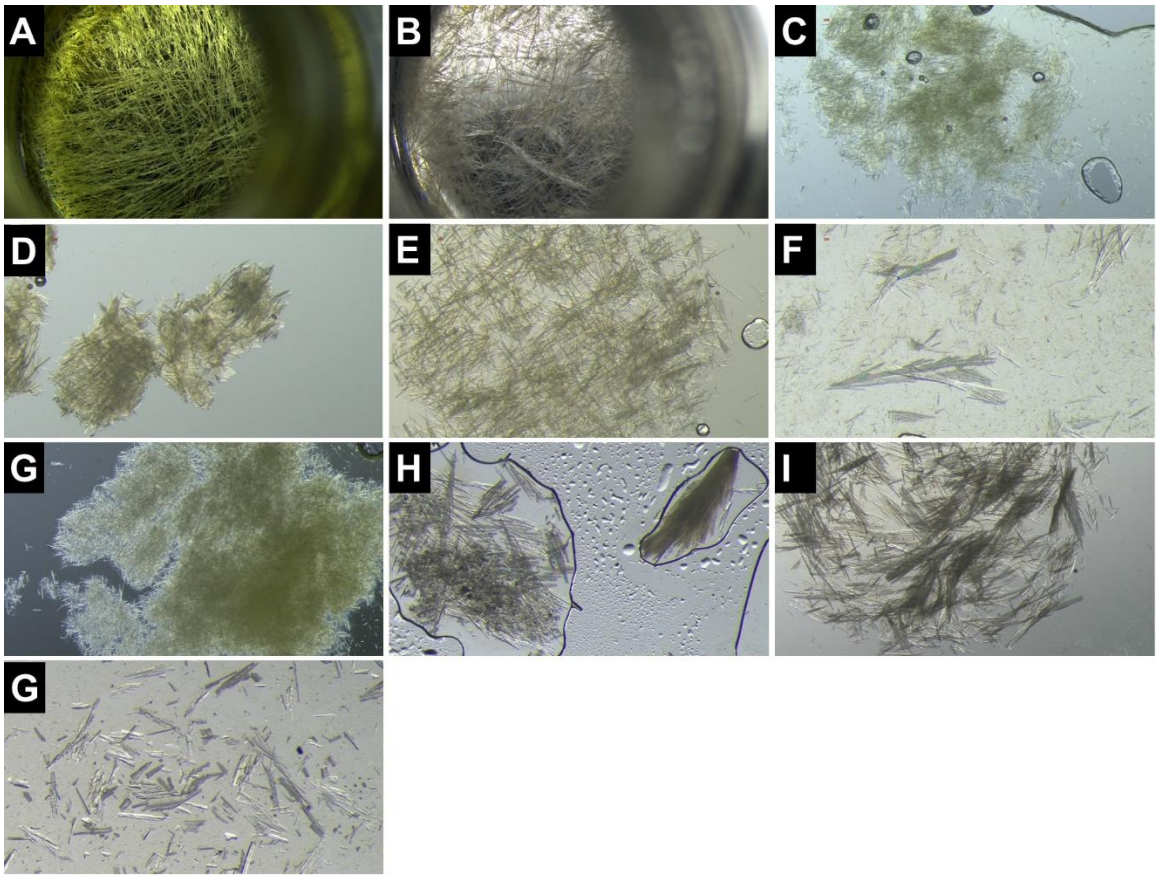

Figure S107: Morphology of the Isonicotinic Acid Hydrazide (ISONIAZID) crystals in 1 wt.% gelator, (**A**,**B**) non-gel (reference sample) nitrobenzene and 1,2,4-trichlorobenzene, (**C**,**G**) 40 mg and 80 mg in **LMWG1d** (nitrobenzene) ×7.5 magnification, (**D**,**H**) 40 mg and 80 mg in **LMWG2f** (1,2,4-trichlorobenzene) ×12 magnification, (**E**,**I**) 40 mg and 80 mg in **LMWG3b** (1,2,4-trichlorobenzene) ×7.5 magnification, and (**F**,**G**) 40 mg and 80 mg in **LMWG3d** (1,2,4-trichlorobenzene) ×7.5 and ×15 magnification, respectively.

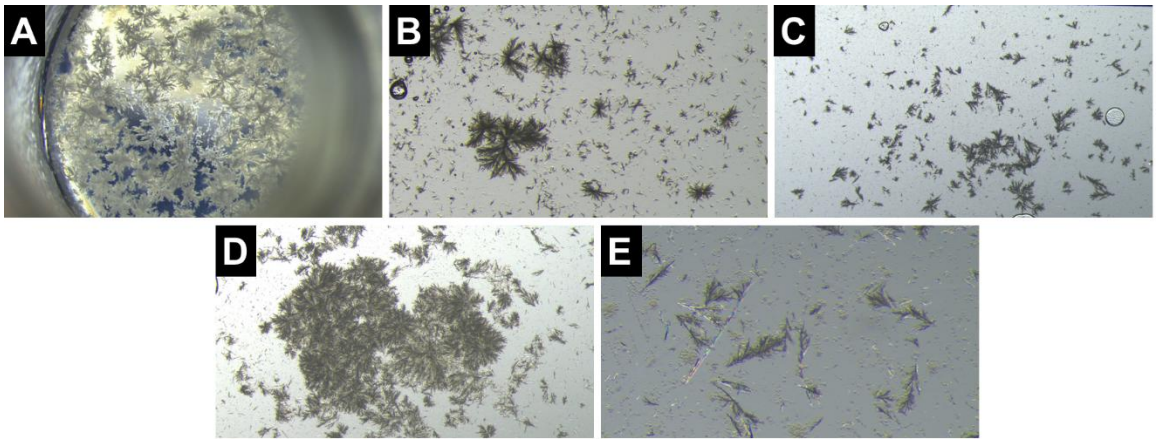

Figure S108: Morphology of the Chlorzoxazone (CHZ) crystals, 10 mg in 1 wt.% gelator, (**A**) **LMWG2f** (1,2,4-trichlorobenzene) ×7.5 magnification, (**B**) **LMWG3a** (DMSO) ×15 magnification, (**C**) **LMWG3b** (1,2,4-trichlorobenzene) ×12 magnification, (**D**) **LMWG3d** (1,2,4-trichlorobenzene) ×12 magnification, and (**E**) **LMWG3e** (1,2,4-trichlorobenzene) ×24 magnification.

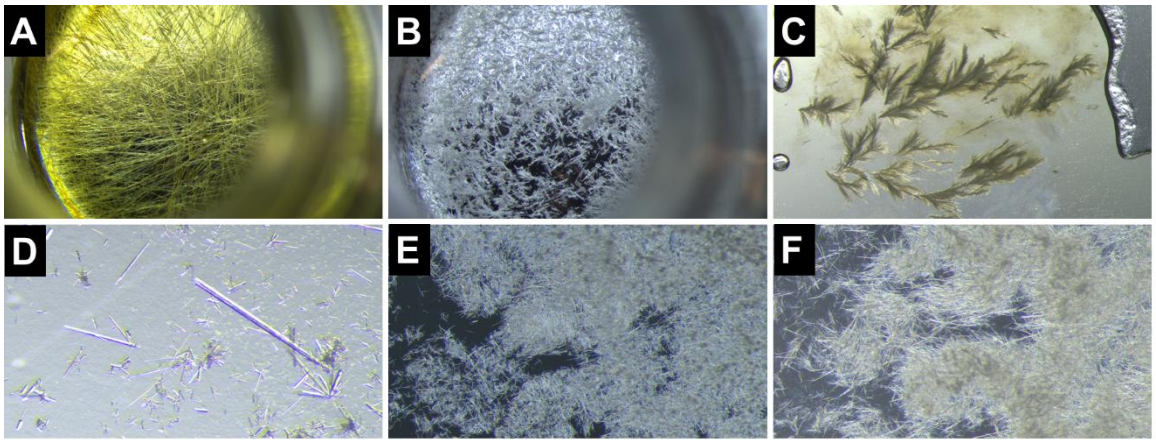

Figure S109: Morphology of the Nicotinamide (NIC) crystals, 10 mg in 1 wt.% gelator, (**A**,**B**) non-gel (reference sample) nitrobenzene and 1,2,4-trichlorobenzene, (**C**) **LMWG1d** (nitrobenzene) ×7.5 magnification, (**D**) **LMWG2f** (1,2,4-trichlorobenzene) ×15 magnification, (**E**) **LMWG3b** (1,2,4-trichlorobenzene) ×12 magnification, and (**F**) **LMWG3b** (DMSO) ×15 magnification.

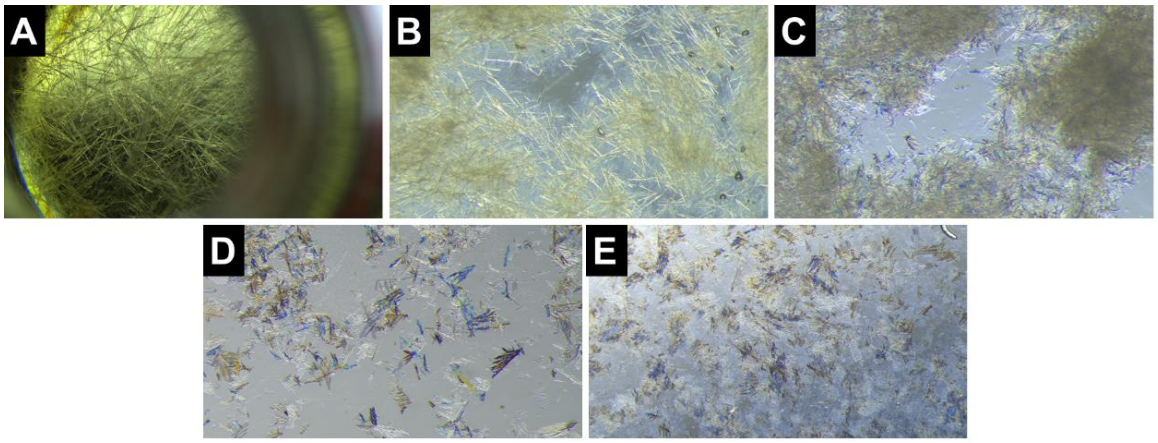

Figure S110: Morphology of the Isonicotinamide (ISON) crystals, 10 mg in 1 wt.% gelator, (**A**) non-gel (reference sample) nitrobenzene, (**B**) **LMWG1d** (nitrobenzene) ×12 magnification, (**C**) **LMWG2f** (1,2,4-trichlorobenzene) ×12 magnification, (**D**) **LMWG3b** (1,2,4-trichlorobenzene) ×12 magnification, and (**E**) **LMWG3b** (DMSO) ×7.5 magnification.

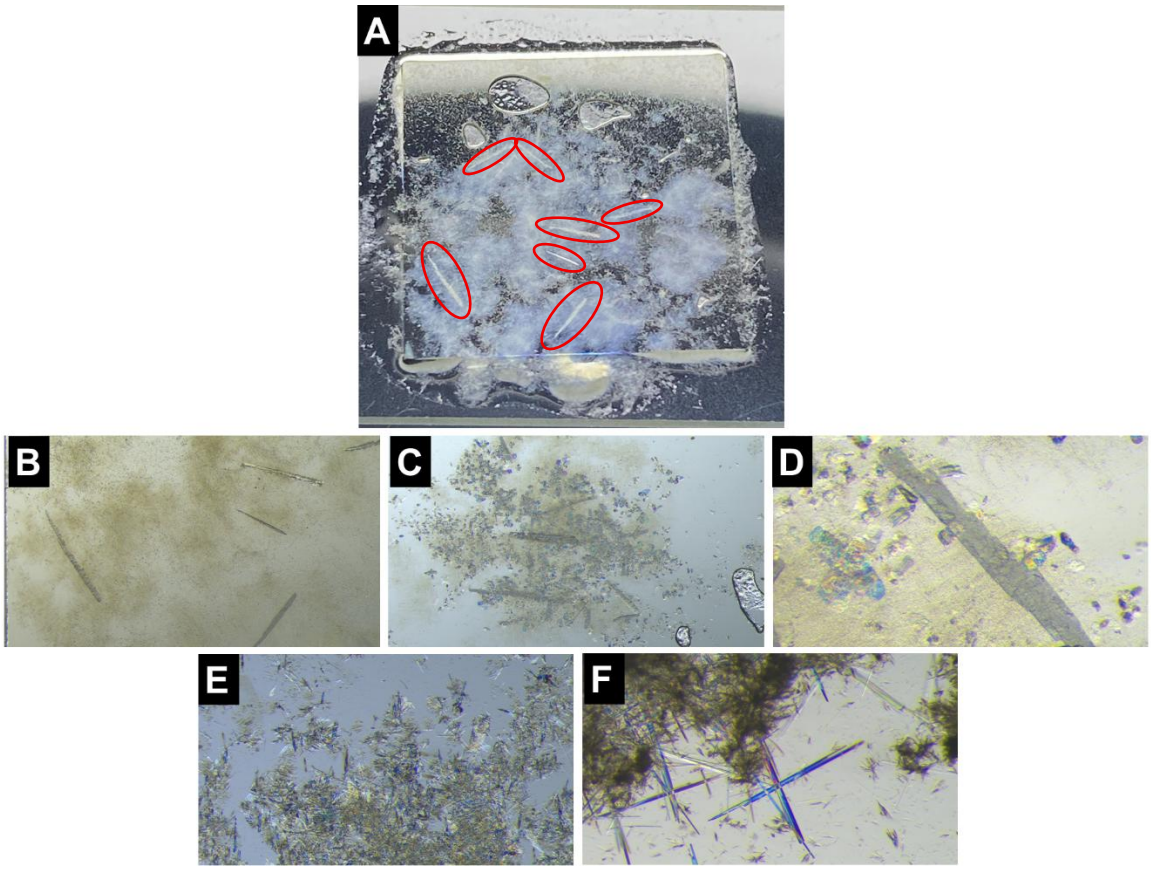

Figure S111: Morphology of the Chloroxazone and Isonicotinamide (co-CHZ-ISON) co-crystals (1:1 mole), (13.88 mg :10 mg) in 1 wt.% gelator, (**A**,**B**) **LMWG1d (**nitrobenzene) after 3 hours (red circles), ×7.5 magnification for image (**B**), (**C**,**D**) **LMWG1d (**nitrobenzene) after 24 hours, ×7.5 and ×30 magnification, respectively, (**E**) **LMWG3e** (DMSO) ×7.5 magnification, and (**F**) Chloroxazone and Nicotinamide (co-CHZ-NIC) co-crystals, (1:1 mole), (13.88 mg :10 mg) in 1 wt% of **LMWG3d** (1,2,4-trichlorobenzene) ×30 magnification.

Table S3. Lattice parameters of novel co-crystals at 100 K

APIs	SG	*a* /Å	*b* /Å	*c* /Å	*V* / Å^3	CCDC deposition	Expt number
CHZ-ISON (1:1)	*P n* 2_1 *a*	12.35473(14)	38.9932(5)	5.33318(6)	2569.26(5)	2468350	2879
CHZ-NIC (1:1)	*P n* 2_1 *a*	11.93448(15)	42.5963(5)	5.05886(7)	2571.75(6)	2490051	3095

Table S4. Crystallographic details of CHZ:ISON (1:1) co-crystal

Formula	$C_7 H_4 Cl N O_2$, $C_6 H_6 N_2 O$
M_r	291.69
Crystal system	orthorhombic
Space group	*P n* 2_1 *a*
Z	8
a / Å	12.35473(14)
b/ Å	38.9932(5)
c / Å	5.33318(6)
V / Å^3	2569.26(5)
D_{calc} / g cm^{-3}	1.508
Crystal habit	Yellow plate
Crystal dimensions / mm	0.023 × 0.079 × 0.117
Radiation	Cu K_α (1.54184 Å)
T / K	100
μ / mm^{-1}	2.754
R(*F*), *Rw*(*F*)	3.68, 9.07
CCDC deposition number	2468350

Table S5: Selected bond lengths (Å) and angles (°) for CHZ:ISON (1:1) co-crystal.

Cl(1) – C(2)	1.743(3)	C(6) – O(7) – C(8)	106.77(18)
Cl(12) – C(13)	1.755(3)	C(16) – O(17) – C(18)	106.56(18)
O(7) – C(6)	1.381(3)	C(4) – N(5) – C(6)	109.0(2)
O(7) – C(8)	1.391(3)	C(18) – N(20) – C(21)	109.1(2)
O(11) – C(6)	1.216(3)	C(28) – N(29) – C(30)	117.1(2)
O(17) – C(16)	1.384(3)	C(37) – N(38) – C(39)	116.9(2)
O(17) – C(18)	1.387(3)	Cl(1) – C(2) – C(3)	117.7(2)
O(19) – C(18)	1.210(3)	Cl(1) – C(2) – C(10)	119.1(2)
O(23) – C(24)	1.238(3)	C(3) – C(2) – C(10)	123.2(2)
O(32) – C(33)	1.245(3)	C(2) – C(3) – C(4)	115.7(2)
N(5) – C(4)	1.388(3)	N(5) – C(4) – C(3)	132.3(2)
N(5) – C(6)	1.354(3)	N(5) – C(4) – C(8)	106.6(2)
N(20) – C(18)	1.353(3)	C(3) – C(4) – C(8)	121.2(2)
N(20) – C(21)	1.393(3)	O(7) – C(6) – O(11)	121.6(2)
N(25) – C(24)	1.339(3)	O(7) – C(6) – N(5)	109.0(2)
N(29) – C(28)	1.352(3)	O(11) – C(6) – N(5)	129.3(2)
N(29) – C(30)	1.339(3)	O(7) – C(8) – C(4)	108.6(2)
N(34) – C(33)	1.327(3)	O(7) – C(8) – C(9)	128.0(2)
N(38) – C(37)	1.331(3)	C(4) – C(8) – C(9)	123.3(2)
N(38) – C(39)	1.344(3)	C(8) – C(9) – C(10)	116.5(2)
C(2) – C(3)	1.395(4)	C(2) – C(10) – C(9)	120.1(2)
C(2) – C(10)	1.389(4)	Cl(12) – C(13) – C(14)	118.5(2)
C(3) – C(4)	1.379(4)	Cl(12) – C(13) – C(22)	117.7(2)
C(4) – C(8)	1.388(3)	C(14) – C(13) – C(22)	123.7(2)

C(8) – C(9)	1.368(4)	C(13) – C(14) – C(15)	120.0(2)
C(9) – C(10)	1.397(4)	C(14) – C(15) – C(16)	115.9(2)
C(13) – C(14)	1.388(4)	O(17) – C(16) – C(15)	127.3(2)
C(13) – C(22)	1.385(4)	O(17) – C(16) – C(21)	109.4(2)
C(14) – C(15)	1.400(4)	C(15) – C(16) – C(21)	123.3(2)
C(15) – C(16)	1.383(4)	O(17) – C(18) – O(19)	121.6(2)
C(16) – C(21)	1.380(3)	O(17) – C(18) – N(20)	108.8(2)
C(21) – C(22)	1.380(4)	O(19) – C(18) – N(20)	129.6(2)
C(24) – C(26)	1.502(3)	N(20) – C(21) – C(16)	106.2(2)
C(26) – C(27)	1.399(3)	N(20) – C(21) – C(22)	132.4(2)
C(26) – C(31)	1.392(3)	C(16) – C(21) – C(22)	121.4(2)
C(27) – C(28)	1.382(4)	C(13) – C(22) – C(21)	115.6(2)
C(30) – C(31)	1.379(4)	O(23) – C(24) – N(25)	122.7(2)
C(33) – C(35)	1.505(3)	O(23) – C(24) – C(26)	119.8(2)
C(35) – C(36)	1.393(3)	N(25) – C(24) – C(26)	117.5(2)
C(35) – C(40)	1.390(3)	C(24) – C(26) – C(27)	118.1(2)
C(36) – C(37)	1.383(4)	C(24) – C(26) – C(31)	123.7(2)
C(39) – C(40)	1.376(4)	C(27) – C(26) – C(31)	118.2(2)
		C(26) – C(27) – C(28)	118.8(2)
		N(29) – C(28) – C(27)	123.1(2)
		N(29) – C(30) – C(31)	123.8(2)
		C(26) – C(31) – C(30)	118.9(2)
		O(32) – C(33) – N(34)	122.9(2)
		O(32) – C(33) – C(35)	119.1(2)
		N(34) – C(33) – C(35)	118.0(2)

		C(33) – C(35) – C(36)	123.3(2)
		C(33) – C(35) – C(40)	118.9(2)
		C(36) – C(35) – C(40)	117.8(2)
		C(35) – C(36) – C(37)	118.4(2)
		N(38) – C(37) – C(36)	124.2(2)
		N(38) – C(39) – C(40)	123.1(2)
		C(35) – C(40) – C(39)	119.5(2)

Table S6: Hydrogen-bond interactions (Å, °) for CHZ:ISON (1:1) co-crystal.

D – H•••A	*D* – H	H•••*A*	*D* •••*A*	*D* – H•••*A*
N(5) – H(51)•••N(29)[i]	0.861(10)	1.923(12)	2.777(4)	171(4)
N(20) – H(201)•••N(38)[ii]	0.855(10)	1.929(11)	2.779(4)	173(4)
N(25) – H(251)•••O(32)	0.861(10)	2.002(11)	2.860(4)	174(3)
N(25) – H(252)•••O(11)[iii]	0.857(10)	2.146(14)	2.972(4)	162(3)
N(34) – H(341)•••O(19)[iv]	0.849(9)	2.137(11)	2.980(4)	171(3)
N(34) – H(342)•••O(23)	0.853(10)	2.017(10)	2.869(4)	178(3)

Symmetry Codes: (i) –*x* + 3/2, *y* + 1/2, *z* + 3/2; (ii) *x*, *y* , *z* – 1; (iii) –*x* + 2, *y* – 1/2, –*z*; (iv) –*x* – 1/2, *y*, *z* + ½.

Table S7: Graph set description of H-bonding in CBZ-ISON (1:1) co-crystal

Descriptor	Atoms	Symmetry Operator	H-bond designation	Level	Period	No. of molecules
D1,1(2)	H51 N29	*x*,*y*,*z* 3/2-*x*,1/2+*y*,3/2+*x*	*a*	1		2
D1,1(2)	H201 N38	*x*,*y*,*z* *x*,*y*,-1+*z*	*b*	1		2
D1,1(2)	H251 O32	*x*,*y*,*z* *x*,*y*,*z*	*c*	1		2
D1,1(2)	H252 O11	*x*,*y*,*z* 2-*x*,-1/2+*y*,-*z*	*d*	1		2
D1,1(2)	H341 O19	*x*,*y*,*z* -1/2+*x*,*y*,1/2-*z*	*e*	1		2
D1,1(2)	H342 O23	*x*,*y*,*z* *x*,*y*,*z*	*f*	1		2
D2,2(9)	H51 N29-C30-C31-C26-C24-N25-H251 O32	*x*,*y*,*z* 3/2-*x*,1/2+*y*,3/2+*z* 3/2-*x*,1/2+*y*,3/2+*z*	*a* *c*	2		3
C2,2(11)	H51 N29-C30-C31-C26-C24-N25-H252 O11-C6-N5	*x*,*y*,*z* 3/2-*x*,1/2+*y*,3/2+*z* -1/2-*x*,*y*,3/2-*z*	*a* *d*	2	2	3
D2,2(8)	H51 N29-C30-C31-C26-C24-O23 H342	*x*,*y*,*z* 3/2-*x*,1/2+*y*,3/2+*z* 3/2-*x*,1/2+*y*,3/2+*z*	*a* <*f*	2		3
D2,2(8)	H201 N38-C37-C36-C35-C33-O32 H251	*x*,*y*,*z* *x*,*y*,-1+*z* *x*,*y*,-1+*z*	*b* <*c*	2		3
C2,2(11)	H201 N38-C37-C36-C35-C33-N34-H341	*x*,*y*,*z* *x*,*y*,-1+*z*	*b* *e*	2	2	3

	O19-C18-N20	-1/2+*x*,*y*,-1/2+*z*				
D2,2(9)	H201 N38-C37-C36-C35-C33-N34-H342 O23	*x*,*y*,*z* *x*,*y*,-1+*z* *x*,*y*,-1+*z*	*b* *f*	2		3
D2,2(5)	O32 H251-N25-H252 O11	*x*,*y*,*z* *x*,*y*,*z* 2-*x*,-1/2+*y*,-*z*	<*c* *d*	2		3
D2,2(6)	H251 O32-C33-N34-H341 O19	*x*,*y*,*z* *x*,*y*,*z* -1/2+*x*,*y*,1/2-*z*	*c* *e*	2		3
R2,2(8)	H251 O32-C33-N34-H342 O23-C24-N25	*x*,*y*,*z* *x*,*y*,*z* *x*,*y*,*z*	*c* *f*	2	2	2
D2,2(6)	H342 O23-C24-N25-H252 O11	*x*,*y*,*z* *x*,*y*,*z* 2-*x*,-1/2+*y*,-*z*	*f* *d*	2		3
D2,2(5)	O19 H341-N34-H342 O23	-1/2+*x*,*y*,1/2-*z* *x*,*y*,*z* *x*,*y*,*z*	<*e* *f*	2		3

Descriptor Graph set type. Capitalised letter identifies pattern: D (= finite discrete) C (= infinite chain), R (= ring); next two numbers give the number of acceptors and donors in the pattern; bracketed number identifies the number of atoms in pattern. **Atoms** CIF labels for the atoms in the pattern. Each line of atoms for a given set lists the participating atoms of one individual molecule in that set; the corresponding symmetry operator identifies the symmetry relationship of the participating atoms relative to the first atom in the set. **H-bond designation** Letters indicate the symmetry equivalence of the H-bonds within a pattern – thus, all H-bonds labelled *a* are symmetry equivalent, but are not symmetry equivalent to H-bonds labelled *b*. The “>“ and “<” symbols indicate the direction of the H bond (D to A or A to D). **Level** Indicates the number of symmetry-independent H-bonds bonds that compose a given pattern. The graph set analysis was conducted with the Mercury default that finds graph sets up to level 2. **Period** The size of the repeat unit (number of hydrogen bonds) for ring and chain patterns. **No. of molecules** The total number of molecules participating in a pattern. The sets are most easily visualised by loading the CIF into Mercury and selecting “Calculate, Graph Sets…”.

Table S8: Crystallographic details of CHZ:NIC (1:1) co-crystal

Formula	$C_7\,H_4\,Cl\,N\,O_2$, $C_6\,H_6\,N_2\,O$
M_r	291.69
Crystal system	orthorhombic
Space group	*P n* 2_1 *a*
Z	8
a / Å	11.93448(15)
b/ Å	42.5963(5)
c / Å	5.05886(7)
V / Å^3	2571.75(6)
D_{calc} / g cm^{-3}	1.507
Crystal habit	Colourless rod
Crystal dimensions /mm	0.023 × 0.036 × 0.257
Radiation	Cu K_α (1.54184 Å)
T / K	100
μ / mm^{-1}	2.752
R(*F*), *Rw*(*F*)	5.31, 12.77
CCDC deposition number	2490051

Table S9: Selected bond lengths (Å) and angles (°) for CHZ:NIC (1:1) co-crystal.

Cl(1) – C(2)	1.749(4)	C(6) – O(7) – C(8)	106.7(3)
Cl(12) – C(13)	1.756(4)	C(17) – O(18) – C(19)	106.6(3)
O(7) – C(6)	1.382(5)	C(4) – N(5) – C(6)	109.7(3)
O(7) – C(8)	1.390(4)	C(15) – N(16) – C(17)	110.1(3)
O(11) – C(6)	1.213(5)	C(27) – N(28) – C(29)	117.4(3)
O(18) – C(17)	1.394(5)	C(36) – N(37) – C(38)	117.4(3)
O(18) – C(19)	1.393(4)	Cl(1) – C(2) – C(3)	117.5(3)
O(22) – C(17)	1.211(5)	Cl(1) – C(2) – C(10)	118.8(3)
O(23) – C(24)	1.249(4)	C(3) – C(2) – C(10)	123.5(4)
O(32) – C(33)	1.245(5)	C(2) – C(3) – C(4)	115.4(4)
N(5) – C(4)	1.391(5)	N(5) – C(4) – C(3)	132.5(4)
N(5) – C(6)	1.347(5)	N(5) – C(4) – C(8)	105.9(3)
N(16) – C(15)	1.385(5)	C(3) – C(4) – C(8)	121.5(4)
N(16) – C(`7)	1.350(5)	O(7) – C(6) – O(11)	121.9(4)
N(25) – C(24)	1.320(5)	O(7) – C(6) – N(5)	108.5(3)
N(28) – C(27)	1.366(5)	O(11) – C(6) – N(5)	129.5(4)
N(28) – C(29)	1.321(5)	O(7) – C(8) – C(4)	109.2(3)
N(34) – C(33)	1.316(5)	O(7) – C(8) – C(9)	127.0(3)
N(37) – C(36)	1.332(5)	C(4) – C(8) – C(9)	123.8(4)
N(37) – C(38)	1.341(5)	C(8) – C(9) – C(10)	115.4(3)
C(2) – C(3)	1.388(6)	C(2) – C(10) – C(9)	120.3(3)
C(2) – C(10)	1.387(6)	Cl(12) – C(13) – C(14)	117.0(3)
C(3) – C(4)	1.380(6)	Cl(12) – C(13) – C(21)	118.9(3)
C(4) – C(8)	1.376(5)	C(14) – C(13) – C(21)	124.1(4)

C(8) – C(9)	1.377(6)	C(13) – C(14) – C(15)	114.9(3)
C(9) – C(10)	1.406(6)	N(16) – C(15) – C(14)	132.2(4)
C(13) – C(14)	1.387(5)	N(16) – C(15) – C(19)	106.3(3)
C(13) – C(21)	1.384(6)	C(14) – C(15) – C(19)	121.6(4)
C(14) – C(15)	1.390(5)	O(18) – C(17) – O(22)	121.8(4)
C(15) – C(19)	1.375(6)	O(18) – C(17) – N(16)	107.9(3)
C(19) – C(20)	1.375(6)	O(22) – C(17) – N(16)	130.3(4)
C(20) – C(21)	1.407(6)	O(18) – C(19) – C(15)	109.1(3)
C(24) – C(26)	1.503(5)	O(18) – C(19) – C(20)	127.1(4)
C(26) – C(27)	1.374(5)	C(15) – C(19) – C(20)	123.8(4)
C(26) – C(31)	1.398(5)	C(19) – C(20) – C(21)	115.6(4)
C(29) – C(30)	1.389(6)	C(13) – C(21) – C(20)	120.1(3)
C(30) – C(31)	1.375(5)	O(23) – C(24) – N(25)	122.4(3)
C(33) – C(35)	1.505(5)	O(23) – C(24) – C(26)	119.7(3)
C(35) – C(36)	1.388(5)	N(25) – C(24) – C(26)	117.9(3)
C(35) – C(40)	1.376(5)	C(24) – C(26) – C(27)	121.5(3)
C(38) – C(39)	1.381(6)	C(24) – C(26) – C(31)	119.6(3)
C(39) – C(40)	1.396(5)	C(27) – C(26) – C(31)	118.8(3)
		N(28) – C(27) – C(26)	122.7(3)
		N(28) – C(29) – C(30)	123.5(3)
		C(29) – C(30) – C(31)	118.9(3)
		C(26) – C(31) – C(30)	118.6(3)
		O(32) – C(33) – N(34)	123.0(3)
		O(32) – C(33) – C(35)	119.4(3)
		N(34) – C(33) – C(35)	117.6(3)

		C(33) – C(35) – C(36)	121.8(3)
		C(33) – C(35) – C(40)	119.7(3)
		C(36) – C(35) – C(40)	118.4(3)
		N(37) – C(36) – C(35)	123.7(3)
		N(37) – C(38) – C(39)	123.2(3)
		C(38) – C(39) – C(40)	118.5(3)
		C(35) – C(40) – C(39)	118.9(3)

Table S10: Hydrogen-bond interactions (Å, °) for CHZ:NIC (1:1) co-crystal.

D – H•••A	*D* – H	H•••*A*	*D* •••*A*	*D* – H•••*A*
N(5) – H(51)•••N(28)^{i}	0.8500(10)	1.999(8)	2.843(5)	172(4)
N(16) – H(161)•••N(37)^{ii}	0.8499(10)	2.003(9)	2.843(5)	172(4)
N(25) – H(251)•••O(23)^{iii}	0.8500(10)	2.086(19)	2.873(5)	154(3)
N(25) – H(252)•••O(32)	0.8499(10)	2.112(7)	2.958(5)	173(4)
N(34) – H(341)•••O(23)	0.8500(10)	2.099 (9)	2.938(5)	169(4)
N(34) – H(342)•••O(32)^{iv}	0.8500(10)	2.10(2)	2.882(5)	152(4)

Symmetry Codes: (i) –*x*, *y* – 1/2, –*z* + 1; (ii) *x* – 1/2, *y* , *z* – 1/2; (iii) *x*, *y*, *z* + 1; (iv) *x*, *y*, *z* – 1.

Table S11: Graph set description of H-bonding in CHZ:NIC (1:1) co-crystal.

Descriptor	Atoms	Symmetry Operator	H-bond designation	Level	Period	No. of molecules
D1,1(2)	H51 N28	*x*,*y*,*z* -*x*,-1/2+*y*,1-*z*	*a*	1		2
D1,1(2)	H161 N37	*x*,*y*,*z* 1/2-*x*,y,-1/2-*z*	*b*	1		2
C1,1(4)	H251 O23-C24-N25	*x*,*y*,*z* *x*,*y*,1+*z*	*c*	1	1	2
D1,1(2)	H252 O32	*x*,*y*,*z* *x*,*y*,*z*	*d*	1		2
D1,1(2)	H341 O23	*x*,*y*,*z* *x*,*y*,*z*	*e*	1		2
C1,1(4)	H342 O32-C33-N34	*x*,*y*,*z* *x*,*y*,-1+*z*	*f*	1	1	2
D3,3(13)	H51 N28-C27-C26-C24-N25-H251 O23-C24-C26-C27-N28 H51	*x*,*y*,*z* -*x*,-1/2+*y*,1-*z* -*x*,-1/2+*y*,-*z* *x*,*y*,-1+*z*	*a* *c* <*a*	2		4
D2,2(8)	H51 N28-C27-C26-C24-N25-H252 O32	*x*,*y*,*z* -*x*,-1/2+*y*,1-*z* -*x*,-1/2+*y*,1-*z*	*a* *d*	2		3
D2,2(7)	H51 N28-C27-C26-C24-O23 H341	*x*,*y*,*z* -*x*,-1/2+*y*,1-*z* -*x*,-1/2+*y*,1-*z*	*a* <*e*	2		3
D2,2(7)	H161 N37-C36-C35-C33-O32 H252	*x*,*y*,*z* 1/2-*x*,y,-1/2-*z* -1/2+*x*,y,-1/2-*z*	*b* <*d*	2		3

D2,2(8)	H161 N37-C36-C35-C33-N34-H341 O23	*x*,*y*,*z* -1/2+*x*,y,-1/2-*z* -1/2+*x*,y,-1/2-*z*	*b* *e*	2		3
D3,3(13)	H161 N37-C36-C35-C33-N34-H342 O32-C33-C35-C36-N37 H161	*x*,*y*,*z* -1/2+*x*,y,-1/2-*z* -1/2+*x*,y,-1/2-*z* *x*,*y*,-1+*z*	*b* *f* <*b*	2		4
D3,3(9)	O32 H252-N25-C24-O23 H251-N25-H252 O32	*x*,*y*,1+*z* *x*,*y*,1+*z* *x*,*y*,*z* *x*,*y*,1+*z*	<*d* *c* *d*	2		4
D2,3(7)	H341 O23 H251-N25-C24-O23 H341	*x*,*y*,*z* *x*,*y*,*z* *x*,*y*,*z* *x*,*y*,*z*	*e* *c* <*e*	2		4
R2,2(8)	H252 O32-C33-N34-H341 O23-C24-N25	*x*,*y*,*z* *x*,*y*,*z* *x*,*y*,*z*	*d* *e*	2	2	2
D2,3(7)	H252 O32 H342-N34-C33-O32 H252	*x*,*y*,-1+*z* *x*,*y*,-1+*z* *x*,*y*,*z* *x*,*y*,*z*	*d* *f* <*d*	2		4
D3,3(9)	O23 H341-N34-H342 O32-C33-N34-H341 O23	*x*,*y*,*z* *x*,*y*,*z* *x*,*y*,-1+*z* *x*,*y*,-1+*z*	<*e* *f* *e*	2		4

Note: See **Table S7** for legend.

References

1. L. R. Hoggard, Y. Zhang, M. Zhang, V. Panic, J. A. Wisniewski and H. Ji, *J. Am. Chem. Soc.*, 2015, **137**, 12249–12260.
2. A. Z. Tareq, M. Hyder, D. H. Merino, A. M. Chippindale, A. Kaur, J. A. Cooper and W. Hayes, *Polymer*, 2024, **302**, 127052.
3. A. Blair, L. Stevenson and A. Sutherland, *Tetrahedron Lett.*, 2012, **53**, 4084–4086.